Improved Tracking of Phosphorus in Wastewater Treatment Works through Anaerobic Digestion of P-rich sludge

Prepared by:

Quevauvilliers Matthieu

Supervised by:

David S. Ikumi (PhD)

Department of Civil Engineering
University of Cape Town, Private Bag Rondebosch, 7700
South Africa 7700

Declaration

I, Matthieu Quevauvilliers, know the meaning of plagiarism and declare that all the work in the document, save for that which is properly acknowledged, is my own. This thesis/dissertation has been submitted to the Turnitin module (or equivalent similarity and originality checking software) and I confirm that my supervisor has seen my report and any concerns revealed by such have been resolved with my supervisor.

Signed: Signed by candidate Date: 31/08/2020

Abstract

This research aims at improving the tracking of phosphorus (P) in wastewater treatment works (WWTWs) by developing a model which accurately explains the intracellular processes of phosphorus accumulating organisms (PAOs). Two major models: the "Comeau-Wentzel" model (Comeau *et al.*, 1987) and the "Mino" model (Mino *et al.*, 1988) were developed to explain PAO intracellular processes but the failure of these models to achieve data reconciliation when modelling the anaerobic digestion of PAOs show that they are still incomplete. Ikumi and Ekama (2019) generated stoichiometry to help model PAO intracellular processes and hypothesised that an energy transfer between the activated sludge (AS) system and the anaerobic digester (AD) might take place. This research generated a steady state (SS) anaerobic digestion model (an extension of Sötemann *et al.*'s (2005) model) to model the treatment of sludge from nitrifying-denitrifying enhanced biological phosphorus removal (NDEBPR) system and assess, through data reconciliation, which of Ikumi and Ekama's (2019) stoichiometry best models PAO behaviour. The AD model generated achieved a high degree of correlation with experimental data but was unable to conclusively identify a single biochemical pathway for PAO processes.

Executive Summary

Anaerobic digestion (AD) is a sludge stabilization process where sludge is treated biologically in the absence of nitrates and oxygen. This process is highly utilized as it allows resource recovery from the sludge in the form of methane gas and precipitates (Henze *et al.*, 2008, Ikumi *et al.*, 2015, Sötemann *et al.*, 2005).

Sötemann *et al.* (2005) developed a steady state (SS) AD model which predicted the effluent COD, amount of methane gas generated, alkalinity and pH of an AD treating primary sludge (PS) (sludge removed through settling before the activated sludge (AS) system) and waste activated sludge (WAS) from Modified Ludzach Ettinger (MLE) systems (nitrogen (N) rich sludge). The Sötemann *et al.* (2005) model, however, was unable to accurately predict the pH of an AD treating sludge from nitrifying denitrifying enhanced biological phosphorus removal (NDEBPR) systems (N and phosphorus (P) rich). Harding *et al.* (2010) extended the SS AD model to begin remediating this issue by modelling the P content of the sludge and ionic releases and speciation of said P content in the bulk liquid. To ensure accurate AD influent characterization, Harding *et al.* (2010) focused on modelling phosphorus accumulating organisms (PAOs), the microorganisms mediating P removal in NDEBPR systems. Harding *et al.* (2010) developed a general PAO composition $C_XH_YO_ZN_AP_B.q_{PAO}[MePO_3]$ (where Me represents an aggregate of all the metals in the biomass and PO_3 represents the polyphosphate (polyP) stored intracellularly). Harding (2009) further extended the polyP composition from $[MePO_3]$ to $Mg_cK_dCa_e.PO_3$ modelling the specific metals (magnesium, potassium, and calcium) associated with the P removal process.

Phosphorus accumulating organisms (PAOs) are a type of ordinary heterotrophic organisms (OHOs) with the ability to remove P in excess of their metabolism requirements in the form of granules called volutins (Henze *et al.*, 2008). These PAOs consist of a group of microorganisms acting as one with the *Accumulibacter* genus representing the largest portion of the bacterial organisms present (Oehmen *et al.*, 2007, Sathasivan, 2011). The PAOs have been seen taking up acetate anaerobically by breaking down polyP and glycogen to manufacture poly-β-hydroxybutyrate (PHB). Two main theories exist regarding this behaviour: the “Comeau-Wentzel” model and the “Mino” model. The “Mino” model is the most accepted model despite being unable to reconcile all variables as it generates more PHB than the “Comeau-Wentzel”

model and correlates better with experimental data. Ikumi and Ekama (2019) modelled PAO processes in the AD following the "Mino" model assumptions and the pH modelled was significantly inferior to the empirical pH as shown in Figure I.

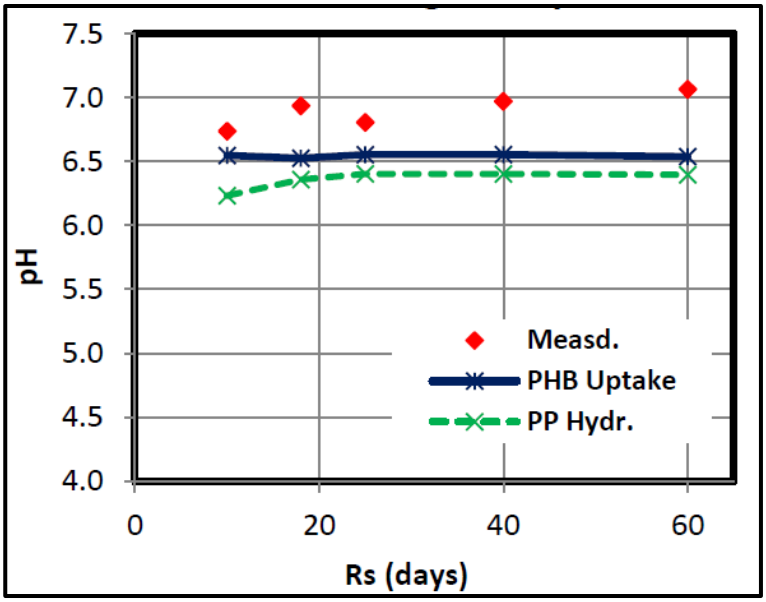

Figure I: Difference between modelled and measured pH (Ikumi & Ekama, 2019)

Several research questions arise from this mismatch between the experimental and modelled pH:

- Since modelling the PAO behaviour in the AD yields a lower pH than the measured pH, is the "Mino" model which is currently being used to model PAO behaviour adequate?
- If glycogen is not the correct reducing agent, does the modelling of polyP (an intracellular, inorganic, product in the PAO) breakdown as the source of energy result in better predictions of the AD system performance?
- If polyP is indeed the direct energy source for anaerobic PHB storage, does this give rise to an energy transfer between the AS system and the AD that current models do not measure because this energy does not take the form of electrons bound in organics (i.e. does not have a COD)?
- What modifications need to be made to the stoichiometric pathways to ensure accurate AD models for EBPR WAS?

This thesis aims at answering these research questions, by building upon the existing work on anaerobic digestion and creating an AD model that accurately predicts the reactor pH and effluent properties of an AD treating NDEBPR WAS. Achieving this new model will help improve the current understanding of PAO processes by ensuring data reconciliation in the AD.

Due to the mismatch between modelled pH and experimental pH, Ikumi and Ekama (2019) generated stoichiometry for PAO bioprocesses in the AD assuming a range of energy sources for anaerobic PHB storage that occurs with polyP release. These include glycogen (as per the "Mino" model), polyP (as per the "Comeau-Wentzel" model) and acetate (as a potential outside carbon source). Modelling of these stoichiometries will allow the identification of the correct PAO biochemical pathway if data reconciliation can be achieved. The AD model generated to allow this analysis was built in five sections:

i) The first section characterized the sludge according to the Harding *et al.* (2010) characterization. The characterization procedure assumed the biomass (PAOs) to have an unbiodegradable fraction of 8% in accordance with the death regeneration model (Dold *et al.*, 1980). The characterization procedure assumed the inorganic portion of the biomass (i.e., the polyP stored in the PAO) to have a general composition of $Mg_cK_dCa_e.PO_3$ (Harding *et al.*, 2010).

ii) The second used saturation kinetics formulation to model the hydrolysis of sludge, as the rate limiting process in AD (the other processes are much faster and allowed to reach completion in the steady state model). Hence, this hydrolysis process was the one that controlled the prediction of the effluent COD, the COD removal and methane gas production. Saturation kinetics formulation was used to model the hydrolysis of the sludge because it replicates hydrolysis as a surface process allowing solids (biodegradable particulate organics) concentrations relative to the biomass (which are mediating the process) to be captured well in the process, as likely to occur in reality.

iii) The third section of the model used the output from the saturation kinetics of hydrolysis as input to the stoichiometries from Harding *et al.* (2010) and Ikumi and Ekama (2019) to predict the final AD products. The various stoichiometries were evaluated towards determining the best stoichiometric pathway for polyP breakdown in the AD (with the other

AD stochiometric processes from Sötemann *et al*. (2005), that relate to organic breakdown, already having a strong validation base; (Ikumi *et al*., 2014))..

iv) The fourth section used the stoichiometric outputs from the third stage of the model as input to calculations used for pH estimation of the AD, at steady state. The pH was calculated for both the conditions where it is assumed that no precipitation took place in the AD (i.e., infinite ionic solubility) and conditions where multimineral precipitation took place in the AD. The multimineral precipitation model developed was an extension of Loewenthal *et al.*'s (1995) model and allowed for the precipitation of struvite, amorphous calcium phosphate (ACP) and newberyite in the AD.

v) The fifth and final section ensured mass balances were maintained over each model. To verify the accuracy of the model, data from a forty (40) day augmented biomethane potential (ABMP) test was used. The influent and effluent data as well as the kinetic constants of hydrolysis, K_M=2.64gCOD organics/gCODorganics.d and K_S=9.11gCOD/l, were sourced from Maake and Ikumi (2020). A comparison between the outputs of each model and the empirical data is presented in Table I.

As shown in Table I, the AD model achieves accurate effluent predictions for COD, VSS, ISS and TSS with respectively 97.5%, 95.8%, 103.0% and 98.5% match. Since Maake and Ikumi (2020) did not have N influent or effluent data, an analysis of the N prediction could not be achieved. Severe discrepancies can be seen between the predicted and measured P and metals effluent concentrations. This difference between measured and predicted readings were attributed to experimental error as P and metal balances were not achieved over the experimental data (see Table 6.10 for details). A comparison between the empirical pH and modelled pH was performed and is presented in Figure I.

Table I: Comparison between ABMP data and model outputs

SS AD model results		Empirical Data	Model Output			
		Maake and Ikumi (2020)	Harding (2009)	Ikumi and Ekama (2019)		
				PolyP	Glycogen	Acetate
Total COD	S_{te}	2520,00	2585,3			
Filtered COD	S_{tse}	-	0			
Unbiodegradable soluble COD	S_{use}	-	0			
TKN	N_{te}	-	366,3			
Filtered TKN	N_{tse}	-	230,2			
Free and Saline Ammonia	N_{ae}	-	230,2			
Influent unbiodegradable N	N_{ouse}	-	0			
Total Phosphorus (TP)	P_{te}	563,40	446,50			
Filtered TP	P_{tse}	-	405,69			
Orthophosphate	P_{ae}	308,70	405,69			
Effluent P	P_{ouse}	-	0			
Particulate Volatile Suspended Solids	VSSe	1660,00	1732,3			
Inorganic Suspended Solids	ISSe	1060,00	1028,6			
Total Suspended Solids	TSSe	2720,80	2760,9			
Total Magnesium	TMg^{2+}_e	-	49,40			
Total Potassium	TK^{+}_e	493,50	245,00			
Total Calcium	TCa^{2+}_e	24,30	42,50			
Soluble Magnesium	SMg^{2+}_e	-	49,40			
Soluble Potassium	SK^{+}_e	-	245,00			
Soluble Calcium	SCa^{2+}_e	-	42,50			
Gas	ml	739,5	771			
pH of effluent assuming infinite ionic solubility		6,69	6,41	6,68	6,68	6,70
pH post struvite precipitation			6,55	6,71	6,72	6,73
pH post ACP precipitation			6,47	6,69	6,69	6,70
pH post newberyite precipitation			6,40	6,67	6,67	6,68

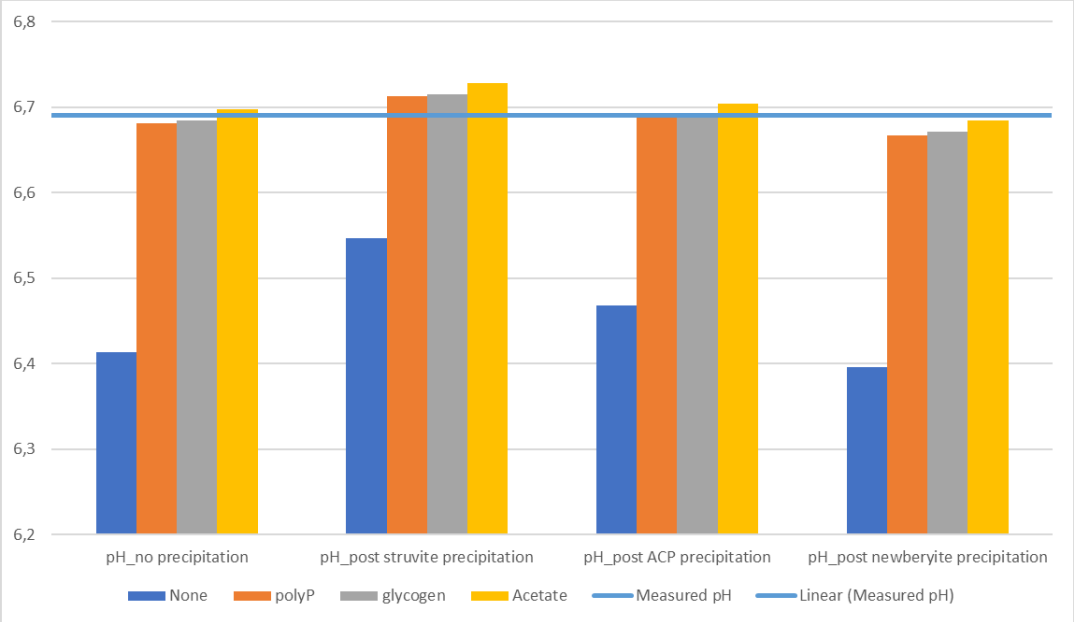

Figure I: Comparison between empirical and model predicted pH

As shown in Figure I, the experimental pH was approximated by:

- The stoichiometry using polyP as reducing agent post ACP precipitation (pH=6.69),
- The stoichiometry using glycogen as reducing agent post ACP precipitation (pH=6.69) and
- The stoichiometry using acetate as reducing agent post multimineral precipitation (pH=6.68).

Conclusion

Due to the high degree of correlation between the model and the experimental data, it can be concluded that a SS AD model accurately predicting reactor and effluent properties when treating NDEBPR sludge was developed meeting this research's objectives.

From the results, it can also be concluded that:

i) PAOs do undergo bioprocesses in the AD confirming the assumption that microorganisms act unconsciously according to the environmental conditions.

ii) The SS AD model generated, by itself, does not allow this research to determine which reducing agent was used by the PAOs for intracellular processes. This implies that if an energy transfer does take place between the AS system and the AD, this energy transfer does not impact the AD at SS (or how it impacts the AD is not yet measured).

iii) The analysis of the precipitation model proposes that the multimineral precipitation model be reduced (assuming polyP or glycogen is used as a reducing agent) to model the precipitation of struvite and ACP only.

The sum of this research and the dynamic analysis presented by Ikumi and Ekama (2019) seems to indicate that the AD model using polyP as a reducing agent should be used as the SS AD model for an AD treating NDEBPR sludge.

Acknowledgements

God Almighty- Thank you Lord for walking with me through this journey. Submitting this thesis has not been easy but it is thanks to your strength and unwavering love and support that I am here today. Thank you.

Dr David S. Ikumi- Thank you David for the opportunity to do this masters research under your supervision. You have been an amazing supervisor and mentor; I wish you nothing but the best.

Prof George Ekama- Thank you Prof for your guidance during this masters. I want to say thank you for being a role model through your humility and kindness. I hope that I one day get to me a fraction of the man you are. I wish you the best of recoveries.

Njabulo Thela and Hector Mufunga- Thank you guys for the help in the lab. Nobody can hope for a better start to a week than having a chat with both of you on a Monday.

My parents Jean-Michel and Corinne and sister Murielle Quevauvilliers - Thanks mom, dad and mumu for your continuous support during this masters. Thank you for accompanying me on this journey and walking with me every step of the way no matter what.

Johanne Cunat- Thank you for your unwavering love and support. This masters thesis is as much yours as it is mine. Thank you for pretending to care about microorganisms.

All my supportive friends- I can truly say that I have been blessed with the most amazing, hardworking and kind friends one could hope for. Your support and dedication will never be forgotten.

The **Water Research Commission** (WRC), The **Water Research Group** (WRG) at the University of Cape Town, The **National Research Foundation** (NRF) for providing financial support.

Table of contents

List of tables

List of figures

List of Equations

List of Symbols, Acronyms, and abbreviations

μ	Growth rate
α	Activity Coefficient
δ	P/O ratio
ΔΨ	Electric Potential Difference across a bacteria's cell membrane
ρCO_2	Partial Pressure of Carbon Dioxide
Ca	Calcium
Ca^{2+}	Calcium ion
CH_3COOH	Undissociated Acetate
CH_3COO^-	Dissociated Acetate Ion
CH_4	Methane
C_i	Concentration of component *i*
f_{av}	Active fraction of sludge in terms of VSS
f_{at}	Active fraction of sludge in terms of TSS
f_i	Fraction of component *i*
f_{iPAO}	The inorganic fraction of PAOs
K	Potassium
K^+	Potassium ion
k_i	Rate of component *i*
Mg	Magnesium
Mg^{2+}	Magnesium ion
s	Acetate

S_{be}	Biodegradable COD in the effluent
x	Biomass
X_{BH}	Biomass concentration in gVSS/l
X_{EH}	Endogenous residue concentration in gVSS/l
X_I	Inert material concentration in gVSS/l
X_{IO}	Inorganic material concentration in gISS/l
X_{BG}	Live PAO biomass concentration in gVSS/l
X_{EG}	Endogenous residue concentration generated from PAOs in gVSS/l
ABMP	Augmented Biomethane Potential Test
AD	Anaerobic Digestion
AOO	Ammonia Oxidising Organism
AS	Activated Sludge
ADP	Adenosine Diphosphate
ATP	Adenosine Triphosphate
BNR	Biological Nutrient Removal
BPR	Biological Phosphorus Removal
COD	Chemical Oxygen Demand
DPAO	Denitrifying Phosphorus Accumulating Organisms
EBPR	Enhanced Biological Phosphorus Removal
GAO	Glycogen Accumulating Organism
HCl	Hydrochloric Acid
K	Potassium
Mg	Magnesium

N	Nitrogen
NaOH	Sodium hydroxide
NDEBPR	Nitrification-Denitrification Enhanced Biological Phosphorus Removal
NOO	Nitrate Oxidising Organism
OHO	Ordinary Heterotrophic Organisms
P	Phosphorus
PHA	poly-β-hydroxyalkanoates
PHB	poly-β-hydroxybutyrate
PHV	poly-β-hydroxyvalerate
PAO	Phosphorus Accumulating Organism
polyP	Polyphosphate
SCFA	Short Chain Fatty Acid
SRT	Sludge Retention Time
SS	Steady State
TSS	Total Suspended Solids
VFA	Volatile Fatty Acid
VSS	Volatile Suspended Solids
WAS	Waste Activated Sludge
WRC	Water Research Committee
WRG	Water Research Group
WWRF	Wastewater Recovery Facilities
WWTP	Wastewater Treatment Plant
WWTW	Wastewater Treatment Works

1. Introduction

This research aims, through the generation of experimental data and the creation of an anaerobic digestion model, to generate knowledge that will help obtain a better understanding of the intracellular bioprocesses of phosphorus accumulating organisms (PAOs). This research is part of a larger research framework that aims at improving the tracking of phosphorus through biological processes, to improve resource recovery from waste and turn wastewater treatment works (WWTWs) to wastewater recovery facilities (WWRFs). The research is carried out in the Water Research Group (WRG) of the Civil Engineering Department at the University of Cape Town supervised by Dr D. S. Ikumi.

1.1 Background

Wastewater treatment aims at the removal of pollutants, toxic material, organic matter, and nutrients (nitrogen (N) and phosphorus (P)) present in wastewaters. This is achieved in wastewater treatment works (WWTWs) through a combination of physical, biological, and chemical treatments. The sizing of settlers, biological reactor size, reactor sequence and the selection of chemicals dosed is based on the WWTWs' influent characteristics and the required effluent quality.

In the 1960s, to reduce eutrophication in open water sources, increased research in the microorganisms involved in the treatment of wastewater took place. The combination of bacteriology and bioenergetics proved most useful as the kinetics of sludge treatment emerged and the first wastewater treatment protocols were created (Henze *et al.*, 2008). However, as the loading to WWTWs increased, the effluent quality declined. The resulting pollution of water sources downstream of the treatment works resulted in an increase in research in wastewater treatment to help stop the eutrophication process and prevent further pollution. As research progressed, the key role of nitrogen (N) and phosphorus (P) in the eutrophication process (the explosive growth of algae and other plants due to the fertilizing effect of nitrogen (N) and phosphorus (P)) was discovered. Further research highlighted the critical role of phosphorus as the limiting factor in the eutrophication process requiring the identification of major P releasers and the creation of effluent quality standards to reduce effluent P concentration back to its

background levels (Henze *et al.*, 2008, Oehmen *et al.*, 2007). Identifying the major P releasers was a particularly difficult task as the phosphorus concentration of a given open-water source is dependent upon upstream factors and atmospheric deposition (Henze *et al.*, 2008, Seviour *et al.*, 2003). The WWTWs were identified as a major P contributor and were required, therefore, to meet stringent effluent requirements. To meet the new effluent requirements, research into chemical and biological P removal treatment processes took place. Because of the increased costs associated with chemical P removal and the adverse effects of the chemicals on the microorganisms mediating sludge treatment, biological P removal was preferred (Lee & Yun, 2014). A process known as the enhanced biological phosphorus removal (EBPR) was developed to help reduce the effluent phosphorus concentration. The EBPR process became and currently is the basis for biological P removal worldwide.

The EBPR process biologically removes the P content of the influent, both in the liquid and solid phase, through the action of microorganisms known as phosphorus accumulating organisms (PAOs). PAOs remove P in excess of their metabolic requirements (anabolism and catabolism) in the form of polyphosphate (polyP) granules called volutins (Henze *et al.*, 2008). Because PAOs thrive under sequential anaerobic-aerobic conditions, most WWTWs use sequential reactors with varying environmental condition (anaerobic-anoxic-aerobic) and recycles (a-, r- and s-) to maximize P removal. Two main theories were developed to explain both PAO intracellular behaviour and their impact on the bulk liquid: the "Comeau-Wentzel" model (Comeau *et al.*, 1987) and the "Mino" model (Mino *et al.*, 1988). The "Comeau-Wentzel" model was developed by assuming the genus of PAOs and uses polyP as the energy source to take up acetate (COD) and generate reducing agents in the manufacture of poly-β-hydroxyalkanoates (PHA). The "Mino" model, on another hand, assigned the energy in the polyP to acetate uptake only and the formation of reducing agents to intracellular glycogen. The "Mino" model is currently preferred as it correlates better with experimental results and produces more PHA (Pereira *et al.*, 1996, Yagci *et al.*, 2003). Smolders *et al.* (1993) continued research into PAOs by investigating their kinetics. Using information from both the "Mino" model and Smolders *et al.*'s (1993) kinetics, models predicting the behaviour of PAOs in the activated sludge (AS) system were developed. These models correlated well with experimental data for activated sludge systems. However, the biological behaviour of PAOs in anaerobic digesters (AD) is still under investigation. The expectation is that PAOs may respond to the anaerobic environment of the

AD in a similar way to the anaerobic zone of the activated sludge system. This is because, besides the environment being anaerobic, readily biodegradable organics such as acetate (which could be used for PHB formation) are known to be generated as intermediate products of the AD process. In the attempts to calibrate the behaviour of PAOs in AD, some measurements, such as the partial pressure of carbon-dioxide, have not yet been reconciled. It is hypothesised that the reason this data reconciliation cannot be achieved is because most of the current models focus on the impact of PAOs on the bulk liquid and do not include the required level of detail regarding intracellular products formed. Ignoring the intracellular products of PAOs, oversimplifies the representation of PAO behaviour in the wastewater treatment systems. Ikumi and Ekama (2019) suggest that because models do not describe these intracellular products, a potential energy transfer between the activated sludge (AS) system and the anaerobic digester (AD) may occur due to these intracellular processes. This may also be the reason behind current model mispredictions of the AD's pH at steady state (SS).

Ikumi *et al.* (2015) anaerobically digested waste activated sludge (WAS) from the AS system of a nitrifying-denitrifying enhanced biological phosphorus removal (NDEBPR) system. When the system was modelled, the modelled reactor achieved a much lower pH than was experimentally recorded. Ikumi and Ekama (2019) suggested that the difference in pH could be traced back to the presence of PAOs in the WAS and the simplified behaviour and lack of data reconciliation previously discussed. Ikumi and Ekama (2019), hence, generated stoichiometry to try and model PAO behaviour with increased complexity in the AD. They modelled PAO bioprocesses in the AD as well as the anaerobic digestion of the bacteria. This AD model with this stoichiometry yielded a much better pH prediction. However, since Ikumi *et al.* (2015) anaerobically digested a mixture of microorganisms, it cannot be conclusively said that the pH prediction issues could be sourced back to PAO behaviour only.

1.2 Research Questions

From the background presented, several questions arise:

- Is the polyp release mechanism as presented in the "Mino" model, which is currently being used to model PAO behaviour, adequate to represent polyP release behaviour in AD systems?

- Does the modelling of polyP as the energy source (via breakdown of polyp chains, without the use of organic reducing agents) for anaerobic PHB uptake result in more accurate prediction in AD system performance? If so, is this process linked to the transfer of energy (not measurable as COD, due to polyp being inorganic) between the AS system and the AD, which does not take What modifications need to be made to the stoichiometric pathways to ensure accurate AD models for EBPR WAS?

1.3 Objectives

This research objectives aims at determining the correct stoichiometric pathway for PAO behaviour in the AD. To address this objective, investigations will aim at:

- Evaluating the stoichiometric pathways of PAO behaviour presented by Ikumi and Ekama (2019) by incorporating them as variable pathways in the AD model generated and to assess the extent to which their predicted outputs match experimental data. This will help validate the concept of polyP contributing to some 'energy' carry over from AS to AD system, as noted by Ikumi and Ekama (2019). The extent to which polyP is released with PHB uptake (resulting in energy generation, alkalinity increase and ρCO_2 decrease) rather than PAO death (results in H_2CO_3 alkalinity drop and ρCO_2 increase) in the AD and the stoichiometric outcome will be investigated. It is expected that if the aerobic PHB uptake rate can be used also in the AD (since PAOs are again exposed to anaerobic conditions with presence of acetate reasonable outputs for pH and ρCO2 will be generated.
- Modification of hydrolysis kinetics to cater for presence of PAOs in AD systems.
- Extension of the weak acid/base chemistry: The current AD weak acid/base chemistry includes the P extension proposed by Harding *et al.* (2010) to model P releases and associated metallic ion releases. Loewenthal *et al.* (1995) developed a procedure to model struvite precipitation but this procedure must now be extended to include additional precipitates such as amorphous calcium phosphate (ACP), struvite, magnesite, calcite and newberyite which are common AD precipitates.

To address investigations extremely careful and exact experimental work on the AD of NDEBPR WAS containing enhanced cultures of PAO biomass.

1.4 Scope and Limitations of this research

This research aims at generating data to inform the behaviour of PAOs in the AD. Although this will also require knowledge on the behaviour of PAOs in the AS system, the previously developed AS system models will not be modified. Data regarding the behaviour of PAOs in the AS system will not be generated as part of this research but sourced from another research.

This research will not consider the thermodynamics of PAO behaviour. This decision was made because since a model explaining PAO behaviour to a high degree of accuracy does not yet exist, a model with an increased level of detail like a thermodynamic model is thought not to be warranted. It is believed that a thermodynamic model will only be required when the current understanding of PAO reaches a consensus. Furthermore, this thesis aims at the generation of a steady state data which will be achieved using Microsoft Excel. A thermodynamic model consists of a dynamic simulation model which requires platforms such as WEST®, SIMBA or MATLAB.

A sensitivity analysis on the SS AD model will not be performed as it is considered outside the scope of this research. Instead a comparative analysis of the stoichiometric pathways generated by Ikumi and Ekama (2019) will be carried out.

1.5 Overview of Report

This section of the introduction aims at presenting a brief overview of the report by focussing on the objectives of each major chapter present within the report. This report is divided into seven major chapters. It starts by presenting the background of the report, the research questions, the objectives, and scope of this report (Chapter 1). It is followed by a literature review (Chapter 2) whereby the research from which this work derives is presented. This section will show that this research, and the claims by Ikumi and Ekama (2019), are grounded in existing knowledge. In Chapter 3, the impact of the new NDEBPR AD model is discussed. The methodology follows in Chapter 4 whereby the experimental set-up used to meet the objectives presented in Chapter 1 will be discussed. Since this research aims at assessing the impact of energy transfer on an AD at SS, the model developed to check this claim is presented (Chapter 5). In Chapter 6, an analysis of said model will be presented to highlight the stoichiometric pathway best representing PAO

behaviour. This will be achieved through a comparative analysis of stoichiometric pathways and data reconciliation. Finally, a conclusion which will present the most important findings of this research and present new research questions and requirements for further research will be developed in Chapter 7. Chapters 1-7 and their relationships to each other are presented graphically in Figure 1.1.

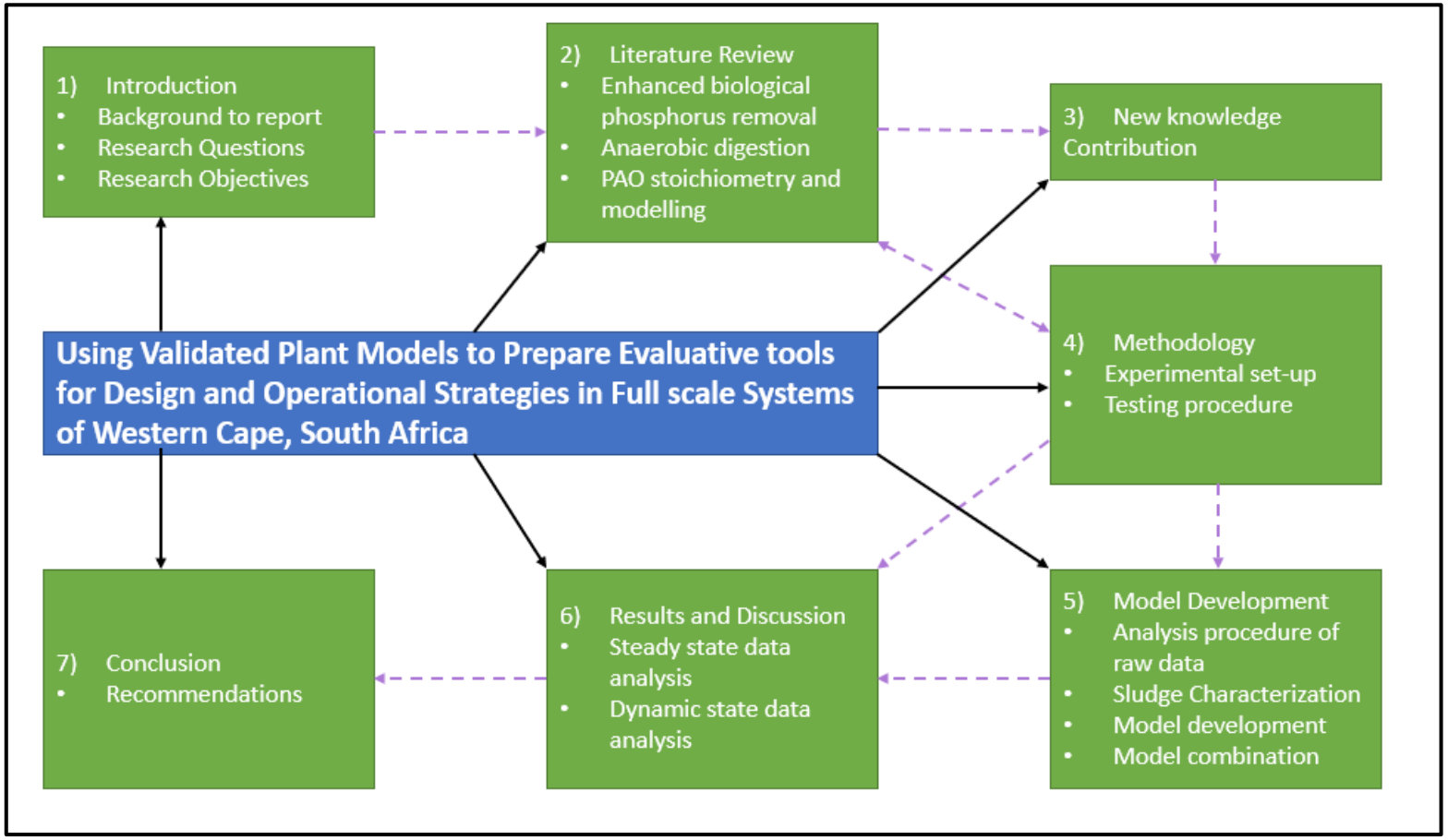

Figure 1.1: Mind-map showing the overview of the and main objectives of each section

2. Literature Review

This literature review was developed with the aim of presenting the research and highlighting the current understanding of the enhanced biological phosphorus removal (EBPR) process, anaerobic digestion, and the stoichiometry of intracellular processes by phosphorus accumulating organisms (PAO).

The literature review is divided into three main sections:

i) The first section will present the current understanding regarding the behaviour of PAOs. This will be achieved by introducing the enhanced biological phosphorus removal process in Section 2.1.1. A good understanding of the EBPR process will lead to a good understanding of PAOs and PAO behaviour. The details of the EBPR process such as the set-up required for phosphorus removal and the processes taking place in each reactor of said set-up will be presented. Section 2.1.2 will contain a more detailed analysis of the behaviour of PAOs in each tank of the activated sludge (AS) system. This section will put forward the most prominent theories regarding PAO behaviour. Understanding these theories is critical for they are the basis upon which the stoichiometry presented by Ikumi and Ekama (2019) was developed. Section 2.1.3 will present a summary of the literature available regarding factors limiting the enhanced biological phosphorus process. Section 2.1.4 will present a brief literature on denitrifying phosphorus accumulating organisms (DPAOs), glycogen accumulating organisms (GAOs) and propionate as a chemical oxygen demand (COD) source and their impact the EBPR process. Although Section 2.1.3 and 2.1.4 are not directly relevant to this research, they were deemed relevant as they help generate a better understanding of PAOs and because an enhanced PAO culture was developed (by MSc. Candidate Njabulo Thela as part of his research) to meet the requirements of this research.

ii) During the experimental phase of this research PAOs will be anaerobically digested and hence it follows that the second section of this literature review will focus on the anaerobic digestion (AD) process. This section is divided into four sub-sections. First the anaerobic digestion process will be introduced in Section 2.2.1. In this section, the different microbial groups present in an AD will be presented. This section will focus on the biochemical reactions (reactants and products) that take place in the AD. The factors which might impede

said microorganisms will also be discussed highlighting the need for a reliable AD model. Section 2.2.2 which follows will discuss the AD of waste activated sludge (WAS). This section will focus on the reasons why WAS is anaerobically digested. The biochemical properties of WAS in the anaerobic digester and good engineering practice when operating anaerobic digester in industry will also be discussed. This will help bridge the gap between research and practice. The anaerobic digestion of P-rich sludge will then be tackled in Section 2.2.3. Because this research aims at producing a better AD model by anaerobically digesting P-rich sludge, this section will discuss the requirements for the generation of a good AD model. Section 2.2.4 will finish this section by introducing the augmented biomethane potential (ABMP) test. The concept behind and the requirements for an ABMP will be explained. Due to the lack of peer-reviewed documentation on ABMPs, the methods utilized to standardise the biomethane potential (BMP) test and how they can be extended to the ABMP will be discussed.

iii) The third section of this literature will discuss the stoichiometry of PAOs in an AD as developed by Ikumi and Ekama (2019). The stoichiometry will be analysed by comparing it to the PAO stoichiometry in anaerobic and aerobic conditions (in the AS system) developed by Smolders *et al.* (1993) and Yagci *et al.* (2003). The PAO anaerobic and aerobic stoichiometry in the AS system could have been introduced at an earlier stage but because this research deals with the possibility of an energy transfer between the AS system and the AD, it seemed useful to introduce them here where the link with Ikumi and Ekama's (2019) stoichiometry. This section is a critical part of this research as it is the basis of the new knowledge contribution of this research.

2.1 Enhanced Biological Phosphorus Removal

In the 1960s, the role and sensitive nature of phosphorus (P) in the eutrophication process was discovered and efforts to decrease the P loading in open water sources were made (Henze *et al.*, 2008, Oehmen *et al.*, 2007). To reduce P loading back to its background levels, stringent effluent requirements for major P contributors such as wastewater treatment plants (WWTPs) were set-up. To meet those new requirements, research into biological and chemical P removal processes took place (Henze *et al.*, 2008). The increased costs of chemical P removal compared to biological P removal and the effects of chemicals on the microorganisms mediating sludge treatment (Lee & Yun, 2014) caused a greater focus in the development of a biological P removal system. From this research, the enhanced biological phosphorus removal (EBPR) was developed. From empirical knowledge, Barnard (Seviour *et al.*, 2003) laid the groundwork for EBPR and developed the three-stage Bardenpho process which is still widely used. Through research, a better theoretical, biochemical and mathematical understanding of the EBPR process was achieved resulting in more advanced P removal systems such as the Johannesburg and modified University of Cape Town (UCT) processes (Henze *et al.*, 2008, Seviour *et al.*, 2003).

2.1.1 Principles of Enhanced Biological Phosphorus Removal

Enhanced biological phosphorus removal is defined as a biological process in the activated sludge system microorganisms known as phosphorus accumulating organisms are employed to remove excess P present in the influent wastewater. PAOs remove P in excess of their metabolic requirements (anabolism and catabolism) in the form of polyphosphate (polyP) granules called volutins (Henze *et al.*, 2008, Oehmen *et al.*, 2007, Wentzel *et al.*, 1990). These heterotrophic were originally described as belonging to the *Acinetobacter* genus but evidence brought forward by molecular microbiology tools such as FISH (fluorescence in-situ hybridisation) have determined that this was not the case (Henze *et al.*, 2008, Sathasivan, 2011). No single bacteria exhibiting the ability to mediate all the EBPR processes was identified which prompted the conclusion that PAOs, rather than belonging to a single bacterial group undertaking all processes, refer to a group consisting of several microorganisms acting in a coordinated manner with the *Accumulibacter* genus representing the largest portion of the bacterial organisms present (Oehmen *et al.*, 2007, Sathasivan, 2011). Despite a change in the PAO genus, the metabolic

pathways available to the micro-organism were not challenged because of the high correlation between predictions and experimental results. Mathematical models have allowed for such changes by grouping all microorganisms contributing to the EBPR process under the PAO classification and modelling them to behave as one organism undertaking all the P removal processes.

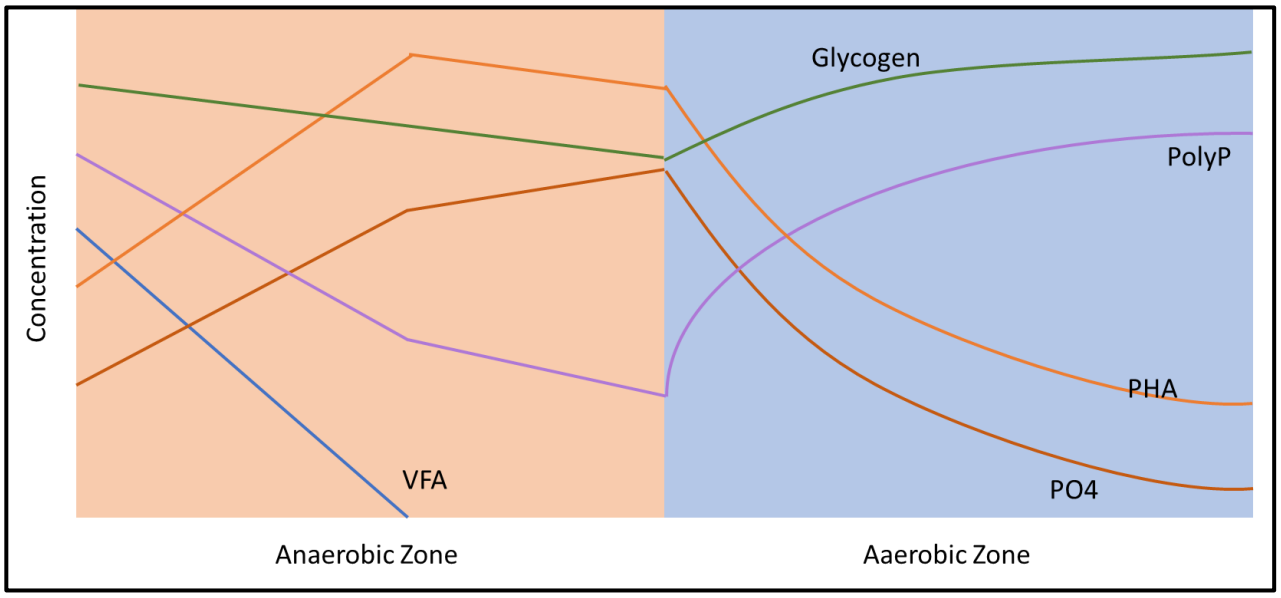

Figure 2.1: VFA, Glycogen, PolyP, PHA and PO4 concentration change over the anaerobic-aerobic EBPR sequence (Henze *et al.*, 2008)

Enhanced biological phosphorus removal takes place in the AS system through a combination of P uptake in the presence of an electron acceptor (aerobically) and P release in the absence of an electron acceptor (anaerobically) as shown in Figure 2.1 (Henze *et al.*, 2008). Since these alternating conditions promote the bacterial dominance of PAOs and maximize P removal, the re-circulation of sludge through the aerobic- anoxic (a-) and anoxic- anaerobic (r-) recycles are implemented (Kuba *et al.*, 1993, Smolders *et al.*, 1993, Wentzel *et al.*, 1988). Anaerobically, PAOs utilize intracellular high energy polyP and glycogen for energy production. The energy from the hydrolysis of polyP (resulting in the release of orthophosphate and metals ions - magnesium, potassium and calcium - in the aqueous phase) and glycogen (resulting in carbon-dioxide release into the aqueous phase) is then used for anaerobic PAO metabolic processes

(Smolders *et al.*, 1993). This energy is used to process simple organics such as acetate and the synthesis of poly-β-hydroxyalkanoates (PHA) a high energy organic molecule that is stored intracellularly. In the presence of an electron acceptor, the PAO biomass then uses the intracellularly stored PHA for biomass growth (anabolism) and energy generation (catabolism). Using some of the catabolic energy, the PAOs take up the aqueous P (stored as polyP) and produce glycogen which will be used as an energy source when the biomass is recycled to the anaerobic zone.

2.1.2 Phosphorus Accumulating Organism processes

2.1.2.1 Phosphorus Accumulating Organism Processes in Anaerobic Conditions

PAO Biochemical Pathways

In the anaerobic tank of the EBPR system, PAOs outcompete other microorganisms (such as ordinary heterotrophic organism (OHOs), ammonia oxidising organisms (AOOs) and nitrate oxidising organisms (NOOs)) and take up the available volatile fatty acids (VFAs). Although they are unable to take up substrate in anaerobic conditions, OHOs generate enzymes that ferment the influent fermentable biodegradable soluble organics (S_{bsfi}) to VFAs increasing the VFA pool available to PAOs (Wentzel *et al.*, 1991). The PAOs take up the VFAs and store them intracellularly releasing phosphorus in the process. The VFAs in a WWTWs' influent consists mainly of acetate, propionate and butyrate. Because the influent VFA composition varies (different percentages depending on the source of the wastewater), it follows that the chemical composition of the PAO intracellular storage was found vary. The intracellular storage organic is often referred to as poly-β-hydroxyalkanoates (PHA) which is the sum of poly-β-hydroxybutyrate (PHB) (80%) and poly-β-hydroxyvalerate (PHV) (20%) (Henze *et al.*, 2008, Mino *et al.*, 1988, Murnleitner *et al.*, 1997). Since much more PHB is formed than PHV and PHB the main product of acetate uptake (as shown by Ikumi and Ekama (2019) and Smolders *et al.* (1995)), this point forward the synthesised intracellular product of PAOs will be referred to as PHB.

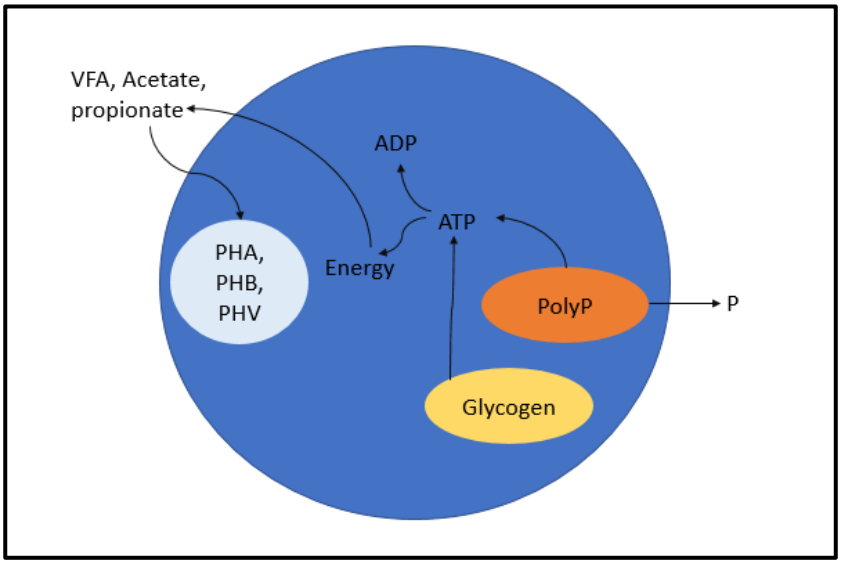

Figure 2.2: Biochemical model of PAO metabolic anaerobic process (Henze *et al.*, 2008)

The uptake of VFAs from the aqueous phase is divided into several steps. The extracellular VFA must first be taken up across the cell membrane, energised into coenzyme A compounds and reduced to PHB (Henze *et al.*, 2008, Mino *et al.*, 1988). However, how this process occurs is subject to debate. The two most prominent models explaining the intracellular behaviour of PAOs are the "Comeau-Wentzel" model and the "Mino" model.

The "Comeau-Wentzel" model

The "Comeau-Wentzel" model is based on the assumptions that PAOs belong to the *Acinetobacter* genus and that the intracellular polyP is the origin of the energy for all processes. Through the genus assumption, Comeau *et al.* (1987) identified the specific biochemical pathways available to the bacteria. Those pathways are dependent upon the ATP/ADP ratio (ATP: adenosine triphosphate, ADP: adenosine diphosphate) and the NADH/NAD^+ ratios. According to this theory, acetate uptake is achieved by simple virtue of diffusion. The ADP bonds in the PAO are energised to ATP using energy stored in the polyP bond. The energy in the ATP is then used to energize acetate to acetyl-CoA reducing ATP back to ADP. In parallel, some of the intracellular VFA enters the tricarboxylic acid (TCA) cycle to produce $NADH_2$ from NAD^+ which acts as a reducing agent used to reduce the acetyl-CoA to PHB (Mino *et al.*, 1988, Wentzel *et al.*, 1991). The breakdown of polyP bonds for energy availability results in the release

cations (Mg^{2+}, $Ca^{2+}$and K^{+}) and anions ($H_2PO_4^-$, HPO_4^{2-}) into the aqueous phase. This is presented graphically in Figure 2.3.

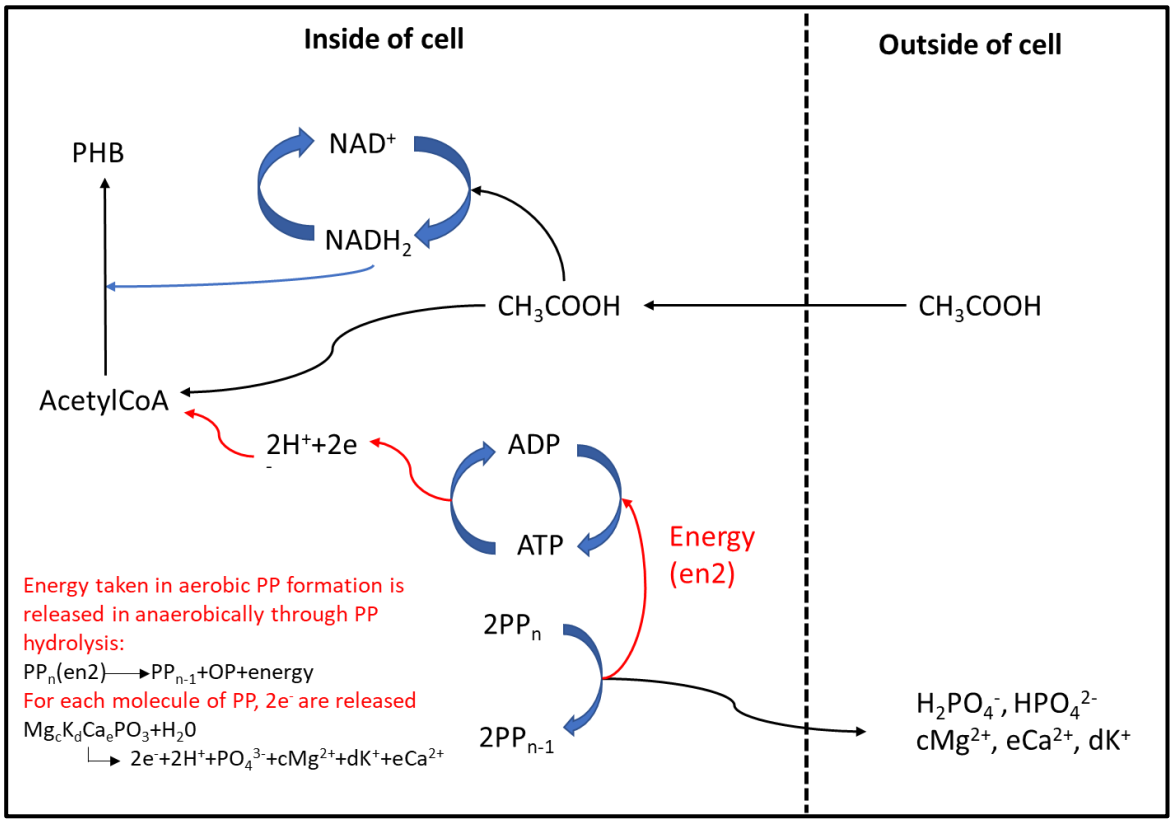

Figure 2.3: "Comeau-Wentzel" Model Anaerobic (Comeau *et al.*, 1987)

The "Mino" model

Although similar in many points to the "Comeau-Wentzel" model, the "Mino" model assumes that glycolysis (degradation/hydrolysis of glycogen) is the source of the intracellular reducing power used to change acetate to PHB and that the energy from polyP hydrolysis is used to take up acetate, storage and cell-maintenance (Pijuan *et al.*, 2008, Smolders *et al.*, 1995, Wentzel *et al.*, 1991, Zhou *et al.*, 2008). The use of glycogen as an energy source significantly reduces the energetic requirements from polyP. The reducing agent required is generated by the conversion of glycogen to pyruvic acid via the Embden-Meyerhof (EM) pathway. The *Acinetobacter* bacteria do not possess the EM pathway and hence was not considered to be a viable pathway in the "Comeau-Wentzel" model. However, since it was established that PAOs are not *Acinetobacter* but rather seem to belong to the *Accumulibacter* genus (Seviour *et al.*, 2003), this

pathway is viable. The pyruvic acid is then converted to acetyl-CoA releasing CO_2 in the process. This reaction produces the $NADH_2$ reducing agent required to transform the coenzyme-A compounds to PHB. An alternative pathway, the Entner-Doudoroff (ED) pathway, was also hypothesised and resulted in different yields of PHB. The "Mino model" is presented graphically in Figure 2.4.

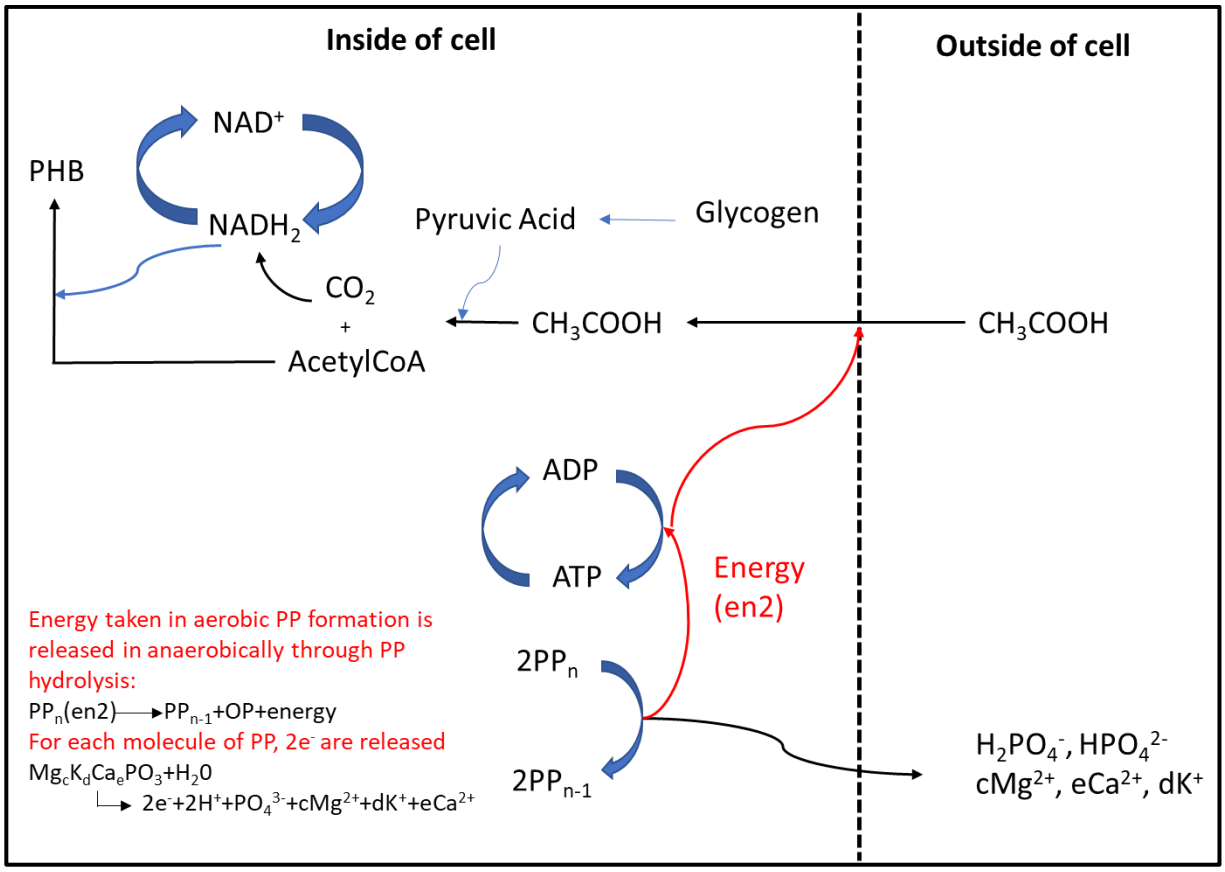

Figure 2.4: "Mino" model (Mino *et al.*, 1988)

A comparison of the "Mino" model and the "Comeau-Wentzel" model was carried out. Modelling of the "Mino" model was found to yield more PHB than the "Comeau-Wentzel" model (Yagci *et al.*, 2003) and correlated better overall with experimental results as shown by Pereira *et al.* (1996). This tends towards validating the model (or at the very least the use of glycogen as an energy source) despite the CO_2 release in the reactor that can be sourced to either a partial or complete TCA cycle associated with polyP hydrolysis and P release. The creation of a validated model linking all processes has not yet been achieved because the EBPR process is highly complex with most of the metabolism described taking place on internally stored substrates and compounds (Smolders *et al.*, 1995).

PAO Acetate Uptake

$$\Delta\Psi = \Delta\mathrm{p} + 2.3\mathrm{RT}(pH_{in} - pH_{out})$$

Equation 2.1: Impact of pH on P releases (Smolders *et al.*, 1993)

As previously mentioned, the P release associated with acetate uptake is one of the defining characteristics of PAOs in the anaerobic zone of the AS system. The ratio of P release to acetate taken up was first thought of as being constant but was found to vary between 0.25-0.75 P-mol/C-mol of acetate as the bulk liquid pH varied between 5.5 and 8.5 (Smolders *et al.*, 1993). This variation was linked to the electric potential difference ($\Delta\Psi$) that is set-up across the cell membrane due to differences between the intracellular pH and the extracellular pH (Nielsen & Villadsen, 1994, Smolders *et al.*, 1993). Indeed, as shown in Equation 2.1, when the intracellular pH is higher than the extracellular pH, the uptake of acetate is done easily due to a low electric potential difference. Since polyP breakdown is used to take up the acetate and assuming the amount of energy in each polyP bond is the same (i.e. contributes the same Gibbs free energy to the process), less energy is required to take up the acetate and therefore less polyP needs to be broken down. When the pH varied between 5.5 and 8.5, the ATP required to take up acetate was seen to vary by 0.57molATP/C-mol as shown by Smolders *et al.* (1993).

PAO Acetate Uptake Kinetics

PAO anaerobic kinetics can be used to gain a better understanding of PAO behaviour. PAO anaerobic kinetics are defined based on two main reactions: the uptake of acetate and the production of anaerobic maintenance energy (m_{an}).

The acetate uptake rate is the defining anaerobic rate as it proceeds uninterrupted if all other participating components (such as polyP and glycogen) are available (i.e. does not stop until either polyP or glycogen runs out when acetate is present in excess) (Brdjanovic *et al.*, 1998, Smolders *et al.*, 1995). The acetate uptake rate was measured through the ratio of P release to change in acetate concentration and found to be 0.8-1.2mol-P/mol-HAc. This is further demonstrated by Brdjanovic *et al.* (1998) who showed that in the absence of intracellular polyP in anaerobic conditions, no acetate uptake took place by PAOs despite acetate being present in excess. This contributes significantly to the concept of polyP carrying energy.

$$q_s = {q_s}^{max} . \frac{C_s}{C_s + K_s}$$

Equation 2.2: Acetate uptake rate (Smolders *et al.*, 1995)

. Where: q_s: refers to the acetate uptake rate (C-mol/C-mol.h)

q_s^{max}: refers to the maximum acetate uptake rate (C-mol/C-mol.h)

Cs: external acetate concentration (C-mol/l)

K*s*: kinetic rate of acetate uptake = 1 C-mmol/l

Smolders *et al.* (1995) concluded that the rate of polyP released was not a defining rate as at high pH the acetate uptake rate was unchanged despite the increased energy transfer requirement. This could indicate that the energy in the polyp bond might be under-estimated in current models. The acetate uptake rate is a Monod type kinetic (shown in Equation 2.2) with a max acetate uptake rate (q_s) of 0.43C-mol/C-mol.h and a K_s constant of 1.6 x 10^{-3} C-mol/l (Smolders *et al.*, 1995).

PAO Maintenance Energy

The anaerobic maintenance rate was determined to also be one of the defining kinetic rates. By testing PAOs in anaerobic acetate free environment, some P release took place to generate maintenance energy at a rate of 2.5 x 10^{-3} molP/C-mol.h or 2.4mgP/gVSS.h. The rate of the reaction equation is shown in Equation 2.3.

$$r_p = 0.44 q_s C_x + m_{an} C_x$$

Equation 2.3: Maintenance energy generation (Smolders *et al.*, 1995)

Where: r_p refers rate of energy generation from P (P mol/m^3.h)

C_x refers to the biomass concentration (mol/m^3)

m_{an} refers to the maintenance energy in anaerobic conditions (mol/C-mol.h)

The maintenance energy is referred to by Smolders *et al.* (1995) as the energy required to keep the biomass functioning when it is not undergoing bioprocesses. No mention of said maintenance energy was found in literature discussing the anaerobic digestion of PAOs. Ikumi *et al.* (2015) showed that the anaerobic digestion of PAOs took place at a slower rate than that of OHOs. It could be conceived that this maintenance energy is used when in the anaerobic digester to "repair" the microorganism's cell membrane and effectively slow down the hydrolysis process. However, the significant difference in hydrolysis rates would allocate more energy to the polyP bond than is currently considered and would confirm the energy transfer between the AS system and the AD.

2.1.2.2 Phosphorus Accumulating Organism processes in Aerobic Conditions

To ensure PAOs grow and enhanced P removal is achieved, PAOs require alternating anaerobic-aerobic environments supplied by the anaerobic and aerobic zones and sludge recycles. The aerobic condition allows for the biomass to utilise an electron acceptor (oxygen) to metabolise the biodegradable organics available (for OHOs) and the PHA stored intracellularly (for PAOs) achieving simultaneous COD and nutrient removal.

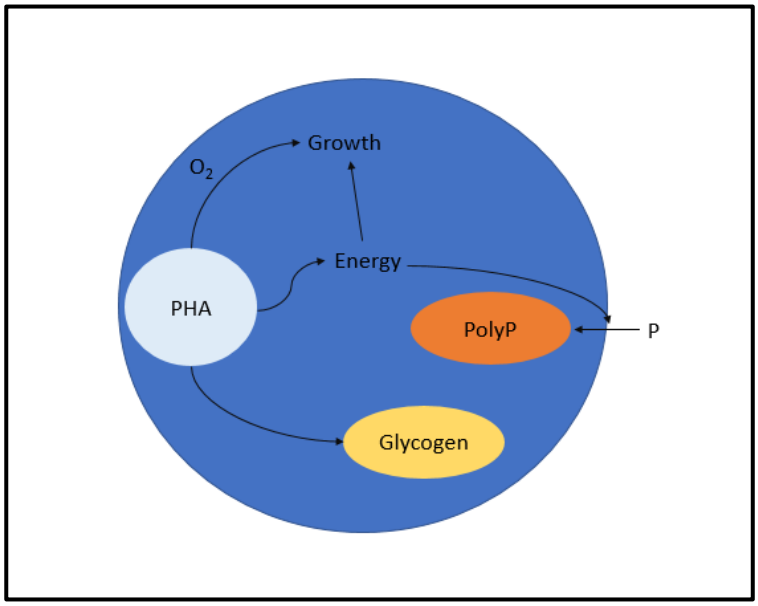

Figure 2.5: Biochemical model of PAO metabolic aerobic process (Henze *et al.*, 2008)

According to both the "Comeau-Wentzel" model and "Mino" model, PAOs use the stored PHB aerobically to generate energy. The PHB is broken down to coenzyme-A compounds, enters the TCA cycle and generates ATP. The ATP is used for biomass anabolism and catabolism:

- The anabolic energy is used to generate new cell mass which increases the P uptake potential of the PAO biomass and leads to increased P removal. This causes a decrease in the aqueous phase and effluent P. The maximum amount of P that can be removed is, however, limited. According to Wentzel *et al.* (1991), PAOs can store a range of phosphorus concentrations but are limited to a maximum of 0.35mgP/mgPAOVSS (Wentzel *et al.*, 1991). In both the "Comeau-Wentzel" and "Mino" models, the amount of new PAO biomass formed is dependent upon the amount of PHA stored in the PAO biomass upon entering the aerobic reactor hence indicating that PHA is the limiting reagent to P uptake (Henze *et al.*, 2008).
- The catabolic energy is used for (i) the synthesis of cations (Mg^{2+}, Ca^{2+} and K^{+}) and anions ($H_2PO_4^-$) to replenish the polyP storage, (ii) glycogen manufacturing* (iii) energy for biomass growth and (iv) cell maintenance (Smolders *et al.*, 1995, Wentzel *et al.*, 1991).

**Unlike polyP resynthesis, no propositions are put forward in the "Mino" model towards the processes used towards the produce intracellular glycogen by PAOs (Wentzel et al., 1991).*

The "Comeau-Wentzel" model and "Mino" model

It seems most likely, at this stage, that the energy source for the synthesis of VFAs to PHB consists of a partial TCA cycle from the "Comeau-Wentzel" model and glycolysis from the "Mino" model (Pijuan *et al.*, 2008, Sathasivan, 2011, Zhou *et al.*, 2008). This is supported by:

- Brdjanovic *et al.* (1998) who has shown that P uptake and release and hence P removal is inhibited by the lack of polyP stored within PAOs making it likely that polyP is an energy carrier;
- Smolders *et al.* (1994) who proved that 60% of the catabolic energy (i.e. electrons to oxygen for energy generation) is used for the producing of glycogen and polyP leading to the conclusion that since energy is used to generate polyP, then polyP must have energy storage capabilities and hence may be used as an energy source;

- Martin *et al*. (2006) who, using microbiology tools, concluded that *Accumulibacter* have the necessary genes for both glycolysis and a full or partial TCA cycle (Oehmen *et al.*, 2007). The presence of multiple paths introduces the idea that the pathway used for the acetate-PHB conversion may be dependent upon environmental and intracellular factors as speculated by Yagci *et al*. (2003); and

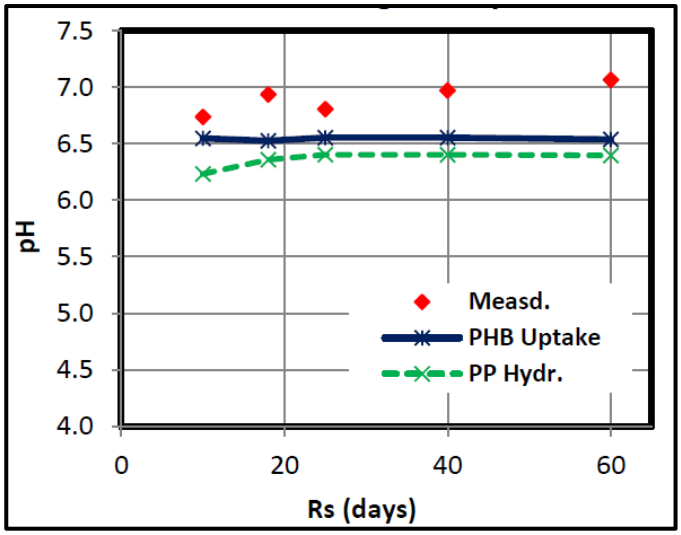

Figure 2.6: Difference between modelled and measured pH (Ikumi & Ekama, 2019)

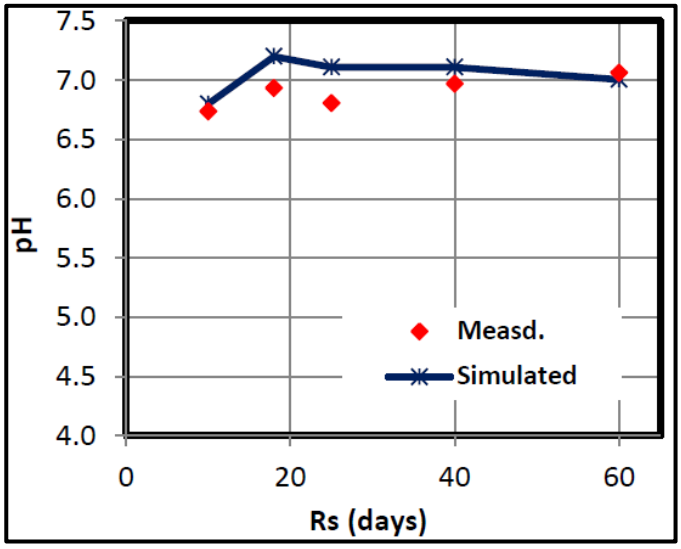

Figure 2.7: Ikumi and Ekama (2019) update model pH prediction

- Ikumi and Ekama (2019) who modelled PAO behaviour in the AD. Ikumi and Ekama (2019) modelled PAO behaviour in the AD based on the "Mino" model and showed that the resulting AD pH did not match experimental data as shown in Figure 2.6. Ikumi and Ekama (2019) therefore modelled for PAO behaviour according to the "Comeau-Wentzel" model, as shown in Figure 2.7, showing that the results might lie somewhere midway between the models.

PAO aerobic kinetics

The PAO aerobic kinetics can be described by four main processes: the growth rate of the organism (μ), the polyP synthesis rate (q_{pp}), the glycogen production rate (q_{gl}) and the aerobic maintenance rate (m_{aer}).

$$\mu = k_x . f_{PHB}$$

Equation 2.4: Growth rate of biomass (Smolders *et al.*, 1995)

Where: μ is the growth rate of the biomass (C-mol/C-mol.h)

k*x* is the rate of growth of biomass *(*C-mol/C-mol.h)

f_{PHB} fraction of PHB (C-mol/C-mol)

The growth rate of PAOs (μ) is assumed to be dependent upon the amount of PHB stored and hence upon anaerobic conditions. The PAO growth rate is hence described as a first-order kinetics with a term expressing the PHB contents in the PAO (f_{PHB}). The growth rate kinetic equation is presented as Equation 2.4 (Smolders *et al.*, 1995).

The polyP formation rate (q_{pp}) is also dependent upon the fraction of PHB within the cell. As the amount of PHB decreases and becomes zero, the rate of P uptake also decreases and stops. However, the polyP uptake is limited as PAOs have a maximum P content at 0.35mgP/mgVSS (i.e. shown as ${f_{PP}}^{max}$ in Equation 2.5). The ratio of P uptake per mol of PHB utilized was calculated and determined to range between 2.2-2.6 mol PO_4-P/mol PHB under aerobic

conditions for a mixed culture aerobic conditions (Comeau *et al.*, 1987, Vlekke *et al.*, 1988) and 0.23mol PO_4-P/mol PHB for an enhanced culture (Kuba *et al.*, 1993).

$$q_{pp} = k_{PP}.\left(\frac{C_P}{C_p + K_p}\right).\left(1 - \frac{f_{PP}}{{f_{PP}}^{max}}\right).f_{phb}$$

Equation 2.5: PolyP uptake kinetics (Smolders *et al.*, 1995)

Where: q_{pp} refers to the polyP synthesis rate (P-mol/h)

k_{PP} refers to kinetic rate of P uptake towards polyP formation (P-mol/C-mol.h)

C_p refers to the external P composition (P-mol/l)

${f_{PP}}^{max}$ refers to the maximum polyP content stored (0.3 P-mol/C-mol)

f_{PP} refers to the current polyP content in the PAO (P-mol/C-mol)

f_{PHB} refers to the PHB content (P-mol/C-mol)

$$q_{gl} = k_{gl}({f_{gl}}^{max} - f_{gl})$$

Equation 2.6: Glycogen uptake kinetics (Smolders *et al.*, 1995)

Where: q_{gl} refers to the glycogen production rate(C-mol/h)

k_{gl} refers rate of uptake of glycogen (C-mol/C-mol.h)

${f_{gl}}^{max}$ refers to the maximum glycogen stored (C-mol/C-mol)

f_{gl} refers to the glycogen stored within the PAO (P-mol/C-mol)

Glycogen manufacture rate (q_{gl}) is a limiting rate in PAO aerobic kinetics. Like polyP, the rate of uptake of glycogen is dictated by the amount of PHB stored intracellularly. The glycogen manufacture rate is likely defined by the difference between the maximum allowable glycogen stored (${f_{gl}}^{max}$=0.27 C-mol/C-mol) and the glycogen currently stored (f_{gl}) within the PAO and

a glycogen production rate k_{gl}=0.8 C-mol/C-mol.h (Smolders *et al.*, 1995). The high degree of resemblance between the polyP and glycogen uptake kinetics equations as well as the factors upon which both processes are dependent show that it is unlikely that glycogen contains energy but not the polyP bond. The energy stored in both need not be the same (i.e. can be measured using the same methods) but it is very likely to be present.

The maintenance aerobic requirement (m_{aer}) was determined by subjecting a sample of an enhanced PAO culture to oxygen till the oxygen consumption rate became constant. The aerobic maintenance was determined to be a constant at 0.25mmol O_2/l (Smolders *et al.*, 1994)

2.1.2.3 Phosphorus Accumulating Organism Composition

The PAO biomass is divided into three main parts:

(i) The organics stored intracellularly (such as glycogen and PHB)

(ii) The inorganics stored intracellularly (such as polyP) and

(iii) The biomass itself.

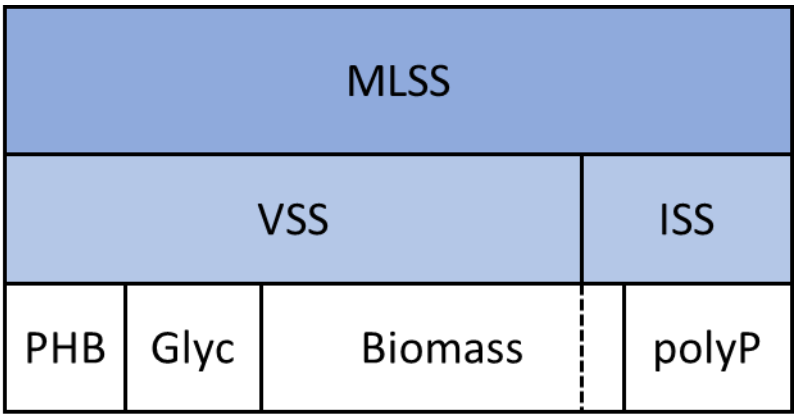

Figure 2.8: PAO Composition (Smolders *et al.*, 1995)

The total suspended solids (TSS) of PAOs is divided between the volatile suspended solids (VSS) and the inorganic suspended solids (ISS). The VSS content of the PAO consists of the glycogen, PHB and the organic part of the biomass. The ISS portion consists of the inorganic portion of the biomass and the precipitates generated from polyP release. The ISS contribution of the organic

portion of the biomass (f_{iPAOBM}) is similar to that of OHOs at 0.15mgISS/mgPAOVSS and the ISS contribution of the polyP is 3.19mg ISS/mgP (Wentzel & Ekama, 2004).

Depending on the sampling point and the influent wastewater composition, the proportions of PHB, glycogen, biomass and polyP in the PAO vary. When samples were taken from the aerobic zone of the AS EBPR system, it was noticed that up to 50% of the PAO mass (VSS) measured was due to the internal storage components of the PAO (Smolders *et al.*, 1995). Because the polyP component of the biomass is inorganic and requires metal ions to maintain charge balance, the polyP storage of the PAO typically modelled as a separate part of the biomass. Harding (2009) recommends $C_XH_YO_ZN_AP_B.q_{\Phi}.[MePO_3]$. This composition includes a linkage factor, q_{Φ}. where Φ is the component it is applied to (q_{PAO}) (Seviour *et al.*, 2003, Smolders *et al.*, 1993, Wentzel & Ekama, 2004).

2.1.3 Enhanced Phosphorus Accumulating Organism Culture

In microbiology, to gain better understanding of a new type of microorganism, its intracellular processes and its genus, research involving a pure culture is undertaken. Such an approach has been attempted with PAOs but has not been successful. This is because, as previously mentioned, PAOs are a consortium of microorganisms most likely composed of different bacteria and hence obtaining a single genus from a consortium of different microorganism with varying microbial pathways is not achievable. Secondly, contrary to most organisms which can develop a colony in static conditions, PAOs require an alternating anaerobic-aerobic condition to multiply and hence would not survive typical microbiological processes (van Loosdrecht *et al.*, 1997). The pure cultures that have been developed have failed to be qualified as phosphorus accumulating organisms due to the inability of the cultured bacteria to either release ortho-phosphate (OP) in significant amount under anaerobic condition in the presence of acetate and/or take up OP under aerobic conditions. Dilution plate techniques are inappropriate when analysing PAOs (van Loosdrecht *et al.*, 1997).

To study PAOs and gain a better understanding of these microorganisms an enhanced culture is hence the best option. An enhanced PAO culture is defined as one where PAOs dominate the system (i.e. are present in majority) but where traces of other organisms remain. Several

methodologies are available in literature regarding the procedure required to grow an enhanced PAO culture. The most common is the use of a sequencing batch reactor (SBR) (a serum bottled in which sludge is placed and subjected to alternating anaerobic-aerobic conditions) or a traditional UCT or JHB system to which a pure synthetic feed is added (Kuba *et al.*, 1993, Wentzel *et al.*, 1988).

To meet this research's objectives and allow a greater focus on PAO metabolism in an anaerobic digester, an enhanced PAO culture will be grown following the procedure detailed by Wentzel *et al.* (1988).

2.1.4 Microorganisms limiting EBPR processes

2.1.4.1 Denitrifying Phosphorus Accumulating Organisms

The metabolic processes explained from Section 2.1.1 to Section 2.1.3 focus on the behaviour of aerobic PAOs. Nitrates are viewed as an EBPR process inhibitor (Kuba *et al.*, 1993) since they can be recycled from the anoxic zone to the anaerobic zone. However, organisms able to undergo the EBPR process in anaerobic-anoxic set-ups have been discovered and have been named denitrifying phosphate accumulating organisms (DPAOs). DPAOs use nitrates as their terminal electron acceptors and can simultaneously remove nitrogen (N) and P from the aqueous phase. This produces less sludge (since nitrates produce less ATP per $(H^+ + e^-)$ pair towards anabolism) compared to oxygen resulting in a smaller yield $Y_{HVanoxic}$=0.54 vs $Y_{HVaerobic}$=0.67 (Hu *et al.*, 2002) and removes the need for aeration. Even if the P uptake rate under anoxic conditions is similar to that under aerobic conditions, less polyP is taken up resulting in high effluent P concentrations (Hu *et al.*, 2002). This process is favoured in wastewaters with inadequate COD/N/P ratio with COD being the limiting reagent in the BNR process.

2.1.4.2 Glycogen Accumulating Organisms

Analysis of EBPR AS system failures (due to high P in the effluent) has led to the discovery of G bacteria or glycogen accumulating organisms (GAOs) (Mino *et al.*, 1988, Oehmen *et al.*, 2007, Seviour *et al.*, 2003). GAOs have been defined as organisms with the capacity to take up acetate anaerobically and storing them as PHA using aerobically intracellularly stored glycogen as an

energy source. GAOs, like PAOs, can thrive in an anaerobic-aerobic sequence. They, however, do not contribute to excess P removal and cannot form volutins. Indeed, no aerobic P uptake has been linked to GAOs and since GAOs and PAOs compete for the same substrate, GAOs represent a burden on the EBPR process (Oehmen *et al.*, 2007).

To be able to prevent GAOs proliferation and/or reduction of the burden they represent in an EBPR system, it is important to understand the mechanisms that determine PAO-GAO bacterial dominance in a system. Research has shown that reactor conditions such as pH, temperature, SRT, carbon source and COD/P ratio play a critical role towards determining whether PAOs or GAOs dominate the reactor (Mino *et al.*, 1988, Varga *et al.*, 2018).

- GAOs have been seen to outperform PAOs at a low anaerobic pH but PAOs outperform GAOs at an anaerobic pH between 7-7.5 (Oehmen *et al.*, 2007);
- Reactor temperature is a key factor regarding GAO dominance in AS systems. At 20°C PAOs outperform GAOs but above 30°C GAOs have been seen to outperform PAOs;
- The sludge retention time (SRT) selected for the AS system was found to be of importance. Short SRTs were found to favour PAO dominance while longer SRTs were found to favour GAO dominance (Oehmen *et al.*, 2007, Seviour *et al.*, 2003). This, however, is limited since significant P removal requires an adequate SRT to allow the PAO biomass to breakdown the stored PHA and generate new mass (Wentzel *et al.*, 1988);
- The uptake rate of GAOs with propionate as a carbon source has been seen to be slower than that with acetate. Indeed, GAOs use up propionate at less than five (<5%) percent the rate at which they use acetate (Oehmen *et al.*, 2007). To return P removal to an EBPR system with a PAO-GAO culture, propionate could be used as an alternate carbon source in view of promoting PAO bioprocesses.
- The COD/P ratio was also determined to be critical. A high COD/P ratio (>50mgCOD/mgP) favours GAOs over PAOs while a COD/P ratio of 10-20mgCOD/mgP, PAOs was found to benefit PAOs. The COD/P ratio must, however, take into account the need for VFAs of PAOs to be able to form PHA (Oehmen *et al.*, 2007).

Some GAOs, just like PAOs have been found to possess denitrifying capabilities. This was observed both in laboratory and full scale EBPR systems. Mixed PAO-GAO bacterial behaviour

in anoxic conditions has led to the conclusion that GAOs have the ability to reduce nitrates to nitrites and provide a terminal electron acceptor to DPAOs enhancing P uptake by DPAOs (Varga *et al.*, 2018).

Very little information is available regarding GAOs and much research is left to be done. Several models such as ASM2d, ASM2d+TUD, ASM3+bio-P and UCTPHO+ model GAO biological processes. These models, however, do not model PAO-GAO competition. The conditions under which GAO bacterial dominance occur are also not modelled.

2.2 Anaerobic digestion

Wastewater treatment works contain a series of interconnected processes where upstream treatments determine the following biological, physical or chemical processes (Henze *et al.*, 2008, Ikumi, 2011, Ikumi & Ekama, 2019). The sludge retention time (SRT) of the AS system was found to be a critical factor that impacted both the quality of the effluent and the WAS active fraction. To achieve increased handling safety and greater sludge stabilization at a reduced cost, research into sludge treatment protocols took place. Anaerobic digestion was found to be a viable alternative which allowed both resource recovery in the form of methane produced and the reduction in aeration requirements of the AS system (Batstone *et al.*, 2002, Henze *et al.*, 2008, Parkin & Owen, 1986).

This section of the literature review will review the biochemical and physico-chemical processes that take place in a mesophilic (35ºC-37 ºC) anaerobic digester. Current AD steady state models will also be discussed to determine the improvements required to generate a model that accurately predicts AD characteristics when treating NDEBPR sludge.

To gain a better understanding of anaerobic digestion and the research objectives, the literature review presented will be organised as follows:

- Section 2.2.1 will introduce the topic of anaerobic digestion. It will focus on the processes taking place in an AD and the microorganisms mediating said processes.
- Since PAOs will be anaerobically digested during the experimental phase of this research, Section 2.2.2 will focus on the anaerobic digestion of WAS of which PAOs are a component. Since no research, except for Ikumi and Ekama (2019), was found relating to the anaerobic digestion of PAOs, inferences about the behaviour of PAOs in the AD will be made from general WAS anaerobic digestion literature. The factors that affect the design and operation of WAS ADs will also be presented as they will inform the design of the experiment that will be carried out in the experimental phase of this research.
- Section 2.2.3 will introduce the modelling of the anaerobic digestion of PAOs. The short comings of current steady state (SS) AD models with respect to the anaerobic digestion of NDEBPR WAS will be highlighted. Advances required regarding the modelling and impact of polyP releases by PAOs on the bulk liquid of the AD will then be investigated.

The modelling of precipitation in the AD will also be researched. A focus on Loewenthal *et al.* 's (1995) struvite precipitation procedure will be carried out since it will be used as the basis of the multimineral precipitation model that needs to be developed for the improved AD SS model.

- Section 2.2.4 will discuss the augmented biomethane potential test (ABMP). As previously mentioned, since peer-reviewed literature on the ABMP test is lacking, Gaszynski *et al.* (2019) will be used as a main reference together with literature on the more popular biomethane potential (BMP) test. The literature that will be presented will represent the basis of the procedures followed during the ABMP tests to ensure scientific rigour is maintained throughout the investigation.

2.2.1 Anaerobic Digestion

Anaerobic digestion is a process mediated by micro-organisms, in the absence of oxygen, where biodegradable organics are fermented to form biogas (consisting of carbon-dioxide, methane and traces of nitrogen gas) and new mass (Henze *et al.*, 2008). The anaerobic digestion process is divided into four (4) main processes: hydrolysis, acidogenesis, acetogenesis and methanogenesis. Acidogenesis, acetogenesis and methanogenesis are respectively mediated by acidogens, acetogens and methanogens while hydrolysis takes place due to the presence of extracellular enzymes produced by acidogens and acetogens. Two types of methanogens are present in the AD namely: acetoclastic methanogens (acetate to methane) and hydrogenotrophic methanogens (hydrogen to methane) (Batstone *et al.*, 2002, Henze *et al.*, 2008). Figure 2.9 shows the phases of the anaerobic digestion process and the microorganisms mediating them.

Hydrolysis is a chemical process whereby long chain biodegradable polymers (particulates) are broken-down to carbohydrates, proteins and lipids by bacterial extracellular enzymes (Batstone *et al.*, 2002, Parkin & Owen, 1986). Hydrolysis is a surface process where particulates are deteriorated from the outside/surface in. As the complexity of the substrate increases, the time required for a complete breakdown increases. Being the slowest process in the AD, hydrolysis is modelled as the limiting process rate and is often incomplete within the solid retention time of the AD at steady state. The hydrolysis process is sensitive to the digester's temperature and pH.

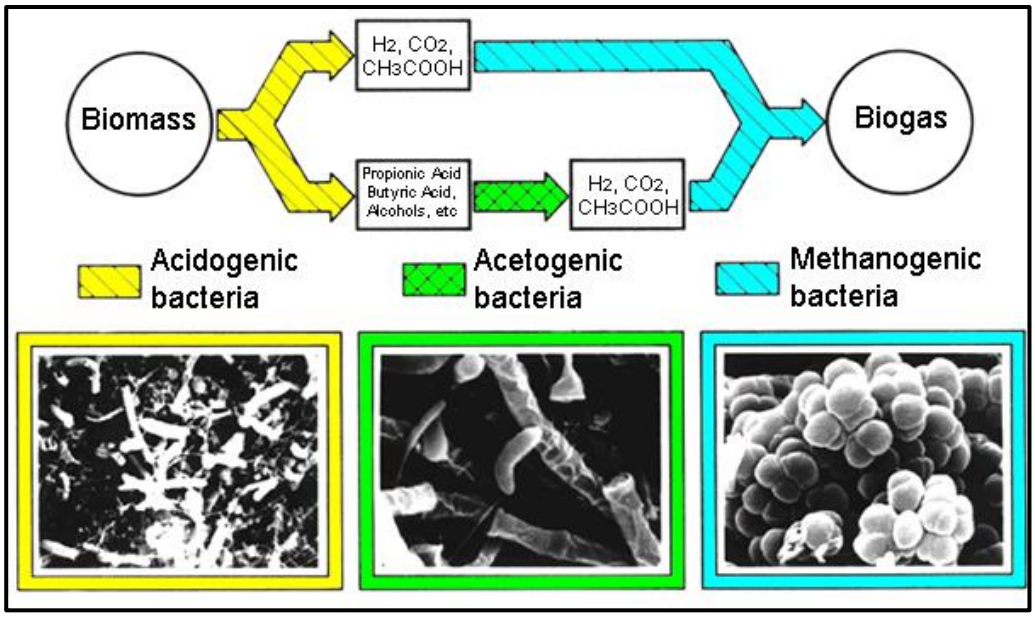

Figure 2.9: Anaerobic digestion bioprocesses and microbial species (WtERT Germany GmbH, 2017)

$$CH_3COOCH_3 + H_2O \rightarrow CH_3COOH + CH_3OH$$

Equation 2.7: Example of a hydrolysis of ester, an organic compound

Equation 2.7 provides an example of the hydrolysis process that takes place in an AD. During the hydrolysis of the influent biodegradables, some acetate and hydrogen is also produced which can be used directly by methanogens to generate methane and carbon dioxide (skip to Equation 2.10). However, most of the biodegradables must first undergo acidogenesis.

$$C_6H_{12}O_6 \leftrightarrow 2CH_3CH_2OH + 2CO_2$$

Equation 2.8: Glucose to acetic acid which is mediated by acidogens

Acidogenesis is the process during which acidogens use the broken-down biodegradables (output from the hydrolysis process) and produce short chain fatty acids (SCFA) (acetic acid (CH_3COOH), propionic acid (CH_3CH_2COOH), butyric acid ($C_4H_8O_2$)…), carbon-dioxide,

hydrogen and generate new cell mass (Batstone *et al.*, 2002, Henze *et al.*, 2008). Due to the high growth rate, high bacterial yield and conversion rate of acidogens, acidogenesis is the fastest process in an anaerobic digester meaning that none of the hydrolysed biodegradables exit the AD at steady state. This high conversion rate, however, makes acidogenesis a sensitive process under dynamic conditions. Dynamically, since acetic acid is produced at a high rate, if methanogens, which operate at a lower rate, are unable to use all the acetate generated, the AD's alkalinity decreases resulting in a pH drop (Henze *et al.*, 2008). This further increases the acid concentration in the digester which further decreases the pH impacting pH sensitive microorganisms and processes (Parkin & Owen, 1986) causing the digester to sour. Equation 2.8 provides an example of the acidogenesis process in an AD.

$$CH_3CH_2COO^- + 3H_2O \leftrightarrow CH_3COO^- + H^+ + HCO_3^- + 3H_2$$

Equation 2.9: Propionate to acetic acid conversion mediated by acetogens

Acetogenesis is the process by which the SCFA (excluding acetate) generated from the acidogenesis process are used up to form acetate (or acetic acid based on pH), carbon-dioxide and hydrogen. These products are then used during methanogenesis to produce methane. Acetogenesis may be inhibited by the pH of the digester as it is dependent on the hydrogen partial pressure. Equation 2.9 provides an example of the acetogenesis process in an AD (Henze *et al.*, 2008).

$$CH_3COO^- + H^+ \rightarrow CH_4 + CO_2$$
$$CO_2 + 4H_2 \rightarrow CH_4 + 2H_2O$$

Equation 2.10: Methane production by methanogens

Methanogenesis is carried out by two sets of bacteria, namely: acetoclastic methanogens (acetate-utilizing bacteria) and hydrogenotrophic methanogens (hydrogen-utilising bacteria). It is in this

final process that the biogas is produced. During the methanogenesis process, the carbon-dioxide in the digester is reduced using the available hydrogen in the aqueous phase as an electron donor. The acetate is also reduced to produce methane gas which, being insoluble, rises to the digester's headspace and exits the digester (Henze *et al.*, 2008, Parkin & Owen, 1986). Equation 2.10 presents chemical reactions detailing the bioprocesses by methanogens.

To maximise methane production, an adequate mesophilic-anaerobic-pH stable environment must be maintained as methanogens are temperature, oxygen, nitrate, and pH sensitive. pH regulation is often achieved by acetoclastic methanogens who have the capacity to take up dissociated acetate ions (CH_3COO^-) together with a proton. This limits acetic acid production and creates a balance between H^+ producing bacteria (acidogens and acetogens) and the H^+ consuming bacteria (methanogens) which gives rise to a balance in the reactor and ensuring a stable pH. This equilibrium is vital as both processes are thermodynamically unfavourable.

$$CH_3COO^- + H_2O \rightarrow CH_4 + HCO_3^-$$

Equation 2.11: Impact of acetate speciation on pH

The operating conditions of the digester (pH, pCO_2, amount of methane produced) are significantly influenced by the composition of the influent biodegradables (i.e. the values of X, Y, Z, a and b in $C_XH_YO_ZN_aP_b$). To achieve an accurate prediction of the digester's alkalinity, pH and the likelihood of precipitation, the influent must be correctly characterized. For example, knowing the influent pH of primary sludge will allow determination of the speciation of acetate in the digester (CH_3COOH or $CH3COO^-$) and its impact on the alkalinity. As shown in Equation 2.11, for every mole of dissociated acetate, one mole of alkalinity is released into the aqueous phase bringing stability to the digester. Knowing the influent characteristics to the AD also facilitates tracking of components of the biodegradables and a higher resource recovery efficiency (Ikumi, 2011).

2.2.2 Anaerobic Digestion of Waste Activated Sludge

To increase the handling safety of sludge, the anaerobic digestion process aims at stabilizing the sludge by reducing its active fraction (f_{av}, f_{at}) (Bolzonella *et al.*, 2004, Parkin & Owen, 1986). To meet this research's objectives and determine whether the anaerobic digestion of PAOs results in an increased death rate, it is first necessary to validate the assumption that PAOs can be anaerobically digested. This will be done by assessing the biodegradability of sludge in an AD and showing that PAOs can be digested.

To inform the experimental methodology that will be followed in this research, key factors towards the anaerobic digestion of WAS will then be presented to link this research to typical guidelines followed in literature and industry.

2.2.2.1 Biodegradability of Waste Activated Sludge

The design of water treatment processes is based upon mass balance principles where the mass of carbon, nitrogen, phosphorus and the number of electrons (amongst many others) into the system must be conserved ($Mass_{in}$ = $Mass_{out}$). To achieve correct predictions, the biodegradability of the sludge is assessed through a characterization process whereby the influent wastewater is divided into two main categories and several subcategories as shown in Figure 2.10. Following this characterization process and depending on the effluent requirements, unit processes are designed. Each of the terms presented in Figure 2.10 is explained in Table 2.1.

Studies by Ekama, Sötemann and Wentzel. (2007) and Ikumi *et al.* (2014) on laboratory scale digesters and full scale WWTPs respectively determined that the biodegradability of sludge organics is consistent in both aerobic and anaerobic conditions. Indeed, they showed that the mass deemed unbiodegradable in the AS system is unbiodegradable in an AD. Since endogenous respiration (or growth regeneration) take place in the AS system (a process whereby part of the biomass is consumed for growth (Dold *et al.*, 1980), it follows that part of the biomass is biodegradable. This idea is further reinforced by Sötemann *et al.* (2005) who anaerobically digested sludge from a Modified Ludzach Ettinger (MLE) system proving that the sludge mass (or active mass) from the AS system could be hydrolysed. Since endogenous respiration was seen

in both PAOs and OHOs, it reinforces the claim that PAOs have a biodegradable portion (Wentzel *et al.*, 1988).

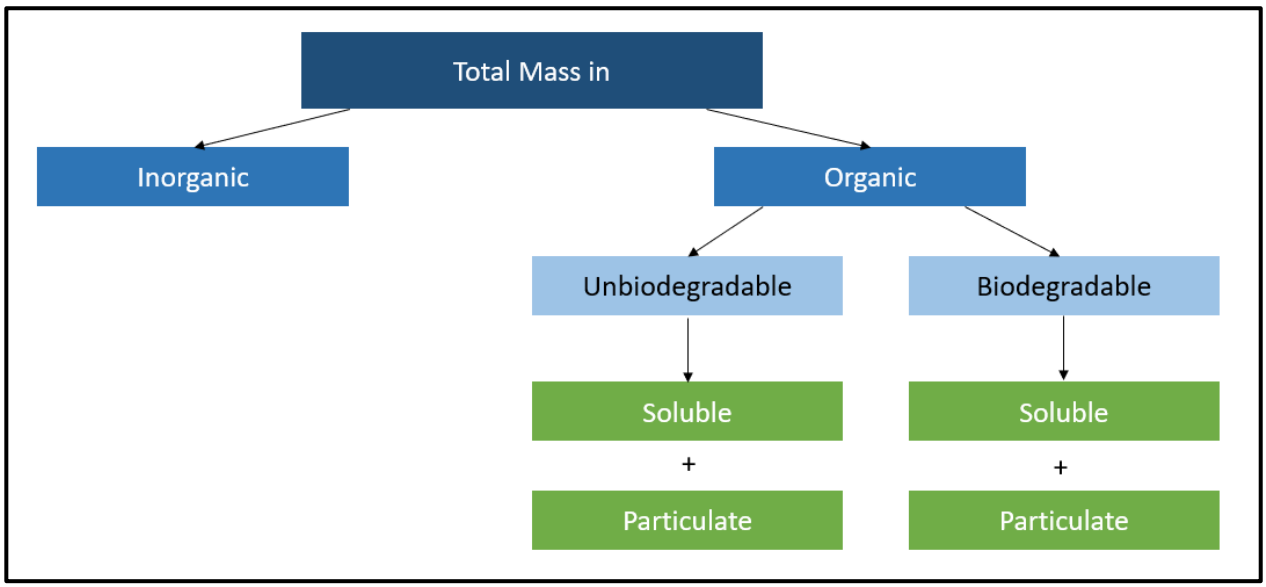

Figure 2.10: Sludge Characterization Process

Table 2.1: Sludge characteristics

Classification	**Properties**
Biodegradable Organics	Organics that are broken down during the SRT of the biological process
Biodegradable Soluble organics	Biodegradable soluble organics are rapidly taken up by microorganisms as they do not need to be broken down before being utilised for growth.
Particulate biodegradable organics	Particulate organics get enmeshed by microorganisms and are broken down from the outside in while being utilised for microorganism growth.
Unbiodegradable Organics	Organics that are not broken down during the SRT of the biological process
Soluble Unbiodegradable Organics	Unbiodegradable soluble organics are not broken down and exit the WWTWs through the effluent.
Particulate Unbiodegradable Organics	Unbiodegradable particulate organics get enmeshed by microorganisms. They cannot, however, be broken down and do not participate in any biological process.
Inorganics	Inorganics are components of the sludge that cannot be broken down. Unbiodegradable organics may not be broken down with the SRT of the WWTWs but they will eventually be degraded. Inorganics cannot be degraded no matter how long they are in the presence of microorganisms

2.2.2.2 Waste Activated Sludge Properties in an Anaerobic Digestor

When anaerobically digesting WAS, the characteristics of the WAS are critical as they impact the AD's weak acid/base chemistry, the magnitude of biogas produced and the SRT required to achieve sludge stabilization. Indeed:

- The amount of methane produced by the AD of WAS was found to be linked to the AS SRT. As the SRT in the AS system increases, the biodegradability (i.e. the active fraction that can be broken down) of the WAS wasted decreases. Because the mass that enters the AD consists mainly of unbiodegradable particulates, which leave the system without contributing to the processes taking place, the specific gas production (SGP) of the AD decreases. Bolzonella et al. (2005) states that AD of WAS yields 0.6-0.8m^3 of biogass/kgVSS destroyed versus 1m^3 of biogass/kgVSS destroyed for a PS-WAS mix. The low biogas production result in WAS ADs having a negative energy balance limiting significantly its resource recovery potential.

**However, one may argue that a positive energy balance may be reached in areas such as Germany from digestion of WAS, due to their less stringent effluent requirements allowing them to operate the AS systems at lower SRTs.*

- Waste activated sludge being a complex substrate (i.e. it consists of live micro-organisms), the retention time necessary to stabilize the sludge is significant. A 20-40 day SRT is commonly used (this is dictated by the influent and required effluent sludge active fraction) at a loading rate of 1 kgVSS/m^3reactor (Bolzonella *et al.*, 2004). Due to the low biogas production, the WAS is often thickened (literature recommends a influent concentration >4% (Bolzonella *et al.*, 2004)) before entering the AD keeping the load on the system constant but reducing the total hydraulic load and hence reactor volume required.

- Due to the low yield of AD bacteria (0.113mgVSS/mgVSS vs 0.45mgVSS/mgVSS for the AS system) the AD of WAS will reduce the mass wasted by the WWTW. Bolzonella et al. (2005) found that anaerobic digestion reduced the suspended solids removal by 84%. This leads to decreased costs associated with sludge transport and disposal.

To help produce more methane from WAS, significant research has been done on methods used to convert unbiodegradable mass to biodegradable mass. Strictly speaking, this is possible because the terms unbiodegradable and biodegradable are time dependent terms. Indeed, in wastewater treatment the term biodegradable refers to the ability of a certain mass to be

biologically broken down within the treatment time of a WWTP. To help reduce the size of ADs used to treat WAS, pre-treatment methods have been researched and were successfully implemented in practice. Due to the low methane production, long SRT and high effluent nutrient concentrations (N and P), the AD of WAS is often not implemented if WAS is to be anaerobically digested as the sole substrate. The savings associated with sludge transport are small compared to the costs required to heat the AD in winter and the high capital cost required in building the ADs. Therefore, it follows, that biodegradable removal is not an adequate measure of the efficiency of a WAS AD (Bolzonella *et al.*, 2004, Parkin & Owen, 1986).

2.2.3 Modelling of Anaerobic Digestion of NDEBPR Sludge

This research aims at determining the impact of the energy transfer from the AS system to the AD at steady state (SS). Current SS AD models are not able identify the impact of this energy transfer since they have not been adapted to consider PAO anaerobic processes. This section of the literature review will aim at pointing out which modification are required to the Sötemann *et al.* (2005) AD SS model to give it the capacity of adequately analysing the experimental data generated during this research.

2.2.3.1 NDEBPR Sludge Characterization

In the aerobic zone of the AS system, PAOs breakdown PHB to generate new mass, take up P as polyP and manufacture glycogen. Since the WAS from a NDEBPR system contains a polyP fraction, it follows that the characterization procedure presented in Sötemann *et al.*'s (2005) AD model is inadequate. Harding (2009) developed a general PAO sludge elemental composition $C_XH_YO_ZN_aP_b.qMePO_3$ (where q represents the number of moles of polyP per mol of PAO) which allows for both characterization of the organic and inorganic portion of the biomass.

2.2.3.2 NDEBPR Steady State AD Model Hydrolysis

An important step in the modelling of anaerobic digestion is the accurate prediction of COD removal. This is achieved through the modelling of the hydrolysis. The hydrolysis rate expression used in the current Sötemann *et al.* (2005) model is inadequate as it does not consider the

particulate nature of the WAS sludge. Sötemann *et al.*'s (2005) AD model relies mostly on Monod kinetics to predict the effluent COD. Monod kinetics perform well for a soluble substrate but are not suited to a particulate substrate like WAS. For the model to predict reasonable outputs, the Monod kinetics need to be calibrated based on both the influent sludge's characteristics and the AD's properties. These two factors require the reactor to be already built and tested. Saturation kinetics, on another hand, are better suited to the general nature of a steady state NDEBPR WAS AD as they are contact kinetics. Saturation kinetics consider the nature of the hydrolysis process (i.e. the breaking down of particulates from the outside in) and the high complexity of the sludge yielding better answers with less calibration. General PAO specific hydrolysis constants can be generated and used in the design of the AD.

The hydrolysis rate of OHOs was found to be lower when compared to that of PS due to the higher complexity of OHOs when compared to PS. No literature is available regarding the sole anaerobic digestion of PAOs. Ikumi and Ekama (2019) reported a slightly lower AD breakdown rate for PAOs than for OHOs from a from a mixed PAO-OHO culture. In the model, this breakdown process includes both the death and hydrolysis of the biomass - there are no studies that have isolated the two processes in AD. However, the PAOs are deemed capable of actively functioning to store PHB in AD as they would in anaerobic zones of AS systems. These PAOs eventually die due to lack of an alternating aerobic zone (hence would not compete with AD biomass for short chain fatty acids; Ikumi and Ekama, 2019). Whether the PAO slower breakdown noted by Ikumi and Ekama (2019) was due to the PAO initial activity in AD systems has not been yet been proven experimentally.

2.2.3.3 NDEBPR Steady State AD Model Stoichiometry

The original stoichiometry presented by Sötemann *et al.* (2005) used carbon (C), N, and hydrogen (water) mass balances to predict the releases in the AD's bulk liquid. Although comprehensive, these releases were insufficient to predict pH adequately when NDEBPR sludge was anaerobically digested as the phosphorus content of the sludge was not represented. Harding (2009) added phosphorus (P) mass balances to the stoichiometry and extended the model by speciating the P releases between the $H_2PO_4^-$ and HPO_4^{2-} ions. This speciation was required as

AD steady state pH vary between 6.8-7.2 which is close to the phosphorus' system second pK value at 7.18 at a temperature of 37°C.

$$H_2PO_4^- + HCO_3^- \rightarrow HPO_4^{2-} + H_2O + CO_2$$

Equation 2.12: Impact of final P releases on pH (Harding, 2009)

From this speciation, Harding (2009) also showed that the organic P releases associated with sludge breakdown result in a decrease in pH. As shown in Equation 2.12, as a proton from $H_2PO_4^-$ is released to form HPO_4^{2-}, the concentration of H_2CO_3 in the system increases. This increases the partial pressure of carbon-dioxide (ρCO_2) and causes the AD's pH to decrease. The amount of H_2CO_3 only decreases once Henry's law constant is exceeded and the H_2CO_3 escapes as CO_2 gas.

2.2.3.4 Precipitation in an Anaerobic Digester

Struvite Precipitation

During the breakdown of polyP in the AD, the metal ions (Mg^{2+}, Ca^{2+}, K^+) used to balance the phosphate charge are also released in the AD's bulk liquid. The increased metal ion concentration in the AD at steady state (pH ranging from 6.8-7.2) increases the likelihood of struvite precipitation (Loewenthal *et al.*, 1995, Musvoto *et al.*, 2000).

When the total species product in the AD bulk liquid is greater than a pH dependent saturation index (pK_{sp}), struvite precipitation takes place (Harding, 2009, Kruk *et al.*, 2014, Loewenthal *et al.*, 1995, Marti *et al.*, 2008). Although the weak acid/base chemistry indicates the likelihood of

$$Mg^{2+} + NH_4^+ + PO_4^{3-} \rightarrow MgNH_4PO_4$$

$$f_t[PO_4^{3-}] * f_m[NH_4^+] * f_d[Mg^{2+}] > K_{sp\_struv}=12.6$$

Where : f_m is the monovalent activity coefficient

f_d is the divalent activity coefficient

f_t is the trivalent activity coefficient

Equation 2.13: Struvite Precipitation

struvite precipitation, it does not indicate the amount of struvite that will be precipitated (Harding, 2009). Loewenthal *et al*. (1995) derived algorithms which accurately predicted the amount of struvite precipitated. Musvoto *et al*. (2000) utilised these weak acid/base equilibrium chemistry principles to model the integrated impact of chemical, physical and biological processes and their interaction towards predicting struvite precipitation.

Modelling Struvite Precipitation

Loewenthal *et al.* (1995) developed the methodology for the modelling of steady state mineral precipitation. Loewenthal *et al.* (1995) modelled struvite precipitation at steady state by assuming that the amount of struvite precipitated:

i) Is small enough that the ionic strength does not need to be recalculated as precipitation occurs, and

ii) Was dependent upon a limiting reagent, the magnesium ion concentration in the bulk liquid.

These assumptions were validated by Musvoto *et al.* (2000) who modelled struvite precipitation with adequate accuracy at Cape Flats (South Africa) WWTWs. A multi-mineral precipitation model will be developed in this research using Lowenthal *et al.*'s (1995) approach.

2.2.4 Augmented Biomethane Potential Test

Anaerobic digestion is a popular treatment process in WWTPs as it enables both sludge stabilization (whether PS or WAS) and resource recovery. During the anaerobic digestion of the AD influent, biogas is produced which, when burnt, can be used to generate electricity. The AD process is a net energy producer as it generates more electricity than it uses (Owen *et al.*, 1978). To provide WWTW designers and stakeholders with the adequate decision-making tools when analysing the need for ADs in the sludge treatment line, the biomethane potential (BMP) test was created. The BMP is a simple and inexpensive test that assesses the maximum amount of methane produced from the AD for a given sludge as a function of the sludge's biodegradability, composition (in particular its protein content) and the AD SRT (Botha & Ekama, 2015,

Gaszynski *et al.*, 2019, Owen *et al.*, 1978, Raposo *et al.*, 2011). The augmented biomethane potential test is a more complex, novel, testing method derived from the BMP test.

2.2.4.1 Augmented Biomethane Potential Test

The augmented biomethane potential test aims at determining the kinetics of the reaction between AD bacteria and a given seed. The use of the term augmented refers to the additional daily measurements of COD, FSA, OP, pH, VFA and settleable solids carried out (Gaszynski *et al.*, 2019). The ABMP relies on the concept that if the products and stoichiometry is known, by applying a reverse mass balance, the influent characteristics can be determined.

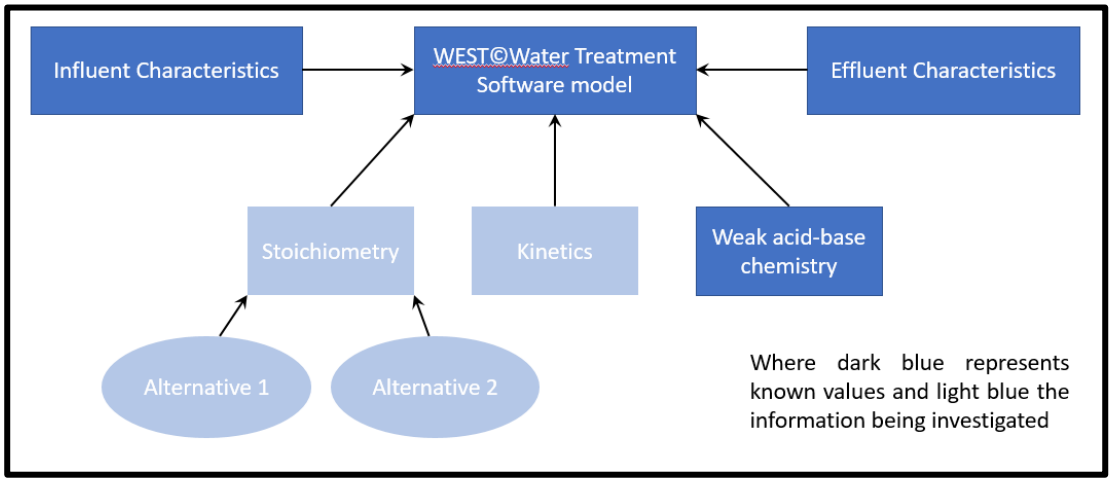

Figure 2.11: Glass box model for WEST©Water Treatment Software model

In this research, the ABMP will be used slightly differently. Using and knowing the influent and effluent characteristics of the ABMP and possible stoichiometric pathways for the PAO-AD interaction (presented in Section 2.3), the most accurate stoichiometric pathway can be validated and the kinetics for this pathway identified. This pathway is the one which will lead to identification of relatively consistent stoichiometric constants (small standard deviation and error) and the best correlation between experimental data and predicted data in future experiments. This is known as a glass box model.

The ABMP procedure is novel and lacks peer reviewed literature towards the methodology required to ensure the production of repeatable and reliable data. To make up for this gap, the literature and procedure for the BMP test was researched. The recommended procedure is

presented in the following section and will be implemented during the experimental phase of this research.

2.2.4.2 Biomethane Potential Test

To carry out a successful BMP and ABMP test, several requirements need to be met:

- The BMP test is run in triplicates to ensure reproducibility of results and statistical significance. Three serum bottles are used for seed-blank BMPs and another three for seed-sludge BMPs with each set of three having identical environmental conditions. Because BMP tests aims at determining the biodegradability of the sludge by measuring the methane produced by the interaction of the AD bacteria and the sludge (seed-sludge BMPs), seed-blanks are required to subtract COD loss due to seed-seed interaction and allow a COD balance to be achieved (Angelidaki *et al.*, 2009, Raposo *et al.*, 2011). The ABMPs will also be run in triplicates. However, contrary to the BMP test, in the case of an ABMP the feed will be used to subtract the kinetics of seed-seed interactions and focus on the seed-feed interaction (Angelidaki *et al.*, 2009, Gaszynski *et al.*, 2019, Owen *et al.*, 1978, Raposo *et al.*, 2011).
- The characteristics of the sludge and the biomass must be known. The biodegradability of sludge being linked to the sludge characteristics, it is essential to know exactly what the sludge characteristics are. The typical tests required are the total suspended solids (TSS), volatile suspended solids (VSS), COD, TP, OP, TKN and FSA concentration (Angelidaki *et al.*, 2009, Raposo *et al.*, 2011).
- A biogas capture method must be selected. During the experiment, biogas is produced from seed-feed and seed-seed interaction. The method selected to capture the gas produced is vital as it must suit the research's objectives required accuracy. Liquid displacement methods are typically used to measure methane gas production as it is insoluble. This gas capture method, however, is inadequate as the carbon-dioxide gas produced is loss to the atmosphere (dissolved in water and escapes as the gas collection is typically an open bath) as it prevents determination of the amount and the nature of trace gasses generated.

Figure 2.12: Typical ABMP set-up with gas displacement columns

- The load applied to the batch must be known. Since the COD in the system must be conserved and the amount of methane generated is monitored, determining the COD load applied will allow the set-up of a COD balance which should be closed within a reasonable range (Raposo *et al.*, 2011).
- The seed used during the BMP test must be active. If the seed is inactive, no reaction will take place and no methane will be produced. This must be coupled with a test to determine the presence of inhibitors or toxic material within the sludge that could result slow down or prevent completion of the test (Raposo *et al.*, 2011). The seed must also contain a wide range of microorganisms to ensure none of the organisms face any substrate limitation during the test (Angelidaki *et al.*, 2009).

- The acclimation of the seed to the sludge must be ensured. If the seed is not adapted to the food source, only a limited amount of biogas will be produced. This will lead to the souring of the batch test as the acidogens and acetogens which adapt faster than methanogens will produce acetate that will be converted to acetic acid. Adequate acclimation will ensure maximum biogas production and a good representation of processes in the AD.
- Stirring is required to ensure adequate interaction between the seed and the sludge and promotes biogas release into the headspace. However, excessive stirring may damage the floc structure and prevent digestion from taking place.
- The serum bottle needs to be purged with a standard gas to remove any oxygen present within the sludge, seed and headspace to create the adequate anaerobic conditions for the experiment. Although literature does not recommend any specific gas for the purging, the most commonly used is a mixture of (20-30%) carbon-dioxide and (80-70%) nitrogen (Angelidaki *et al.*, 2009, Raposo *et al.*, 2011).
- Tests are carried out every second day after the tenth day and it is recommended that the BMP test last 30 days (Raposo *et al.*, 2011).

The requirements presented above be met during the experimentation phase of this research and any departure from the method above will be justified.

2.3 Phosphorus Accumulating Organism Stoichiometry and modelling

The stoichiometry generated by Harding (2009) and Ikumi and Ekama (2019) is presented in this section of the literature. It aims at describing the intracellular processes and anaerobic digestion of PAOs in an anaerobic digester. It will be analysed through comparison with Yagci *et al.* (2003), Smolders *et al.* (1994) and Smolders *et al.* (1995) which describe the behaviour of PAOs in anaerobic conditions. Since the aerobic stage products (polyP and glycogen) influence the characteristics of the WAS in the AD, the aerobic zone PAO metabolism will also be used as a point of reference as it contributes useful information towards the pathways available to PAOs in the AD. The multiple comparisons will help build confidence that the stoichiometry being analysed in this report is based in existing knowledge.

In Section 2.3.1, acetate uptake and PHB production in anaerobic conditions will be analysed. The stoichiometry by Ikumi and Ekama (2019) will allow PAOs multiple stoichiometric pathways with the use of glycogen, polyP and acetate as an energy source for the generation of reducing agents. Several comparisons will then take place:

- The first comparison will take place between Ikumi and Ekama's (2019) stoichiometry and Smolders *et al.*'s (1994). Smolders *et al.* (1994) developed aerobic stoichiometry for the formation of poly P and assuming the reverse reaction to polyP formation, polyP hydrolysis, requires the same amount of energy, the concept of energy transfer will be confirmed
- The use of glycogen as a reducing agent will be analysed through the comparison of Ikumi and Ekama's (2019) stoichiometry with Yagci *et al.*'s (2003). The concept of glycogen being produced anaerobically, which is supported by Yagci *et al.* (2003), will be discussed as an alternative to Ikumi and Ekama's (2019) stoichiometry.

In Section 2.3.2, the anaerobic digestion of PAOs in P-rich sludge will be analysed. Since no other stoichiometry regarding the breakdown of PAOs is available, this section will highlight the similarities between Ikumi and Ekama's (2019) stoichiometry and Sötemann *et al.*'s (2005).

Finally, the requirements for a complete PAO AD model will be discussed.

2.3.1 Acetate uptake in anaerobic conditions

2.3.1.1 Acetate uptake

The first step in PHB formation is the uptake of acetate anaerobically by PAOs. Ikumi and Ekama (2019), Smolders *et al.* (1993), Smolders *et al.* (1994) and Yagci *et al.* (2003) all agree that energy from polyP is used to take up the extracellular acetate. Once intracellular, energy from polyP is again used to activate it to acetylCoA according to the "Comeau-Wentzel" model.

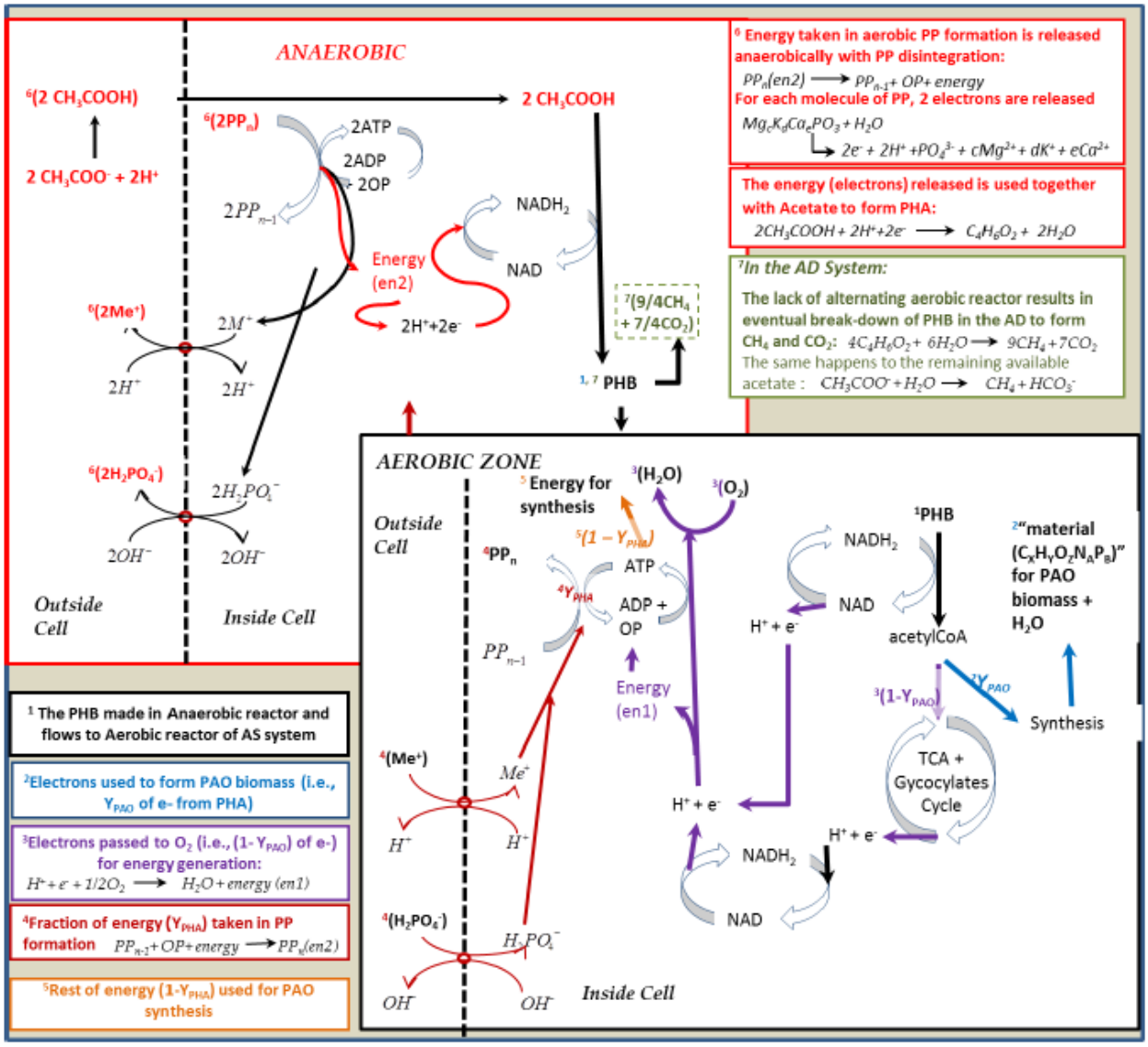

Figure 2.13: Schematic representation of processes taking place in an anaerobic-aerobic reactor sequence (Ikumi & Ekama, 2019)

$$HPO_3 + H_2O \rightarrow \alpha_2 ATP + H_3PO_4$$

α_2: is the amount of ATP per electron pair = 1

Equation 2.14: ATP per mole of polyP (Smolders *et al.*, 1993)

$$(PolyP)_n + ADP \rightarrow (PolyP)_{n-1} + ATP$$

Equation 2.15: PolyP used as an energy source (Ikumi & Ekama, 2019, Rittmann & McCarty, 2001)

$$(PolyP)_n + H_2O \rightarrow (PolyP)_{n-1} + H_3PO_4$$
$$Mg_cK_dCa_ePO_3 + H_2O \rightarrow cMg^{2+} + dK^+ + eCa^{2+} + H_2PO_4{}^-$$

Equation 2.16: Overall polyP breakdown stoichiometry (Ikumi & Ekama, 2019)

$$Acetate + energy \rightarrow Acetyl - CoA$$

Equation 2.17: Activation of Acetate to AcetylCoA (Ikumi & Ekama, 2019)

$$Acetate + \left(\frac{1}{2} + \alpha\right) ATP \rightarrow Acetyl - CoA$$

Equation 2.18: Activation of Acetate to AcetylCoA (Smolders *et al.*, 1993, Smolders *et al.*, 1994)

The use of polyP as an energy source is shown in Equation 2.14 and Equation 2.15. Since the hydrolysis of one mole polyP can be seen to energise one mole of ADP to ATP, it follows that one mole of polyP contains 2 useful moles of $(H^+ + e^-)$ (an unknown portion is lost due the inefficiency of bioprocesses). This causes a release of P into the aqueous phase as per Equation 2.16. Using the energy available from Equation 2.15, acetate is taken up and activated to acetyl CoA as shown in Equation 2.17. Although Ikumi and Ekama (2019) do mention the use of polyP to uptake acetate and reduce it to acetyl-CoA, detailed equation towards this process is provided. The equation provided by Smolders *et al.* (1993) and Smolders *et al.* (1994) is presented to provide more details towards P releases into the aqueous phase. Similar stoichiometry is presented by Yagci *et al.* (2003) for acetate uptake to acetyl-CoA but said stoichiometry yields a much larger P release than Smolders *et al.*'s (1993). The use of this α term in Smolders *et al.* (1993) is very useful stoichiometrically because it allows the energy for acetate uptake to be

modified depending on pH as per Smolders *et al.* (1993) allowing for the variations in P/HAc ratio present in literature.

$$Acetate + (1 + 2\alpha)ATP \rightarrow Acetyl - CoA$$

Equation 2.19: Activation of Acetate to Acetyl-CoA (Yagci *et al.*, 2003)

Yagci *et al.*'s (2003) stoichiometry for acetate uptake and its reduction to acetylCoA is presented in Equation 2.19. At a pH of seven, an $\alpha = 0.25$ is used (this is equivalent to Smolders *et al.* (1993) $\alpha = 0.5$) yielding a 0.5mol of ATP/mol of acetate taken up as assumed by Comeau *et al.* (1987) to do work against the bacteria's electric potential difference ($\Delta\Psi$) across the cell membrane. However, compared to Smolders *et al.* (1993), Yagci *et al.* (2003) uses one mole of ATP versus 0.5mol of ATP by Smolders *et al.* (1993) for the conversion of one mole acetate to one mole acetylCoA releasing twice the amount of P in the aqueous phase for the same ATP available per polyP. This seems to contradict AS system observations and might be a source of error.

2.3.1.2 $NADH_2$ formation using Polyphosphate as an Energy Source

1. $ATP + H_2O \rightarrow ADP + H_3PO_4(H^+ + H_2PO_4{}^-)$
2. $NAD^+ + 2(H^+ + e^-) \rightarrow NADH - H^+ \qquad \Delta G^{0\prime} = 62kJ$

Equation 2.20: PolyP used as an energy source intracellularly in anaerobic conditions

Once manufactured intracellularly, acetyl-CoA needs to be reduced to form PHB. One option is that the reducing agent is produced through the TCA cycle as per Equation 2.20. The source of the energy used in this process has not been confirmed and as such, alternatives to the use of polyP in the formation of $NADH_2$ will be provided the following equations.

2.3.1.3 PHB synthesis using polyP as an energy source

$$Y_{PP}Mg_cK_dCa_ePO_3 + 2CH_3COO^- + (2 - 2Y_{PP})H^+ + 2(H^+ + e^-) \rightarrow C_4H_6O_2 + (2 - Y_{PP})H_2O + Y_{PP}PO_4{}^{3-} + Y_{PP}cMg^{2+} + Y_{PP}dK^+ + Y_{PP}eCa^{2+}$$

Y_{PP} in the equation is the number of moles of P released per mole of PHB formed.

Equation 2.21: Stoichiometry of polyP release in anaerobic conditions (Ikumi & Ekama, 2019)

Equation 2.21 presents the overall stoichiometry of acetate uptake using polyP and glycogen as an energy source. In Equation 2.21, the H^+ present in the term $(2 - 2Y_{PP})H^+$represents the protons available from glycogen breakdown and the $2(H^+ + e^-)$ are used to represent the reducing agent $NADH_2$ formed (in terms of protons and electrons) using energy from polyP as shown in Figure 2.13. This equation provides more energy to polyP than current models do.

This stoichiometry is viable as experimentation by Brdjanovic *et al.* (1998) showed that for a pure acetate substrate, PAOs were not able to uptake the acetate with glycogen in excess but no polyP stored. This observation aligns with the amount of energy in polyP as suggested in Equation 2.21 (i.e. with one of the components lacking no reaction takes place). The presence of glycogen as a second energy source possibly explains the under-prediction in anaerobic digester pH noted during anaerobic digestion of P-rich WAS modelling (Ikumi & Ekama, 2019). Indeed, because glycogen ($C_6H_{10}O_5$) does not contain any N in its chemical equation, this implies that upon breakdown of the PAO biomass, the glycogen will increase the partial pressure of CO_2 which causes a decrease in pH and under-predictions since no alkalinity is released simultaneously. To achieve correct a pH prediction, a potential combination between the "Mino" model and the "Comeau-Wentzel" model may be the solution.

2.3.1.4 PHB synthesis with Glycogen as an Energy Source

Equation 2.22 presents stoichiometry using glycogen as the source of all reducing agents in PHB synthesis. Analysis of this stoichiometry, presented by Ikumi and Ekama (2019), has shown that more glycogen is used in PHB formation than is manufactured in the aerobic stage of the AS. It is therefore suggested that the difference in the amount of energy required for PHB synthesis may originate from the production of glycogen anaerobically. If polyP has more energy than is

currently being reported, some of the energy present within the polyP bond may be used to manufacture glycogen intracellularly which is then broken down for PHB synthesis. This allows for the PAO releases to be adequate while producing the required reducing agents. However, if polyP is used to generate glycogen, the breaking down of the anaerobically generated glycogen without alkalinity release would cause pH to decrease significantly creating a mismatch between theoretical prediction and experimental observation by Harding (2009) and Ikumi and Ekama (2019).

$$Y_{PP}Mg_cK_dCa_ePO_3 + 2CH_3COO^- + Y_{gl}C_4H_7O_{3.5} \rightarrow \left(\frac{7Y_{gl}}{18} - Y_{PP} + \frac{4}{9}\right)H_2O + \left(\frac{4Y_{gl}}{9} + \frac{2}{9}\right){CO_3}^{2-} + \left(\frac{8Y_{gl}}{9} + 2Y_{PP} - \frac{5}{9}\right)H^+ + Y_{PP}{PO_4}^{3-} + Y_{PP}cMg^{2+} + Y_{PP}dK^+ + Y_{PP}eCa^{2+} + \left(\frac{8Y_{gl}}{9} + \frac{4}{9}\right)C_4H_6O_2$$

Where Y_{gl} is the number of moles of glycogen used per mole of PHB formed.

Equation 2.22: Stoichiometry of polyP release with glycogen as an energy source (Ikumi & Ekama, 2019)

An analysis of the stoichiometry of Yagci *et al.* (2003) was performed and it was found that this stoichiometry also allows energy from polyP to anaerobically produce glycogen if PHB is the only product stored by the PAO. Using the model in Figure 2.14, one mole of glycogen and one mole of acetate can be used to generate three moles of PHV using the glyoxylate cycle as shown in Equation 2.23.

$$Glycogen + Acetate + 1.5PolyP \rightarrow 4NADH_2 + 3CO_2 + 1.5ATP + 1.5P + 3PHV$$

Equation 2.23: Glyoxylate cycle glycogen utilization to form PHV

Two additional moles of acetate are taken up to form PHB:

$$2Acetate + 2ATP + 3PolyP + NADH_2 \rightarrow 3PHB + 3P$$

Equation 2.24: Glyoxylate cycle acetate utilization to form PHB

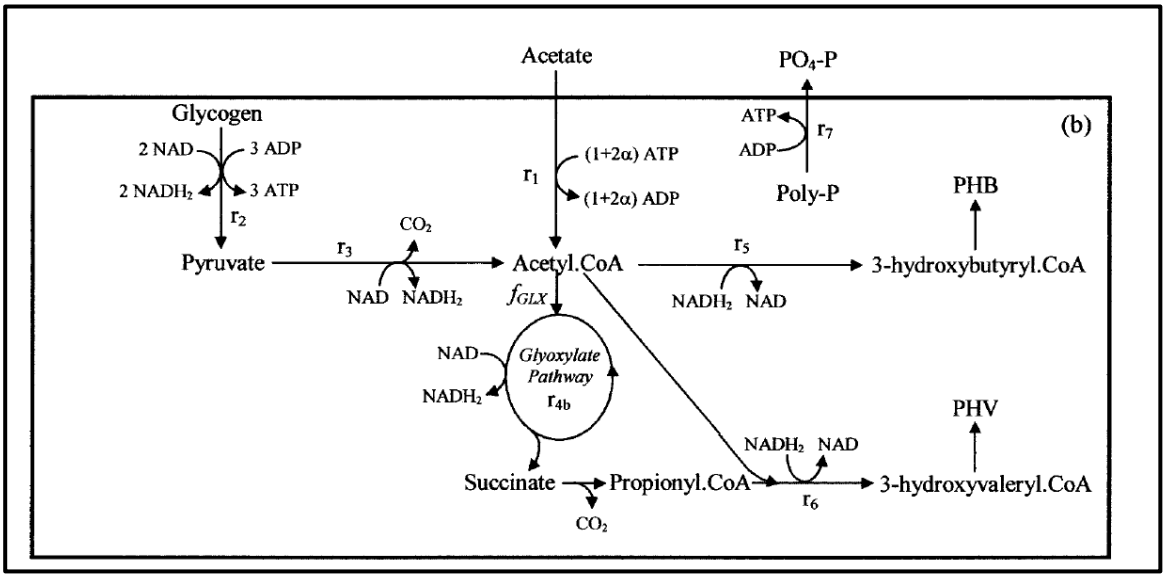

Figure 2.14: PAO stoichiometry (Yagci *et al.*, 2003)

The sum of these Equation 2.23 and 2.24 yields Equation 2.25:

$$Glycogen + 3Acetate\ + 4.5polyP \rightarrow 5.5ATP + 3CO_2 + 4.5P + 3PHB + 3PHV$$

Equation 2.25: Overall Glyoxylate pathway

$$Glycogen + 3Acetate \rightarrow \beta ATP + 3CO_2 + 3PHB + 3PHV$$

Equation 2.26: Overall Glyoxylate pathway

As shown by the ATP present on the right hand-side of Equation 2.25, Equation 2.25 is not energy balanced. The energy leftover may make up for the difference in glycogen seen in Ikumi and Ekama's (2019) stoichiometry. If the energy is stored in polyP, this energy would not be measured during a COD test (measures energy in organic material) and supports the hypothesis that polyP contains energy. This stoichiometry, although different to Ikumi and Ekama (2019), shows that polyP may be an energy carrier and that glycogen generation anaerobically is possible.

Furthermore, this stoichiometry has several advantages as the use of glycogen as an electron donor allows for carbon-dioxide release which matches well with carbon-dioxide generation from the TCA cycle, a biochemical pathway available to PAOs by virtue of their genus. Secondly, the release of carbon-dioxide can be used to explain changes in pH that are associated by P release from polyP. The data reconciliation regarding CO_2 release, pH, H_2CO_3 alk and H_3PO_4 alk will be a major part of this research as it will allow correct aqueous chemistry prediction.

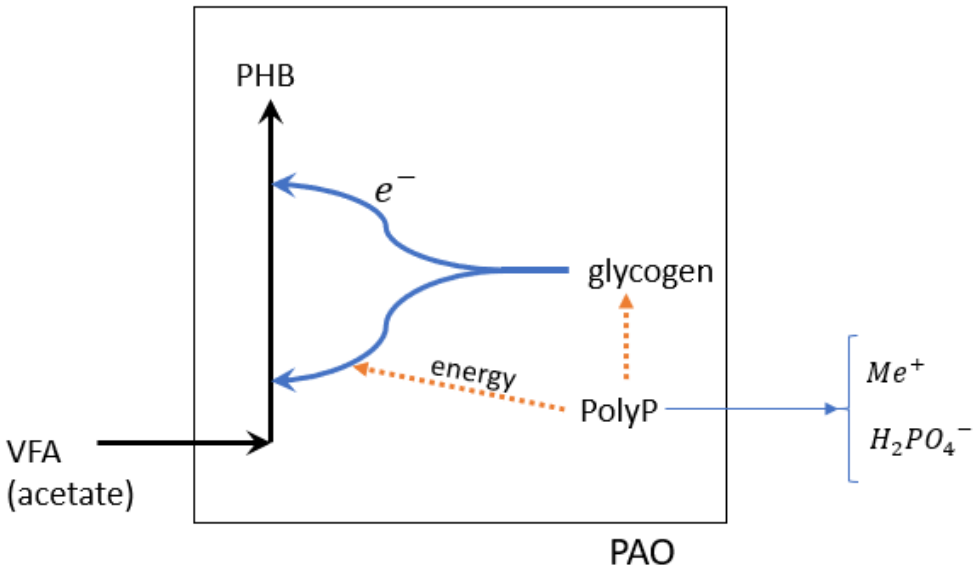

Figure 2.15: Possible use of polyP as an energy contributor

2.3.1.5 Impact of P releases on pH

As shown in Equation 2.27 and Equation 2.28, the manner in which released orthophosphate is speciated in the aqueous phase, during acetate uptake in the anaerobic zone of the AS or in an AD, is dependent on the system pH. Since both the anaerobic zone of the AS and the AD operate at a pH of about 7, the main species of the P group alternate between $H_2PO_4^-$and HPO_4^{2-}. The release of polyP as PO_4^{3-}causes an increase in phosphorus alkalinity and total alkalinity as shown in Equation 2.22. The amount of $H_2PO_4^-$and HPO_4^{2-}ions in the aqueous phase is dependent upon how far the pH of the system is from the 2nd dissociation constant inorganic

$$PO_4^{3-} + \alpha H^+ \rightarrow f_p H_2PO_4^{2-} + (1 - f_p) HPO_4^{2-}$$

Equation 2.27: P releases impact on alkalinity

$$Total\ P_{released} = f_p H_2PO_4^{2-} + (1 - f_p) HPO_4^{2-}$$

Equation 2.28: PolyP digestion in an anaerobic digestion

phosphate system pK_{p2} ~7.21 at 20°C (adjusted to 7.18 according to Debye Hückel law) (Loewenthal *et al.*, 1995). A fraction f_p of $H_2PO_4^-$ is produced and a fraction (1- f_p) HPO_4^{2-} is released where f_p is a pH dependent factor. The f_p fraction can be estimated by knowing the pH, which is predictable from AS and AD stoichiometry for the best calibrated model – i.e., the polyphosphate release model that agrees best with data.

2.3.2 Anaerobic Digestion of PAOs

$$C_4H_6O_2 + 6H_2O \rightarrow 4CO_2 + 18(H^+ + e^-)$$

Equation 2.29: PHB digestion in an anaerobic digester (Ikumi & Ekama, 2019)

$$Mg_cK_dCa_ePO_3 + fH_2O + (1 - f_c)HCO_3^- \rightarrow (1 - f_c)CO_2 + f_pH_2PO_4^- + (1 - f_p)HPO_4^{2-} + cMg^{2+} + dK^+ + eCa^{2+}$$

Equation 2.30: PolyP digestion in an anaerobic digestion (Ikumi & Ekama, 2019)

As mentioned, upon entering the AD, PAOs take up acetate, manufacture PHB and release 80.5% of the polyP as P in the aqueous phase (Wentzel *et al.*, 1988). Due to the long SRT associated with the AD of WAS, PAOs are hydrolysed and used as a substrate by the AD bacteria. The PHB, glycogen and polyP stored intracellularly in the PAOs are also broken down as the PAOs get hydrolysed. The PHB is digested releasing carbon dioxide, protons and electrons as shown in Equation 2.29. The polyP remaining in the PAOs is digested as shown by Equation 2.30. This

final P release increases the system's overall alkalinity due to the additional $H_2PO_4^-$ but causes a decrease in pH. Equation 2.30 is interesting stoichiometrically, as it is similar for a steady state model whether glycogen or polyP is used as a reducing agent with differences only in a dynamic model. Since the stoichiometry of only polyP as a reducing agent and only glycogen as a reducing agent does not seem to agree with experimental results then this shows that the use of polyP and glycogen as a combined source of reducing agent is possible.

2.3.3 Modelling of the Anaerobic digestion of PAOs

As was previously mentioned, PAOs consist of several microorganisms acting in a coordinated manner which, when modelled, are assumed to behave as one organism. This level of organisation is chosen because several processes take place intracellularly (formation of Gibbs free energy to fuel reactions, building block formation from substrate, polymerization of building blocks into macromolecules…) and modelling each one individually is not practically possible (Nielsen & Villadsen, 1994). For this reason, the stoichiometry presented by Ikumi and Ekama (2019) seems relevant as it lumps them together.

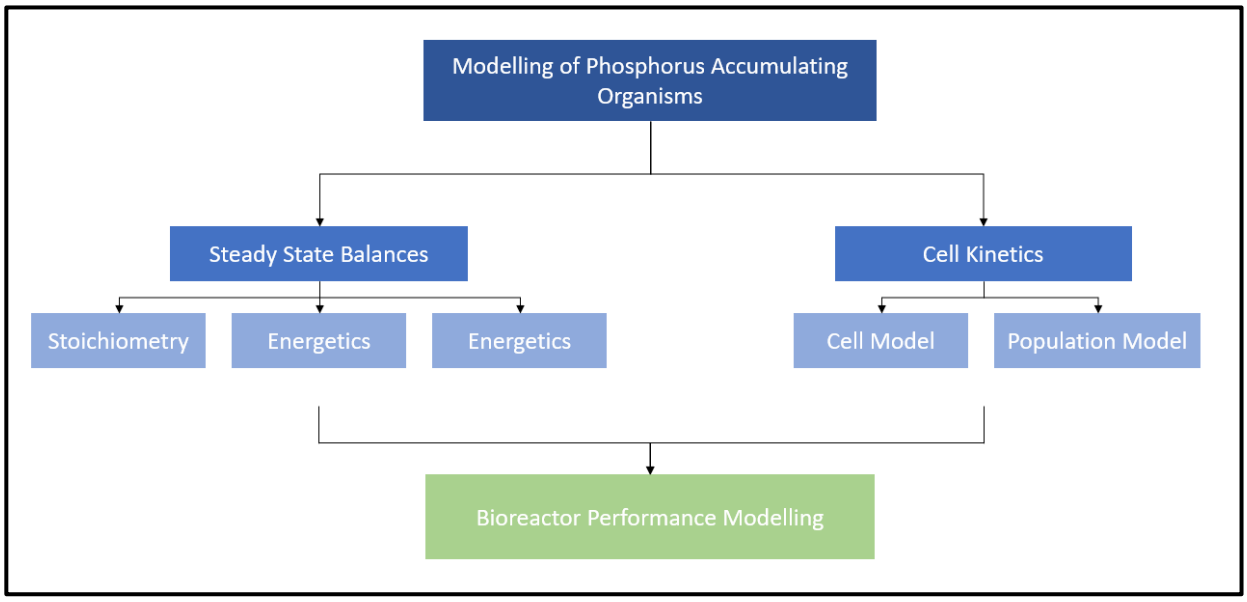

Figure 2.16: Steps in accurate modelling of bioreactor performance (adapted from Nielsen &Villadsen (1994))

From Ikumi and Ekama's (2019) stoichiometry and analysis of Smolders *et al.*'s (1993) kinetics, as a proxy (at this stage) of AD-PAO kinetics, the three major processes that need to be considered during modelling are:

1. The acetate uptake and its transport through the cell membrane;
2. The overall intracellular reactions; and
3. The metabolic products released into the aqueous phase (Nielsen & Villadsen, 1994).

During the AD of an enhanced PAO culture, the biodegradable fraction of the WAS will consist of the active (live) PAO biomass present in the WAS. In current mathematical models (such as PWM-SA), the polyP content of the PAOs is usually not included in the PAO particulate organics characteristics but rather attached to it ($C_XH_YO_ZN_AP_B$. $q_\Phi[MePO_3]$) using a linking factor q_{PAO} (q_Φ is a general term) (Harding, 2009, Ikumi *et al.*, 2014).

The use of a linking term allows the modelling of the polyP as a separate component of the biomass which simplifies the stoichiometric and kinetic bioprocesses in which PAOs are modelled to participate. For example, since the hydrolysis of the BPO portion of PAOs occurs slower than polyP hydrolysis, having separate equations simplifies the model (Harding, 2009). The use of a linking term also allows an analysis of the impact of releases separately, whether organic or inorganic) on pH. By linking this information with the Ekama & Wentzel (2004) ISS model through data reconciliation, a validated PAO AD model will be generated.

The Ekama & Wentzel (2004) ISS model, from the analysis of AS system data, determined that the ISS of the organic part of the PAOs (f_{iPAOBM}) is the same as the ISS of the organic part of OHOs (f_{iOHO}) at 0.15 mgISS/mgVSS. However, since polyP is an inorganic compound and is stored within PAOs, it contributed to the measured ISS. The ISS generated from polyP stands from the presence of counter charge ions within the molecule which when subjected to heat break their bonds and precipitate giving rise to addition mass. At a PAO-P concentration of 0.38mgP/mgPAO-VSS, the PAO ISS content totals at 1.3mgISS/mgPAO-VSS or approximately 10 times that of the OHO biomass (Wentzel & Ekama, 2004).

3. Anaerobic digestion model for NDEBPR sludge

As shown in the literature review, the enhanced biological phosphorus removal (EBPR) process is a widely implemented process. Despite its overwhelming acceptance, several questions are left pending regarding the metabolic behaviour of the microorganisms mediating P removal. Uncertainties linked to these questions prevent the formulation of an accepted theory regarding the behaviour of phosphorus accumulating organisms (PAO) and their impact on anaerobic digesters (AD) when treating waste activated sludge (WAS) from nitrification-denitrification enhanced biological phosphorus removal (NDEBPR) systems.

3.1 AD Model Description

3.1.1 Hydrolysis of PAOs in an AD

In the anaerobic zone of the activated sludge (AS) system, PAOs break down polyP and glycogen releasing respectively polyphosphate (polyP) and carbon-dioxide (showing as pCO_2) to take up acetate and manufacture poly-β-hydroxybutyrate (PHB) (Smolders *et al.*, 1995). Since there is acetate produced during intermediate AD processes, it follows that PAOs should be able to manufacture PHB in the AD. How these processes impact the death and hydrolysis of PAOs in AD systems is still unknown, and two hypotheses are presented towards improving our understanding of the hydrolysis process:

i) Hypothesis One:

The first hypothesis suggests that the PAO BPO hydrolysis is initially simultaneous with the anaerobic PHB uptake bioprocesses and PHB hydrolysis taking place with the death of PAO biomass. The bioprocess-hydrolysis process is thought to take less than 10 (ten) days since Harding (2009) reported that initial polyP release in AD (which is taken to occur with PHB uptake; Ikumi (2011)) stopped after 8-10days and Brdjanovic *et al.* (1996) reported that no bioprocesses were seen by PAOs in the absence of polyP. After those first 10 (ten) days, the hydrolysis process continues and PAOs and the intracellular PHB formed are hydrolysed. This

hypothesis is in line with current assumptions since hydrolysis takes place from the entrance of PAOs into the AD till their exit. This is shown by the black line in Figure 3.1.

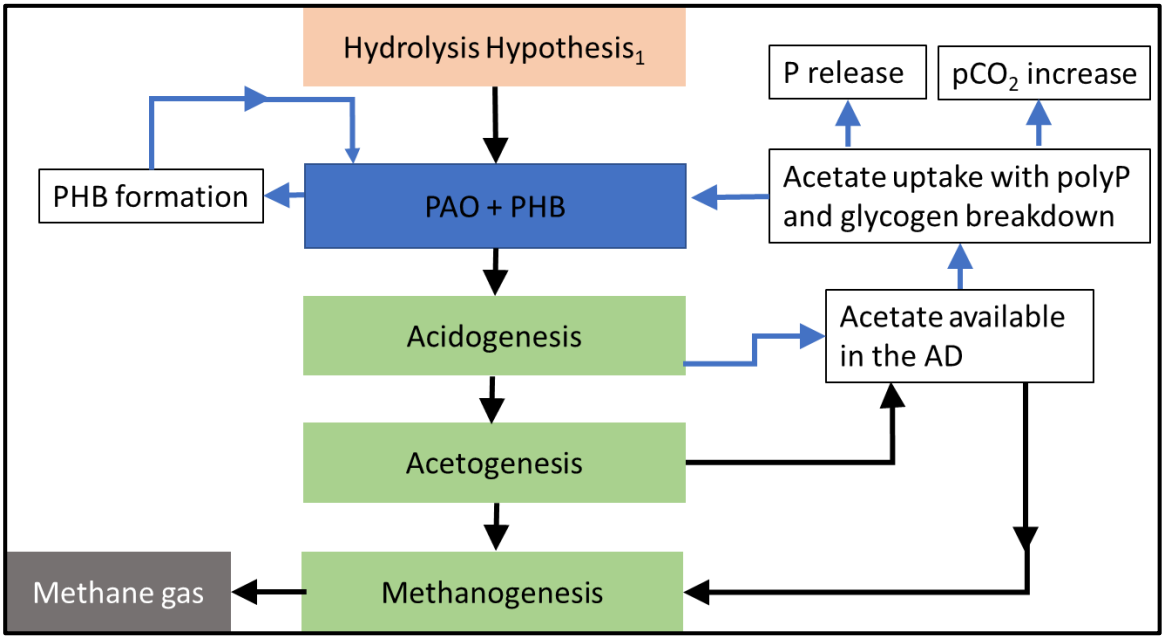

Figure 3.1: Hydrolysis Hypothesis 1

As shown by the green arrow in Figure 3.3, at short SRTs (where the SRT <10d) or under dynamic conditions, PAOs take up acetate present in the AD to manufacture PHB reducing the pool of acetate that goes to methanogens and hence the amount of methane generated. Hence, a hydrolysis process modelled inadequately causes an error in the effluent residual COD prediction and methane gas production.

At a long SRT (larger than 10d), despite the initial PAO bioprocesses (i.e., polyP release and accompanying PHB formation), all the acetate taken up by PAOs ultimately returns to the acetate pool when PAOs and PHB are fully hydrolysed. This allows for both an accurate methane prediction and effluent COD prediction.

ii) Hypothesis Two:

The second hypothesis assumes that upon entry into the AD, PAOs are not impacted by hydrolysis due to their ability to undertake bioprocesses.

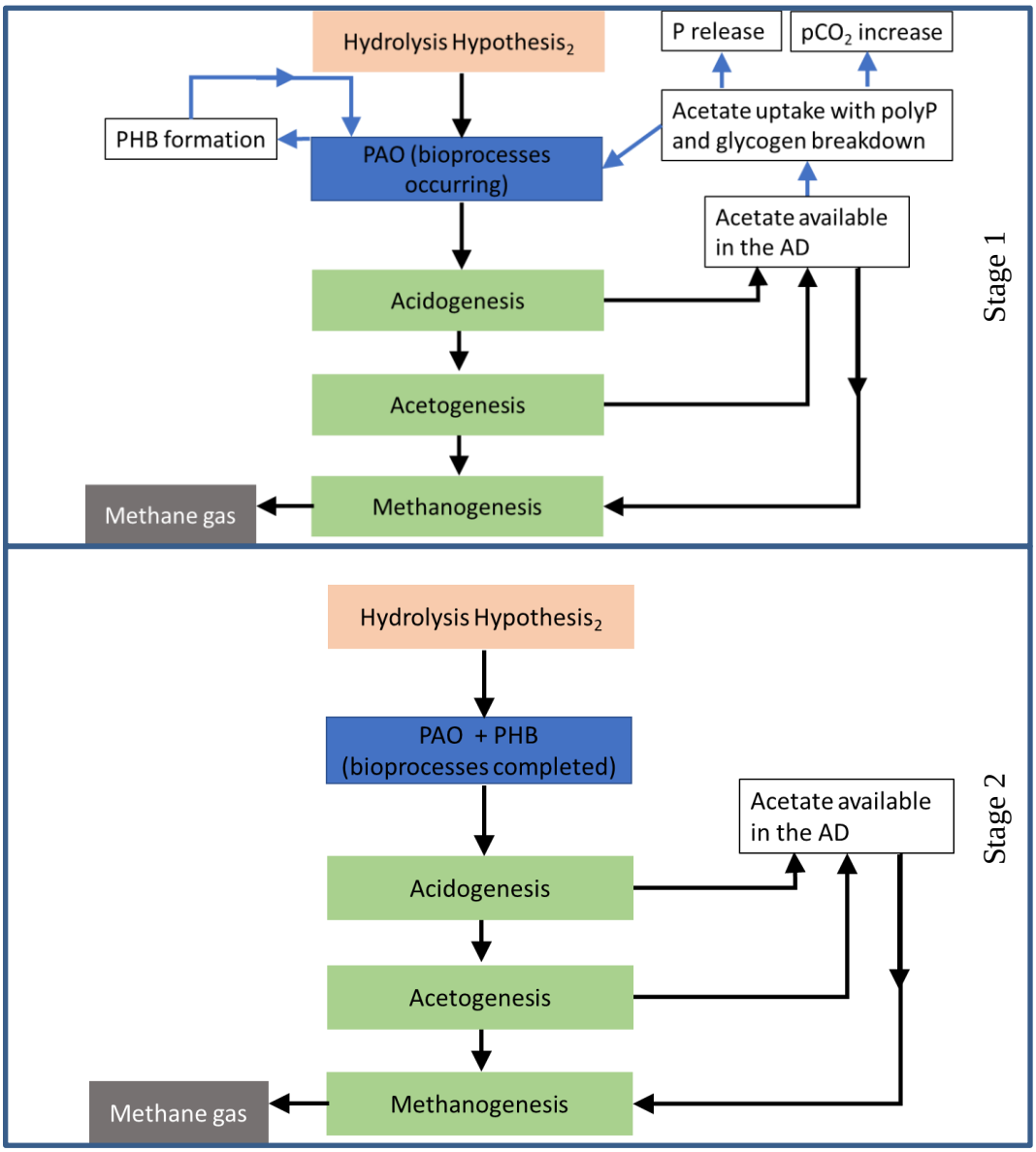

Figure 3.2: Hydrolysis Hypothesis 2

Upon entry into the AD, PAOs are exposed to hydrolysis. However, due to the maintenance energy described by Smolders *et al.* (1995), the hydrolysis process is either slowed down or prevented. Once the polyP stored intracellularly is used up, in accordance with Brdjanovic

(1996), acetate uptake stops and the hydrolysis process continues unencumbered breaking down the PAOs and PHB formed in parallel. This is presented as Figure 3.2 as Stage 1.

Based on this hypothesis, the hydrolysis process is very slow since Smolders *et al.* (1995) only assigns 2.5 x 10^{-3} P-mol/C-mol.h of maintenance energy to PAOs. Assuming 1 ATP/P-mol (Smolders *et al.*, 1995), this results in 2.5 x 10^{-3} mol ATP/C-mol.h.

Another possible conclusion, however, suggest the hydrolysis rate is high but so is the amount of energy in the polyP bond resulting in an effectively low perceived breakdown of PAO biomass. This hypothesis would confirm the claim by Ikumi and Ekama (2019) that energy transfer does take place between the AS system and the AD but split the energy in the polyP bond towards acetate uptake and PHB formation as per Smolders *et al.* (1995).

Once P release and the corresponding acetate uptake stops, the PAO and PHB formed are anaerobically digested. This is presented in Figure 3.2 as Stage 2.

3.1.2 Multimineral Precipitation

Harding (2009) describes the metal ions and phosphate releases associated with PAO processes in a SS AD. These releases are likely to give rise to mineral precipitation. To model multi-mineral precipitation in an AD at SS, the methodology described by Loewenthal *et al.* (1995) for struvite precipitation will need to be applied to each mineral. This multi-mineral precipitation in the AD

Table 3.1: Multimineral Precipitation: Precipitates and Limiting reagent (Ikumi, 2011, Musvoto *et al.*, 2000)

Chemical name	Chemical composition	Limiting reagent
Amorphous Calcium Phosphate (ACP)	$Ca_3(PO_4)_2$	Calcium (Ca)
Struvite	$MgNH_4PO_4$	Magnesium (Mg)
Magnesite	$MgCO_3$	Magnesium (Mg)
Calcite	$CaCO_3$	Calcium (Ca)
Newberyite	$MgHPO_4$	Magnesium (Mg)

is vital in assessing the impact of the energy transfer on a steady state AD as accounting for as many variables as possible in the model will increase confidence in the results generated. The minerals that will be considered in this multimineral precipitation process are presented in Table 3.1.

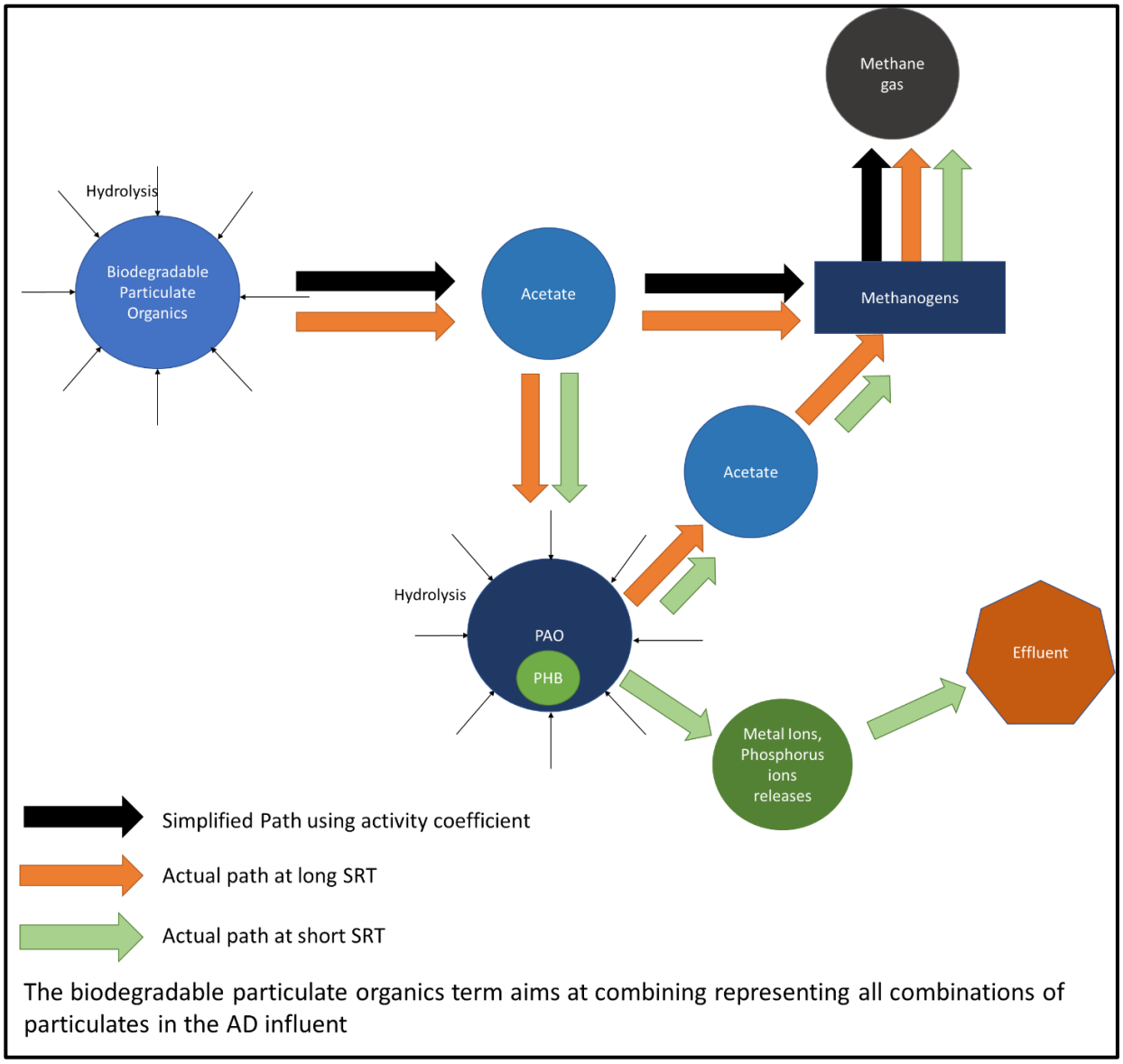

Figure 3.3: Available AD pathways due to PAO presence in the AD

3.2 The Impact of Energy transfer

Since WAS is typically removed from the aerobic tank of the AS system, the live PAO biomass have used up the PHB stored for growth, replenished on glycogen and stored the P available from the aqueous phase intracellularly as polyP (see Section 2.1.2.2 for details). When subjected to the anaerobic conditions in the AD, the biomass behaves as per its normal characteristics unable to differentiate between the anaerobic conditions of the anaerobic tank of the AS system and that of the anaerobic digester. Having a metabolizable food source available; acetate from acidogens and acetogens bioprocesses, PAOs use their intracellularly stored glycogen and polyP to uptake the acetate releasing P in the AD aqueous phase. Since energy is assumed to be used in the anaerobic phase of the AS system for uptake of acetate, it follows that energy is present within the PAO's polyP bond to take up COD in the AD (Smolders *et al.*, 1994). This energy is not accounted for in current models and its impact on the AD pH is unknown.

This energy transfer, however, does not put into question the COD balance as it is currently being performed but rather the understanding linked to the COD balance. Indeed, there seems to be a common misunderstanding behind the COD balance. The COD balance is often thought of as being analogous to an energy balance which is not the case. The COD balance measures electrons, a form through which energy can be measured but not the only form energy takes. For example, energy is loss within biological processes due to the inefficiencies of the bacteria mediating the bioprocesses is not modelled since this energy does not take the form of electrons.

In the AS system, energy from PHB breakdown is assumed to be used solely for catabolism and biomass growth (Henze *et al.*, 2008, Smolders *et al.*, 1994, Wentzel *et al.*, 1988). The hypothesis presented in Figure 3.4 and 3.5 suggests that some of the energy assumed to be used during the catabolism process could be stored within the inorganic polyP bond. This assumption, although not yet proven to be valid, is credible since although the amount of energy generated from catabolism can be measured from oxygen usage, how this oxygen is used is based upon biological assumptions of intracellular behaviour. Figure 3.5 provides a schematic diagram explaining the proposed energy utilization by PAOs. If this is the case, to predict reasonable outputs, the stoichiometry regarding AD polyP release will need to be adjusted to ensure the right reducing agents are utilized which will result in correct AD output (including pH) prediction. This would then confirm the energy transfer from the AS system to the AD through PAOs. This hypothesis

as shown in Figure 3.5 does not impact the yield (Y_H) value (i.e., the amount of energy used for new cell mass formation) but rather decreases the energy used for catabolism by dividing the energy used for catabolism between energy stored in PAOs through the polyP bond (Y_{PAO}) and the catabolic energy (1- Y_H - Y_{PAO}). The yield can then be separated into two portions: the PAO biomass itself (Y_{PAO}) and the glycogen yield (Y_{GLY}) both of which show up as VSS and COD when testing PAOs (i.e. $Y_{PAO} + Y_{GLY} = Y_{HV} = 0.66$).

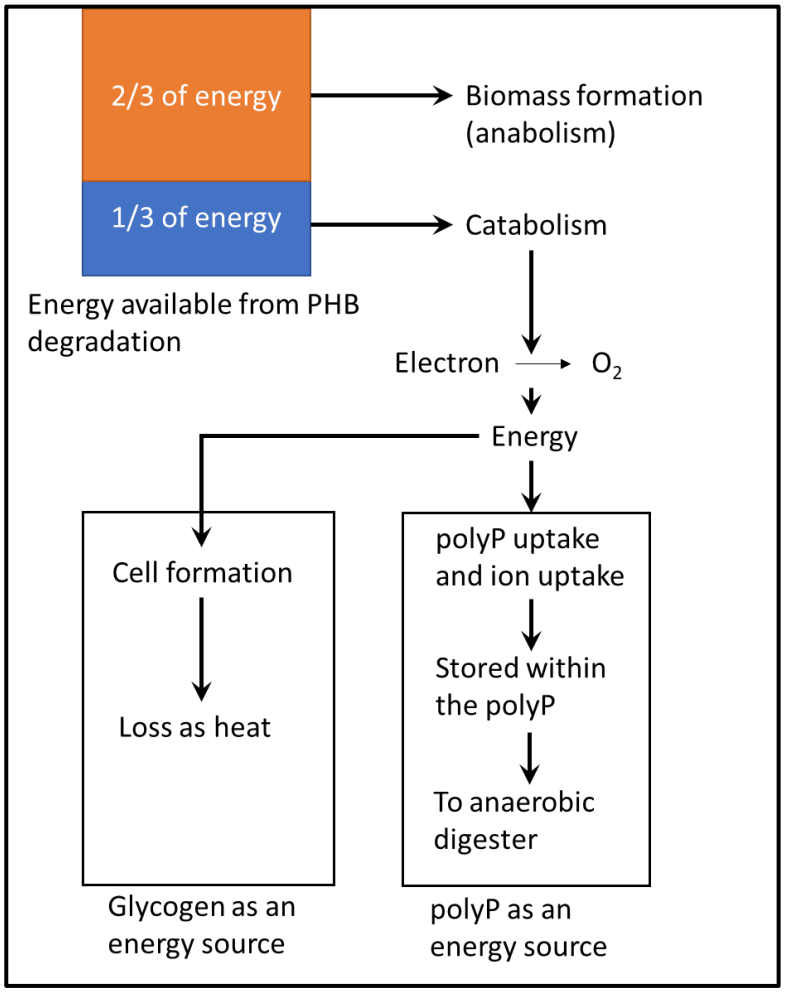

Figure 3.4: Proposed hypothesis

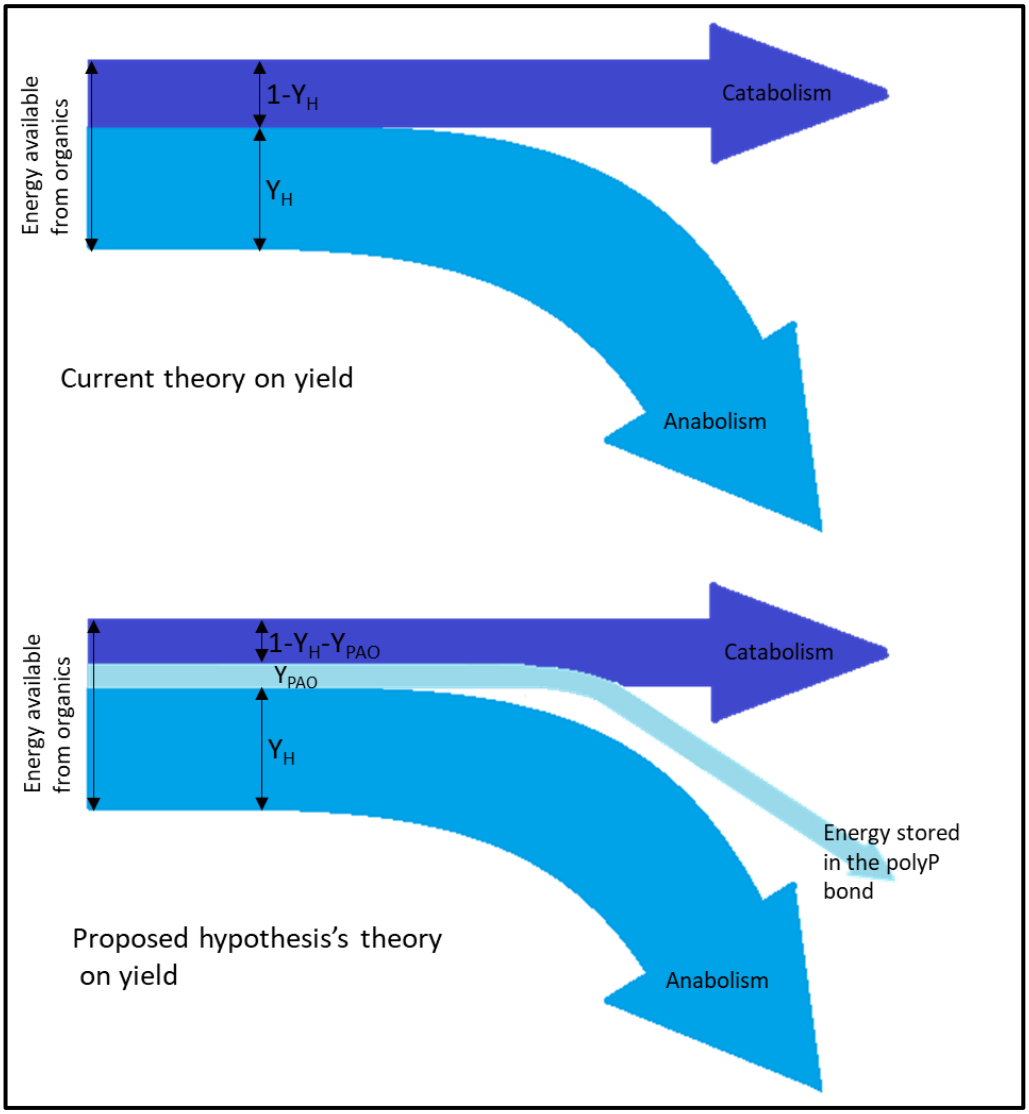

Figure 3.5: Proposed Hypothesis impact on Yield

4. Methodology

The objective of this section is to present the experimental set-up, testing methodology and tests performed during the experimental phase of this research. To generate the data required, three systems were set-up:

- System 1 consisted of a nitrifying-denitrifying enhanced biological phosphorus removal (NDEBPR) Modified University of Cape Town (UCT) membrane system used to grow an enhanced phosphorus accumulating organism (PAO) culture. The enhanced PAO culture, also referred to as the parent system, was constructed as detailed in Section 2.1.3 to allow a greater focus on PAO behaviour in the anaerobic digester (AD) when the waste activated sludge (WAS) from the enhanced culture was anaerobically digested.
- System 2 consisted of two anaerobic digesters. These digesters were run to generate data regarding the anaerobic digestion of PAOs. The data generated from these ADs were used to understand the behaviour of PAOs in AD system, including the verification of potential links between the catabolic PAO activity in aerobic reactors of activated sludge (AS) systems (including polyphosphate (polyP) uptake) and the metabolic PAO activity in AD systems (which includes the potential polyP release for PHB formation).The ADs were run at different sludge retention times (SRTs) to ensure this research's findings were not sludge age specific. The information generated was also used to understand the hydrolysis kinetics and the impact of multiple mineral precipitation on a steady state (SS) AD's pH prediction.
- System 3 consisted of augmented bio-methane potential (ABMP) test reactors. The ABMPs were performed using WAS from the enhanced PAO culture and seed from the AD. The ABMPs were used to allow a focus on the dynamics of the interaction between the AD biomass and PAOs. The data produced was also used to assess the combined behaviour of PAOs and AD biomass in the AD, the death rate of PAOs in the presence of AD biomass and the unbiodegradable fraction (f_{EG}) generated from PAO death. From the information generated, a PAO intracellular model that reconciles PHB production, partial pressure of carbon dioxide (pCO_2) and pH can be created.

All three systems were interconnected as part of the experimental campaign. An overview of the experimental set up is shown in Figure 4.1.

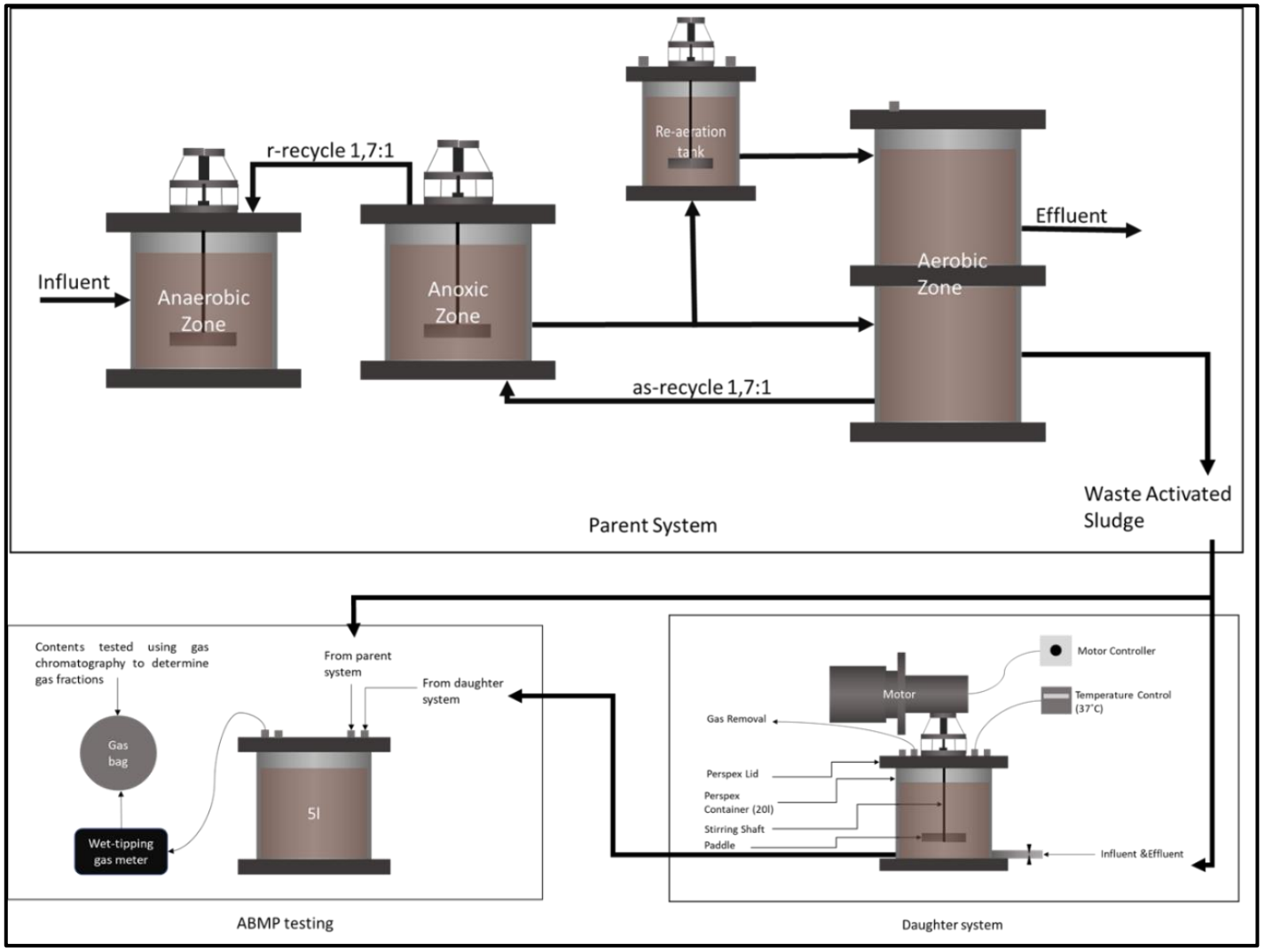

Figure 4.1: Overview of Experimental Set-Up

This section of the report is presented in four main sections. The first three will detail each of the main systems focussing the operational details of each component of the set-up. They will create a link between the literature presented in Chapter 2 and the experimental phase showing that the data generated was based on existing peer reviewed information. Section 4.4 will present the tests carried out to generate the information analysed in this research. The procedure followed for each test is presented in the APHA (1975) standard methods for the examination of water and wastewater.

4.1 Enhanced PAO culture

The system used to grow the enhanced PAO culture was a sixty-three and a half litre (63.5l) EBPR UCT membrane system. The system had a 27l anaerobic zone, a 4.5l anoxic zone, 29*l* aerobic zone and 3*l* reaeration tank. The set-up is presented in Figure 4.2.

The enhanced PAO culture was achieved by gradually shifting from a settled wastewater (WW_ feed to a synthetic feed. This shift gradually eliminated bacterial groups other than PAOs present in the system (Wentzel *et al.*, 1988). This shift also promoted the activity of PAOs by ensuring they were given an advantage over other microorganisms. Both the set-up and the operation of the parent system were based on Wentzel *et al.*'s (1988) enhanced PAO culture except for the secondary settling tank which was replaced by a membrane system. The inoculum used to grow the enhanced culture was obtained from Bellville Wastewater Treatment Works' (WWTW) UCT system. The settled WW fed to the culture was sourced from Mitchel's Plain WWTWs.

As the feed to the parent system was being gradually switched from a settled feed to a synthetic feed, great care was taken in minimizing the growth of glycogen accumulating organisms (GAOs) and ensuring PAO dominance over them (see Section 2.1.4 which presents the procedure required to ensure PAO dominance). A solids retention time (SRT) of 10days was selected as it provided enough time for PAOs to metabolise the influent, ensuring GAO presence was minimal in the system (Oehmen *et al.*, 2007) and achieving a reasonably high active fraction of PAOs in the WAS. To further favour PAOs, it was decided that the system would be carbon (limited by the influent chemical oxygen demand(COD)) limited and not P-limited (GAOs have been seen to be present especially in P-limiting EBPR systems) (Yagci *et al.*, 2003).

The influent to the AS system are presented in Table 4.1.

An enhanced PAO culture was only briefly achieved. Settling issues gave rise to the loss of a significant portion of the biomass by causing the aerobic tank containing the membrane to overflow. Most of the lost mass was recuperated but the system was unable to fully recover and the enhanced PAO culture remained unstable. This caused the AD to also remain unstable and prevented it from reaching steady state. The enhanced PAO culture WAS was, however, used during Maake & Ikumi's (2020) ABMP tests. The data from those tests will be used during this research.

Table 4.1: AS system influent properties

Characteristic	Value
Influent feed	60l/d
SRT	10 days
Influent COD	1000 mg/l
Influent settled WW	150 mg/l
Influent synthetic WW	850 mg/l
Influent orthophosphate (OP) concentration from dipotassium hydrogen orthophosphate (K_2HPO_4)	80 mg/l
Magnesium from Magnesium Chloride Hexahydrate ($MgCl_2$.6H2O)	50 mg/l
Calcium from Calcium Chloride di-hydrate ($CaCl_2.2H_2O$)	50 mg/l
Yeast	0.57 mg/d
Boron from boric acid (H_3BO_3)	43.68 mg/d
Copper from copper sulphate ($CuSO_4$.5H2O)	63.84mg/d
Iodine as potassium iodide (KI)	47.88mg/d
Manganese as manganese chloride ($MnCl_2$.4H2O)	462mg/d
Molybdate as sodium molybdate (Na_2MoO_4.2H2O)	49.56mg/d
Zinc as zinc sulphide ($ZnSO_4.7H_2O$)	286 mg/d
Cobalt as cobaltous chloride ($CoCl_2.6H_2O$)	62.16mg/d

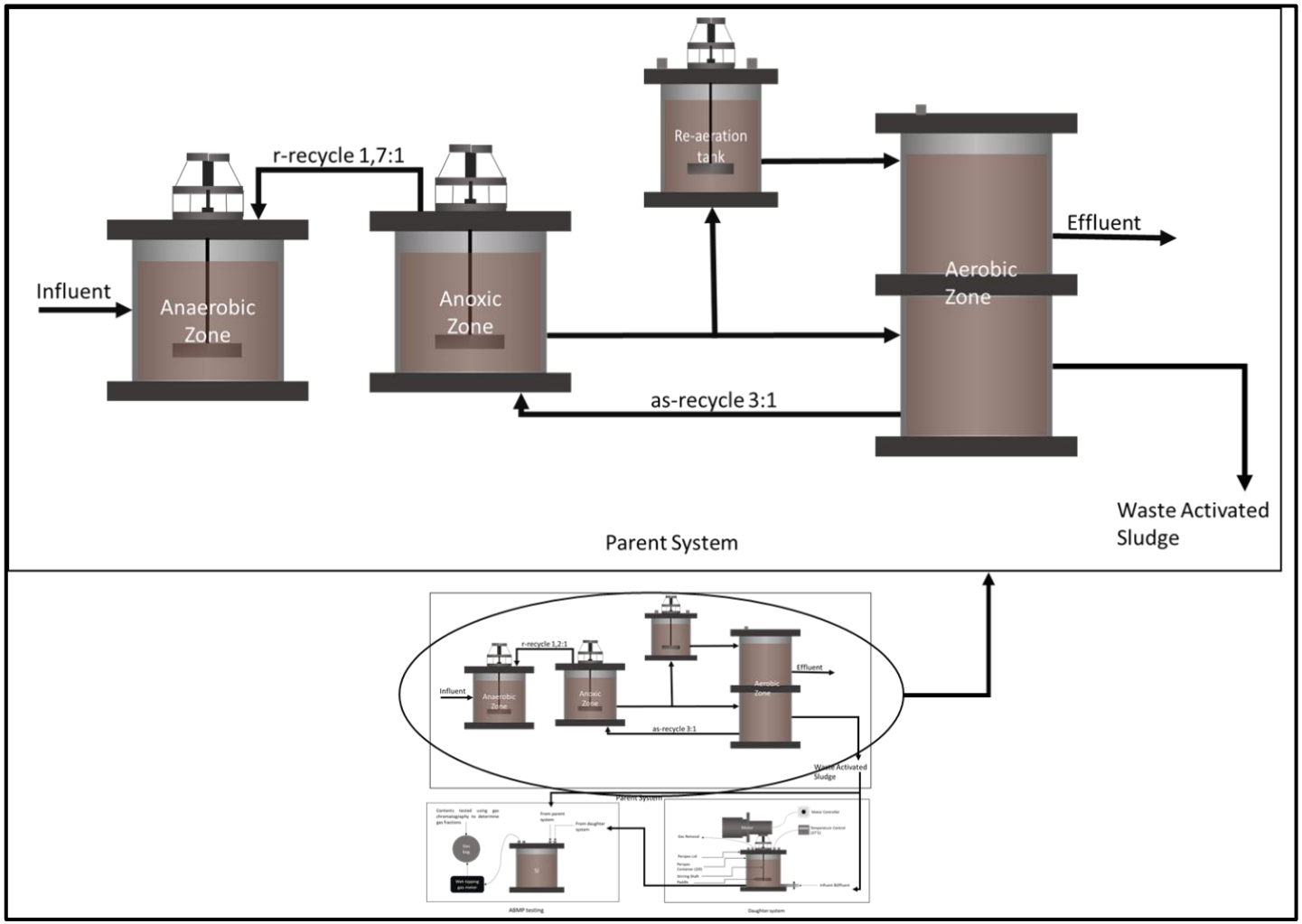

Figure 4.2: Enhanced Phosphorus Accumulating Organism culture

4.2 Anaerobic Digestion

4.2.1 Anaerobic Digestion Experimental Details

Two batch continuously stirred (CSTR) 22*l* mesophilic (36°C) anaerobic digesters were used during the experimental phase of this research. They both operated at 20*l* with a 2*l* headspace. They were respectively running at 15 and 30 days SRT to ensure the findings of this research were not sludge age specific and to increase the confidence in the results generated. The details of the AD set-up are shown in Figure 4.3.

As mentioned, the feed to the AD consisted of WAS from the parent system. This WAS contained mainly PAO biomass (biodegradable) and endogenous residue (unbiodegradable). Since the WAS was wasted from the aerobic tank of the AS system, to limit oxygen transfer to the AD, it was allowed to deoxygenate for 10 mins. The WAS from the parent system was fed to the digester before steady state of the parent system was reached to ensure conversion of the bacteria to an enhanced PAO feed and reduce the time for the AD to reach steady state once the parent system was at steady state. Steady state of the system was confirmed by monitoring the influent and effluent COD, total kjeldahl nitrogen (TKN), free and saline ammonia (FSA), total phosphate (TP) and OP concentrations and ensuring that they stayed constant for at least seven consecutive measurements after three SRTs. The details of sampling and testing procedures are presented in Section 4.4.

4.2.2 Anaerobic Digester Contribution to Objectives

Information from the anaerobic digesters was used towards calibration of the steady state AD model for the anaerobic digestion of EBPR WAS. This process involved the evaluation of the theoretical models against experimental data to answer the research questions: (i) Is there any significant energy transfer from the AS system to the AD with polyP disintegration processes when EBPR WAS is fed to AD systems and (ii) the kinetics of hydrolysis of PAO biomass when fed to the AD system. During the AD of the P-rich WAS (i.e. the disintegration of the PAO biomass and polyP from EBPR AS systems), metallic and phosphorus ions get released in the AD mixed liquor. The extent to which these ions are released, and the weak acid/base conditions of the aqueous phase shall determine the potential for multiple mineral precipitation (i.e., some

ions could bind shifting from the liquid to the solid phase). This also impacts the accuracy of the predicted AD effluent aqueous phase concentrations and the system pH. Hence, the experimental data used towards characterisation of the influent organic and inorganic components is important, to ensure that the biodegradable organics from PAO biomass and polyP (inorganics) to be disintegrated as input to the hypothesized model stoichiometry are correct. The inorganic particulates that are not polyP (i.e., ISS from the influent wastewater that accumulated in the AS reactor and any mineral precipitates) shall be distinguished from polyP. In this experiment the influent to the NDEBPR AS system is largely soluble (i.e., negligible influent WW ISS) but there is uncertainty on whether the mineral precipitation during feeding of WAS and redissolution during the AD process would result in the generation of a reservoir of alkalinity which is not detected by a 5-point titration (Lahav & Loewenthal, 1993).

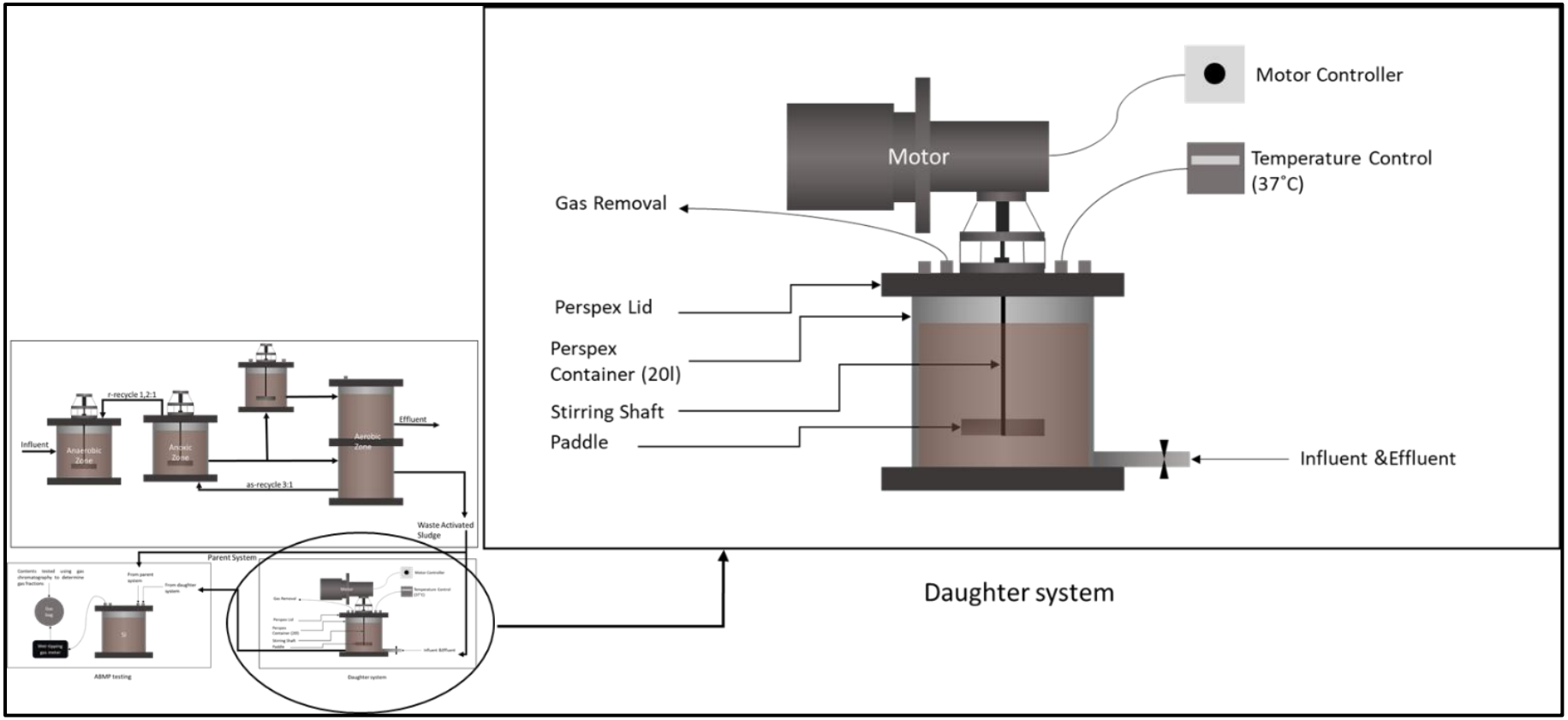

Figure 4.3: Anaerobic digester set-up

4.3 Augmented Biomethane Potential

An augmented biomethane potential test (Botha & Ekama, 2015, Gaszynski *et al.*, 2019) was carried out using feed from the parent AS system (MBR UCT) and seed from the SS AD(s). This test was performed to determine the polyP release kinetics of PAOs in AD conditions, the hydrolysis of PAOs in AD, the PAO favoured stoichiometric pathways in AD and to determine the PAO endogenous residue (ER) fraction and the PAO ER elemental composition.

4.3.1 ABMP Experimental Details

4.3.1.1 Operational Details

The ABMP tests were carried out using 5*l* serum bottle despite Angelidaki *et al.* (2009) 2l recommendation. 5*l* serum bottles were selected over 2*l* ones because:

i) They allowed for larger seed and feed samples which were more likely to be representative of the AD characteristics and parent system respectively;

ii) The use of larger ABMP serum bottles also allowed for larger sampling volumes for testing; and

iii) The use of 5*l* serum bottles ensured that more than 50% of the initial volume was left at the end of the testing phase.

The ABMP bottles selected in Figure 4.4 and the setup is presented in Figure 4.5.

Figure 4.4: ABMP serum bottle selected

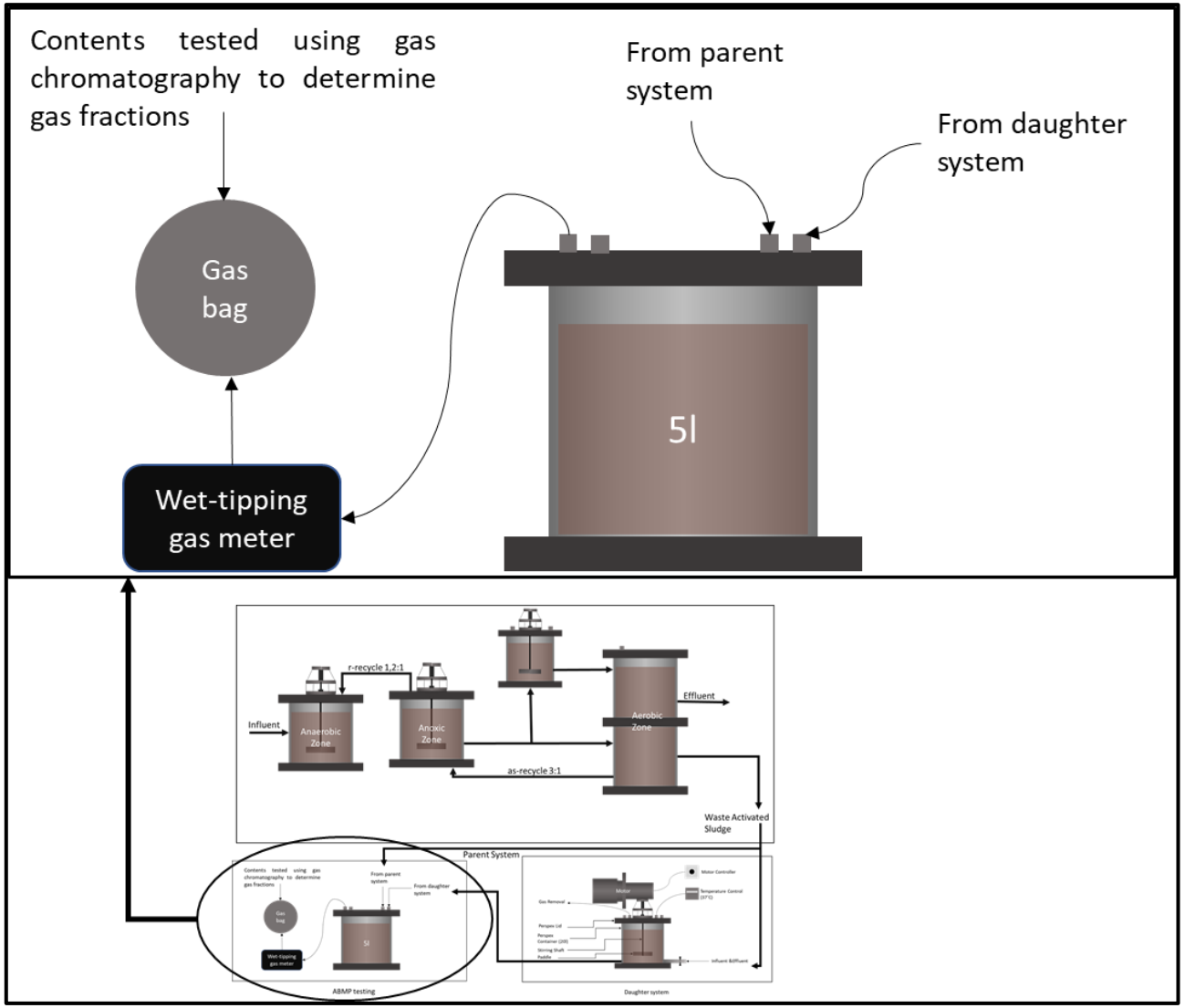

Figure 4.5: Augmented biochemical methane potential test set-up

- The seed to the ABMP was sourced from the CSTR ADs. The AD being continuously stirred, it was assumed that the biomass content of each serum bottle was an adequate representation of the AD (i.e. that the ratio of acidogens to acetogens to methanogens was consistent with that of the AD).
- The seed was sourced from an AD fed the same feed as that which was added to the ABMP serum bottles. Since the AD was at steady state, the seed was fully acclimatized to the feed which confirmed the activity of the seed as well as the lack of toxic or inhibitory solutions (this was also confirmed by control of the parent system influent and ensuring no heavy metals were added to the AD) in the parent system. This allowed the assumption that the metabolic requirements of each bacterial group were met.
- To ensure anaerobic conditions in the ABMP, the serum bottles were purged by bubbling nitrogen gas. Since the composition of the gas produced was important and some nitrogen gas is produced in an AD, the presence of the purging nitrogen gas would yield inaccurate results. To remove the nitrogen gas, it was proposed that the seed from the AD be added to the serum bottles and purged 24hrs before the beginning of the experiment. During the 24hrs, as seed-seed interaction took place, the biogas generated would displace the nitrogen gas present in the headspace while ensuring the AD bacteria's health. The feed was added by connecting the ABMP to a transfer bottle. As the feed was added, an equivalent biogas volume was displaced into the transfer bottle.

4.3.1.2 Gas Capture methods

Keeping in mind the need for accurate gas fractions, a wet-tipping gas meter was selected to measure the volume and properties of the biogas generated during the test. A wet-tipping gas meter uses a combination of liquid displacement and magnets to measure the number of tips experienced within a certain time frame is counted. The product of the number of tips by the volume of gas per tip gives the total volume of gas generated in said time frame. A typical wet-tipping gas meter is shown in Figure 4.6. The combination of the gas meter and gas chromatograph will provide information as to the volume and constitution of the biogas formed during the ABMP test.

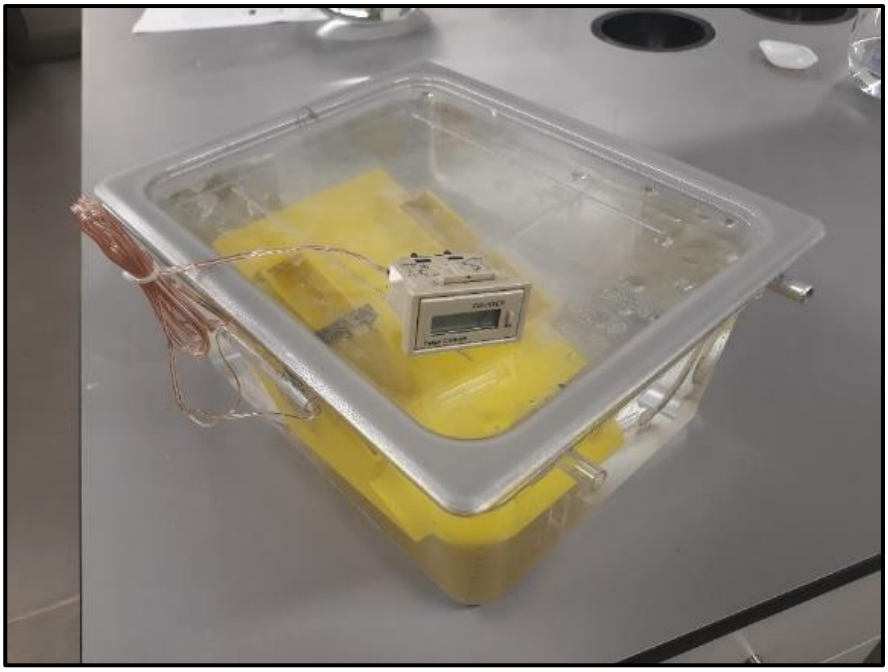

Figure 4.6: Gas meter

4.3.1.3 Testing Period

The ABMP test aimed at generating data to allow the measurement of kinetic rates of the interaction between PAOs and AD biomass. To be able to do so, all the tests described in Section 4.4 were performed daily for the first 10 days, last 5 days and every second day during the thirty (30) days (Gaszynski *et al.*, 2019)

The data from the first ten days was used to generate dynamic data for kinetics calibration as most polyP is released as OP during the first 8-10 days in anaerobic conditions (Harding *et al.*, 2010). During the last five days of testing, COD removal decreased and stopped, the data generated was used to determine the unbiodegradable fraction of PAOs (Owen *et al.*, 1978). The ABMP experiment lasted 30 days as recommended in literature but a reading was taken at 60 days to verify the composition of UPOs generated by PAOs and verify that they, indeed, have the same chemical composition as the influent PAO biomass (excluding the polyP storage).

4.3.2 ABMP Contribution to Model Validation

In current steady state models, the inorganic suspended solids (ISS) is the sum of the polyP and the influent ISS component (Wentzel & Ekama, 2004). To achieve adequate calibration of polyP release, experimental data that characterises the ISS towards the location of the particulate phosphorus (from this set up, it may largely be in the form of polyP or P precipitates) is required. To identify the hypothetical stoichiometric pathway of polyP release, the AD pH and pCO_2 were monitored closely. According to Ikumi and Ekama (2019), AD polyP release for PHB uptake results in energy generation, alkalinity increase and ρCO_2 decrease while the polyP release with PAO death results in total alkalinity decrease and ρCO_2 increase. The ABMP tests (which are described in the following section) shall be useful towards generating data that calibrates the PHB uptake rate with polyP release and associated pH and pCO_2 changes. The ABMP will also allow the calibration of the kinetics of hydrolysis with AD of PAO biomass and the endogenous mass fraction of these PAOs. In the AS system the PAOs endogenous respiration rate is known to be at about 0.04/d, with the endogenous residue being about 0.25 of the PAO biomass (Wentzel *et al.*, 1991). In the AD system, it is likely that the PAOs die at a faster rate since they are hydrolyzed. However, rather than their death rate, of importance is the rate at which their biodegradable particulate organics hydrolyse. Ikumi *et al*. (2014) reports the biodegradability and kinetics of hydrolysis of WAS from NDEBPR AS system, as similar to that of primary sludge. However, this information was obtained from the AD of WAS containing mixed cultures of OHO and PAO biomass. This research could validate this information, extending PAO modelling.

4.4 Testing Methodology

Table 4.2: Summary of Sample and Tests Carried-Out During Experimental Phase

Test	COD	VFA	TKN	FSA	TP	OP	NO_2	NO_3	VSS	TSS	Gas production	pH	Total Alkalinity
Waste Activated Sludge	Filt & Unf	Unf	Filt & Unf	Filt	Filt & Unf	Filt	Filt	Filt	Unf	Unf		Dir	
Anaerobic Digester	Filt & Unf	Unf	Filt & Unf	Filt	Filt & Unf	Filt	Filt	Filt	Unf	Unf	Dir	Dir	Filt
Augmented Biomethane Potential Test	Filt & Unf	Unf	Filt & Unf	Filt	Filt & Unf	Filt	Filt	Filt	Unf	Unf	Dir	Dir	Filt
Abbreviation	**Meaning**												
COD	Chemical Oxygen Demand, Open Flux Method												
VFA	Volatile Fatty Acid (as mgHAc/l), 5-point titration												
TKN	Total Kjeldahl Nitrogen, micro-Kjeldahl Method												
FSA	Free and Saline Ammonia, titrimetric method												
TP	Total phosphorous, sulphuric acid/ persulphate digestion at 100°C followed by molybdate-vanadate colour development for ortho-phosphate												
OP	Ortho-phosphate, molybdate vanadate colour development												
NO_2	Nitrites, Discrete Analyser												
NO_3	Nitrates, Discrete Analyser												
VSS	Volatile suspended solids, sample ignited at 600°C												
TSS	Total suspended solids, sample dried at 103-105 °C												
pH	Concentration of H^+ ions, pH meter												
Total Alkalinity	Total Alkalinity (as mg$CaCO_3$/l), 5-point titration												
Filt	Filtered												
Unf	Unfiltered												
Dir	Direct Measurement												

This section aims at presenting all the tests carried out on samples during the experimental phase of this research. A broad range of tests were carried out to ensure multiple data points were available for reconciliation. For example, filtered and unfiltered measurements were taken during the ABMP to measure the hydrolysis rate of PAOs. A drop in unfiltered COD concentration coupled with changes in particulate P, OP and gas production would indicate the breakdown of PAOs.

The metal ion concentration, FSA, nitrates, nitirites and orthophosphate concentration (with the exemption of OrgN) were measured during a gallery analyser. The gallery was calibrated daily. Calibration fluids expiry date were monitored and kept in a cold fridge except for calibration.

5. Model Development

This section of the report aims at presenting the model used to analyse the data collected during the experimental phase. The model developed is instrumental in answering the research questions and meeting the objectives outlined in Chapter 1. The model was developed in three main stages:

- Stage 1 aimed at assessing the quality of the data produced during the experimental phase of the research. This was achieved by evaluating the data produced through mass balance calculations over the anaerobic digesters (ADs) and augmented biomethane potential (ABMP) tests. Good mass balance results would show that the data generated was reliable and could be used to answer the research questions presented in Chapter 1.
- Stage 2 aimed at characterizing the influent and effluent to the AD. This step was crucial because an incorrectly characterized influent would lead to an inaccurate analysis of the data and a model that does not accurately predict the AD system's effluent. The characterization proposed by Harding (2009) was implemented. Since the Harding (2009) characterization is uncommon, a sample calculation of the procedure used to model the inorganic part of the phosphorus accumulating organisms (PAOs) is also presented.
- Stage 3 aimed at extending Sötemann *et al.*'s (2005) steady state (SS) AD model. This was achieved through the introduction of the stoichiometry by Ikumi and Ekama (2019) and the modelling of multimineral precipitation. Each extension is explained and its role within the larger framework of the AD model is discussed.

This section was divided into four main subsections. The first three will detail the first three stages of the model development. The fourth and final section will present the various models set-up through combinations of proposed changes to the AD model modification to assess the importance of each modification.

5.1 Stage 1: Analysis of raw data

The raw data generated was assessed by means of mass balances. Mass balances aim at tracking electrons, nutrients and minerals through physical, chemical, biological and biochemical processes. Mass balances as detailed by Sötemann *et al.* (2005) were carried out.

5.2 Stage 2: Sludge Characterization

The UCT AD SS model presented by Sötemann *et al.* (2005) was originally developed to model the anaerobic digestion of primary sludge (PS). It was first extended to model the treatment of sludge from N removal systems. This research aims at further extending this model by modelling the anaerobic digestion of sludge from a nitrifying-denitrifying enhanced biological phosphorus removal (NDEBPR) AS system. To allow the adequate modelling of NDEBPR sludge, a characterization procedure reflecting the properties of the sludge is required. The characterization procedures presented by Sötemann *et al.* (2005) and Harding (2009) were reviewed to determine Their applicability to the extended AD model.

5.2.1 Sötemann et al. (2005) characterization

The Sötemann *et al.* (2005) sludge characterization aims at using the wastewater's characteristics to determine the various organic and inorganic components of the sludge and their mass fractions (i.e. f_{cv}, f_c, f_n, f_p). These ratios are then used to formulate the sludge's elemental composition (i.e. determine the values of X, Y, Z, a and b in $C_XH_YO_ZN_aP_b$). This characterization is used as an input to the AD model stoichiometry which predicts the system's performance in terms of biomass formation, methane production and nutrient releases. The procedure used to characterize the influent and effluent are respectively presented graphically in Figure 5.1 and 5.2.

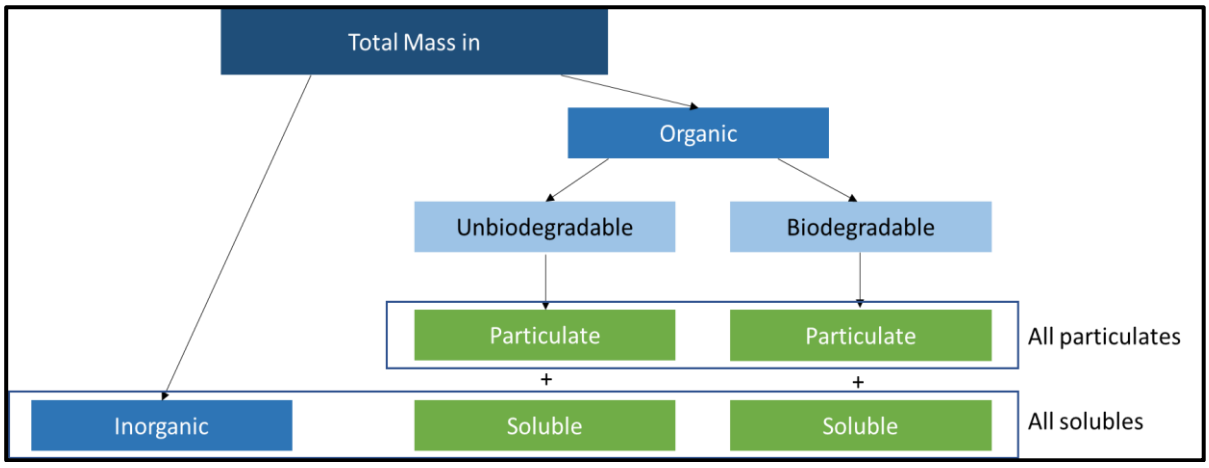

Figure 5.1: Sötemann *et al.* (2005) characterization of influent AD sludge

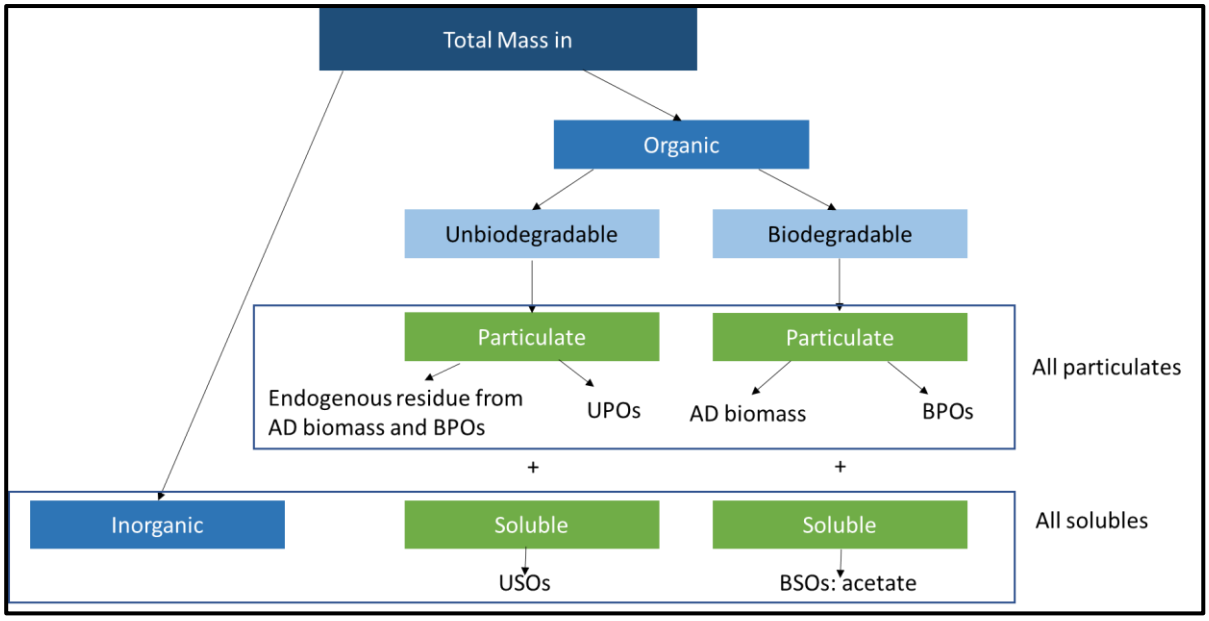

Figure 5.2: Sötemann *et al.* (2005) characterization of effluent AD sludge

5.2.2 Harding (2009) characterization

The Harding (2009) characterization procedure was introduced to allow the improved modelling of sludge from an NDEBPR system. It was developed as an extension to the Sötemann *et al.* (2005) characterization method by allowing the modelling of polyphosphate (polyp) and metallic ions within the sludge's empirical formula. According to Harding (2009), the sludge's elemental composition is $C_XH_YO_ZN_aP_b.qMePO_3$ where q represents the number of moles of polyP per mol of biomass, "Me" the aggregate of all metals used for charge balancing and "PO_3" the polyphosphate ions. The Harding (2009) characterization separates the inorganics between intracellular/bound inorganics (metals (Me) and polyP (PO_3)) and extracellular/unbound inorganics (soluble metals and OP). The sludge's properties are then recalculated yielding the sludge's mass ratios (i.e. f_{cv}, f_c, f_n, f_p). These are then calculated to determine the values of X, Y, Z, a and b used in the sludge's empirical formula.

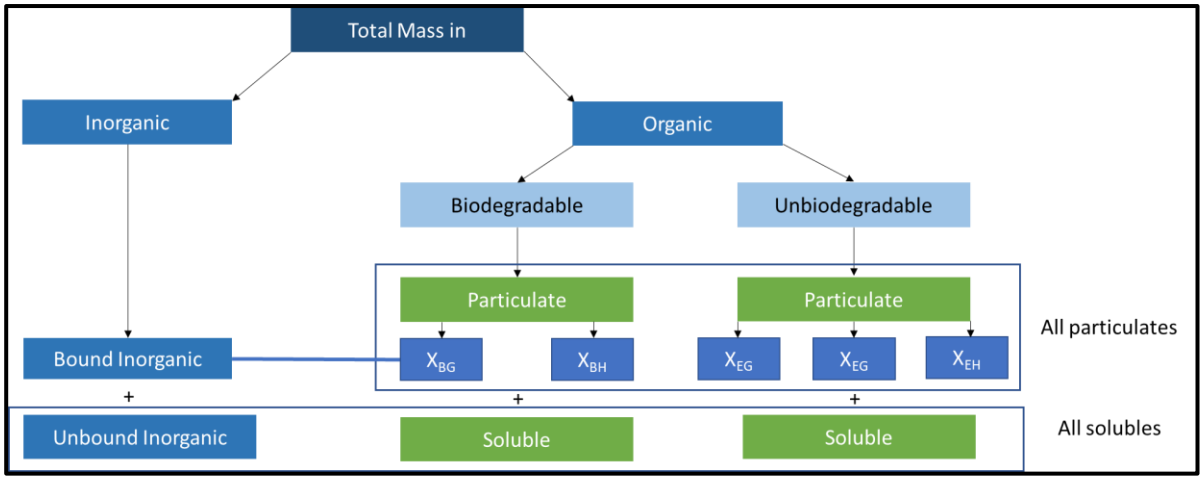

Figure 5.3: Harding (2009) influent AD characterization

The influent NDEBPR sludge to the AD is divided into three main categories: the biodegradable organics, the unbiodegradable organics and the inorganics. The influent characterization assumes that influent sludge does not contain precipitates which means that the inorganic ions released into the aqueous phase are entirely sourced from polyP. The block procedure used to characterize the influent NDEBPR sludge is presented in in Figure 5.3.

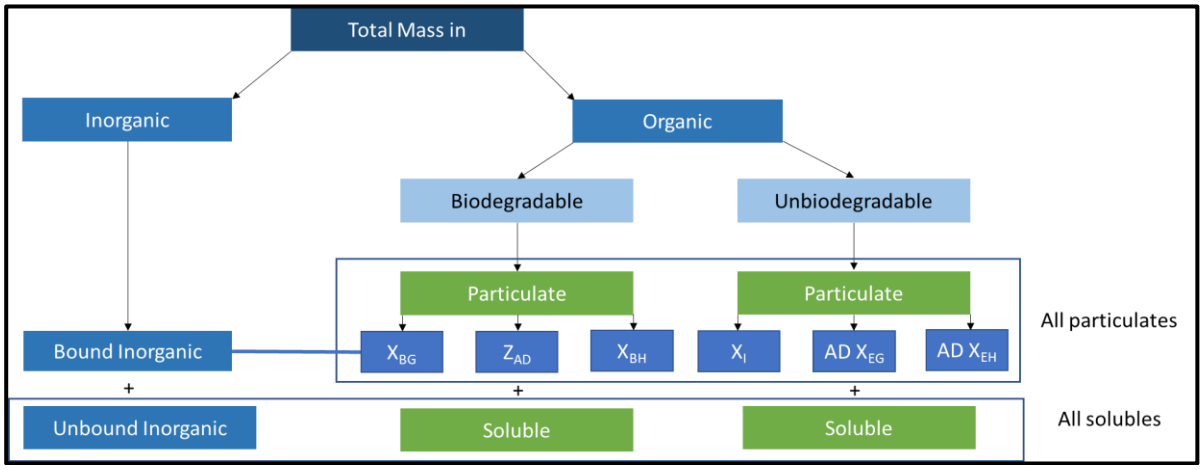

Figure 5.4: Harding (2009) effluent AD characterization

Similarly to the influent characteristics, the effluent characteristics of the AD is expected to be characterized three main categories: the inorganic mass, the biodegradable organic mass and the unbiodegradable organic mass:

- In the experiments conducted, the SRT is longer than ten (10) days and hence all the metals and polyP bound in the NDEBPR sludge are expected to be released. This means that the

inorganic mass measured in the effluent during experimentation can be assigned to the inorganic portion of the biomass and the precipitates formed from metal and polyP release.

- The biodegradable mass refers to the AD biomass (acidogens, acetogens, and methanogens) generated and modelled as acidogens, and
- The unbiodegradable mass refers to the influent UPOs and endogenous residue generated during the stabilization of the NDEBPR sludge

The block procedure used to characterize the effluent sludge is presented in Figure 5.4.

5.2.3 Inorganics Characterization

The Harding (2009) characterization procedure is not common when modelling AD influent sludge. An example of the procedure used to characterize the polyP in the PAO is presented.

Example of polyphosphate characterization

Objective: Simulate the procedure used in the characterization process of polyP in Harding (2009) characterization.

Influent metals concentration and accepted metal ratios

Name	Ions	Concentration (mg/l)
Magnesium	Mg^{2+}	30,00
Potassium	K^{+}	40,00
Calcium	Ca^{2+}	8,00
Phosphate	PO_3^{-}	125,00

Step 1: Assessing charge balance

Since the metal ions aim at balancing the polyP charge, it is critical that the sum of the metallic charge is equal to that of polyphosphate ions.

$$Total\ metallic\ charge = (number\ of\ moles\ of\ Mg * Mg\ charge) + (number\ of\ moles\ of\ K * K\ charge) + +(number\ of\ moles\ of\ Ca * Ca\ charge)$$

$$= \left(\frac{30}{24.31} * 2\right) + \left(\frac{40}{39.1} * 1\right) + \left(\frac{8}{40.08} * 2\right) = 3.89$$

$$Total\ phosphate\ charge = (number\ of\ moles\ of\ phosphate * PO_3{}^{-} charge)$$

$$= \frac{125}{30.97} * -1 = -4.04$$

$Net\ charge = 3.89 - 4.04 = -0.15$ which shows that a charge balance is not achieved. Assuming that the charge in excess is the source of error, the concentration of phosphate ions is recalculated to ensure a total phosphate charge of -3.89 is achieved.

Step 2: Determining error to ensure charge balance is achieved

The phosphorus (P) concentration required to obtain a charge of 3.89 is calculated and found to be

$P\ concentration = -3.89 * \frac{30.97}{-1} = 120.5$ which shows that an experimental error of 4.5mgP/l occurred. A new revised phosphate concentration of 120.5mg/l is used in the calculation.

Step 3 Determining the charge ratio

Since the polyphosphate composition is $Mg_cK_dCa_e.PO_3$, the value of c, d and e are calculated ensuring that the c + d + e =1. This is achieved by dividing the charge contribution of each metal ion by the total metal ion charge (3.89). Therefore,

$$c = \frac{number\ of\ moles\ of\ Mg * Charge\ of\ Mg}{Total\ charge} = \frac{\left(\frac{30}{24.31}\right)}{3.89} = 0.61$$

$$d = \frac{number\ of\ moles\ of\ K * Charge\ of\ K}{Total\ charge} = \frac{\left(\frac{40}{39.1}\right)}{3.89} = 0.25$$

$$e = \frac{number\ of\ moles\ of\ Mg * Charge\ of\ Mg}{Total\ charge} = \frac{\left(\frac{8}{40.08}\right)}{3.89} = 0.10$$

Yielding a polyphosphate composition of $Mg_{0.61}K_{0.25}Ca_{0.10}PO3$

According to Ekama and Wentzel (2004), the ISS contribution from OHO biomass is relatively small (f_{iOHO} = 0.15 mgISS/mgOHOVSS) compared to that of PAOs (about 1.2 mgISS/mgPAOVSS). This is mainly due to the presence of polyP ($Mg_cK_dCa_ePO_3$) that is known to have a maximum of 0.35mgP/mgPAOVSS (Wentzel *et al.*, 1990). However, to have accurate polyP characteristics in WAS (i.e. the concentration and the empirical formula - c, d and e). The Wentzel *et al.* (1990) mass and charge balanced steady state model is used together with reconciliation of P, Mg, K, Ca and ISS measurements over the NDEBPR AS system. The inorganic solubles (mainly ammonia and orthophosphates) are measured directly from the AS system reactor.

5.2.4 The adopted sludge characterisation Method

The characterisation method presented by Harding (2009) was adopted because it allows for the separation of organic and inorganic particulate P (largely taken to be the polyP in WAS), together with the metals associated with the inorganic P. This was important for the AD of NDEBPR WAS because Harding (2009) showed that P release associated with polyP breakdown takes place over the first eight (8) to ten (10) days in the AD while Bolzonella *et al*. (2005) reports complete WAS anaerobic digestion in twenty (20) to thirty (30) days. The accurate quantification of polyP in the WAS is necessary to ensure correct prediction of P releases into the aqueous phase and associated changes to the system's alkalinity and pH. Furthermore, the hydrolysis of polyP is also accompanied with release of its component metal ions which may result in the formation of mineral precipitates such as struvite ($MgNH_4PO_4.6H2O$) which can impact the effluent AD ISS and aqueous phase ionic concentration.

$$C_xH_yO_zN_aP_bS_c^{ch} + \left(2x-z+a+b(2+f)+2c-ch-E\frac{Y_S}{Y_B}[2k-m+n+p(2+f)+2s]-\frac{2Y_S}{8}(1-E)\right)H_2O \Rightarrow + \left(c-sE\frac{Y_S}{Y_B}\right)SO_4^{2-}$$
$$\left(x-a+b(2-f)+2c+ch-E\frac{Y_S}{Y_B}[k-n+p(2-f)+2s]-\frac{(1-E)Y_S}{8}\right)CO_2 + \left(\frac{Y_S}{8}(1-E)\right)CH_4 + \left(E\frac{Y_S}{Y_B}\right)C_kH_lO_mN_nP_pS_s + \left(a-nE\frac{Y_S}{Y_B}\right)NH_4^+$$
$$+ f\left(b-pE\frac{Y_S}{Y_B}\right)H_2PO_4^- + (1-f)\left(b-pE\frac{Y_S}{Y_B}\right)HPO_4^{2-} + \left(a-b(2-f)-2c-ch-E\frac{Y_S}{Y_B}[n-p(2-f)-2s]\right)HCO_3^-$$

Equation 5.1: AD stoichiometry taking phosphorus into account (Harding, 2009)

Harding (2009) models the inorganic P and metals as separate entities joint to the biomass. As previously stated, this characterization procedure considers the metallic ions as a charge balance to the polyP intracellularly stored. This characterization allows the inorganic and organic P release to be modelled at different rates with metal releases being modelled at the same rate as inorganic P releases. The metal releases allow for a more accurate modelling of the aqueous phase by shifting from a two phase (gas-liquid) to a three phase (gas-liquid-solid) weak acid base chemistry through the modelling of precipitation.

5.3 Stage 3: AD Model Development

Sötemann *et al.* (2005) developed an integrated two phase (aqueous-gas) mixed weak acid/base chemical, physical and biological process kinetic model for the AD of sewage sludge. The model generated is applicable to PS and WAS from nitrifying-denitrifying (ND) plants. To further the AD model and allow the anaerobic digestion of NDEBPR sludge (P rich), several modifications were made:

i) The stoichiometry was extended by modelling Ikumi and Ekama's (2019) stoichiometry. This modification allowed the hypothesis that energy transfer takes place between the AS system and the AD to be tested.

ii) The weak acid/base chemistry section was extended through the inclusion of multimineral precipitation. Multimineral precipitation was included due the high ionic release associated with the breakdown of polyP into the AD and the release of phosphorus and metals in the aqueous phase. The inclusion of precipitation extended the model from a two phase to a three phase (aqueous-gas-solid) model.

5.3.1 Model Stoichiometry

Using the outputs from the kinetics section of the model, the AD releases and partial pressure of carbon dioxide (CO_2) are determined from the AD model's stoichiometry. The stoichiometric section of the model uses the empirical composition of the organic substrate ($C_XH_yO_ZN_A$), its concentration (determined from the hydrolysed COD and molar mass from the empirical composition of the influent) and a generalized reaction stoichiometry for an overall AD system

developed by McCarty (1974) to predict the AD's weak acid/base chemistry. The stoichiometric equation comprising the anabolic and catabolic processes is shown by Equation 5.2 (McCarty, 1974).

$$C_X H_Y O_Z N_A + \left(2X + A - Z - \frac{9ED}{20} - \frac{(1-E)D}{4}\right) H_2O \rightarrow$$
$$\rightarrow \left(X - A - \frac{ED}{5} - \frac{ED}{8}\right) CO_2 + \frac{(1-E)D}{8} CH_4 + \frac{ED}{20} C_5H_7O_2N + \left(A - \frac{ED}{20}\right) NH_4^+ + \left(A - \frac{ED}{20}\right) HCO_3^-$$

Equation 5.2:Sötemann *et al.* (2005) and McCarty (1974) stoichiometry

Where: D is the electron donating capacity of the influent. It is given by:

$$D = 4X + Y - 2Z - 3A \quad \text{[e- equiv/mol]}$$

E is the ratio of biomass to hydrolysed biodegradable organics. It is given by:

$$E = \frac{Z_{AD}}{S_{bpi} - S_{bp}} \text{ (Sötemann } \textit{et al.}\text{, 2005)}$$

In the extension of the current UCT SS AD model, Harding *et al.* (2010) added biomass P to the existing stoichiometry and extended the characterization procedure to include the polyP component which consists of the phosphate (PO_3^-) and metals ions (Mg^{2+}, Ca^{2+} and K^+). The complexities of including P in the mass balanced stoichiometry of the different WWTP unit operations were considered to hinge around:

i) The different rates at which polyP and organically bound P are released in anoxic/aerobic and anaerobic digestion (i.e. the need to consider kinetics due to the presence of PAOs),

ii) The effect of the 2nd dissociation constant of the OP weak acid/base system (pK_{p2}~7.18) and

iii) The precipitation of metal phosphates (such as struvite) because polyP has a high metal (Mg^{2+}, K^+, Ca^{2+}) content which is released with the OP in aerobic and anaerobic digestion.

$$C_X H_Y O_Z N_A P_B . q[MePO_3] + \left(2X - Z + A + 2B - E\frac{\gamma_S}{\gamma_B}(2k - m + n + 2p) - \frac{2\gamma_S}{8}(1-E)\right)H_2O \rightarrow$$
$$\left(X - A + 2B + q - E\frac{\gamma_S}{\gamma_B}(k - n + 2p) - \frac{(1-E)\gamma_S}{8}\right)CO_2 + \left(\frac{\gamma_S}{8}(1-E)\right)CH_4 + \left(E\frac{\gamma_S}{\gamma_B}\right)C_k H_l O_m N_n P_p$$
$$+\left(A - nE\frac{\gamma_S}{\gamma_B}\right)NH_4^+ + \left(B + q - pE\frac{\gamma_S}{\gamma_B}\right)HPO_4^{2-} + \left(A - 2B - q - E\frac{\gamma_S}{\gamma_B}(n - 2p)\right)HCO_3^- + qMe^+$$

Equation 5.3: AD stoichiometry assuming P releases as HPO_4^{2-}

and,

$$C_X H_Y O_Z N_A P_B . q[MePO_3] + \left(2X - Z + A + 3B + q - E\frac{\gamma_S}{\gamma_B}(2k - m + n + 3p) - \frac{2\gamma_S}{8}(1-E)\right)H_2O \rightarrow$$
$$\left(X - A + B - E\frac{\gamma_S}{\gamma_B}(k - n + p) - \frac{(1-E)\gamma_S}{8}\right)CO_2 + \left(\frac{\gamma_S}{8}(1-E)\right)CH_4 + \left(E\frac{\gamma_S}{\gamma_B}\right)C_k H_l O_m N_n P_p$$
$$+\left(A - nE\frac{\gamma_S}{\gamma_B}\right)NH_4^+ + \left(B + q - pE\frac{\gamma_S}{\gamma_B}\right)H_2PO_4^- + \left(A - B - E\frac{\gamma_S}{\gamma_B}(n - p)\right)HCO_3^- + qMe^+$$

Equation 5.4: AD stoichiometry assuming P releases as $H_2PO_4^-$

Harding *et al.* (2010) determined the mass balanced redox half-reactions by splitting phosphate products between HPO_4^{2-} and $H_2PO_4^-$ to include the effect of the 2nd pKa value of the ortho-phosphate weak acid/base system. These reactions are given in Equation 5.3 and Equation 5.4. The phosphate products $H_2PO_4^-$ and HPO_4^{2-} products of each reaction are equal to the total ortho-phosphate (OP) released from the biomass and polyP assuming infinite solubility. Harding *et al.* (2010) then noted, that in the AD, the OP species almost entirely comprises of $H_2PO_4^-$ and HPO_4^{2-} ions due to the operating pH ranging between 6.8-7.2. a generalisation of the releases was achieved by splitting the phosphate ions based on AD pH. The equations used towards this phosphorus split is presented using Equation 5.5 (a-e) This gave rise to a pH sensitive f term. The combination of Equation 5.3 and 5.4 with this f term yields Equation 5.6.

(a) $f\left[H_2PO_4^-\right] + (1-f)HPO_4^{2-} = P_t$ (b) $K'_{P2} = \frac{\left(H^+\right)\left[HPO_4^{-2}\right]}{\left[H_2PO_4^-\right]}$ (c) $\left[H_2PO_4^-\right] = fP_T = \frac{P_T \cdot \left[H^+\right]}{\left[H^+\right] + K'\,p_2}$

(d) $\left[H^+\right] \cdot (f-1) = -f \cdot K'\,p_2$ (e) $\left[H^+\right] = \frac{-f \cdot K'\,p_2}{(f-1)}$

Equation 5.5 (a-e): Phosphorus Weak acid/base system speciation equations

In the AD stoichiometry of Harding *et al.* (2010), it is noted that at a sludge age of five (5) to eight (8) days, only a part of the biodegradable organics of the NDEBPR WAS biomass are degraded but all the polyP inside the phosphorus accumulating organisms (PAOs) is released. Since in the empirical composition of the PAO there is a fixed ratio (q) between the PAO biomass and polyP, it is better to separate the biomass P from the polyP in the general reaction stoichiometry. This yields Equation 5.6 and 5.8 which can be applied to any biodegradable organics.

$$C_X H_Y O_Z N_A P_B + \left(2X - Z + A + (2+f)B - E\frac{\gamma_S}{\gamma_B}(2k - m + n + (2+f)p) - \frac{2\gamma_S}{8}(1-E)\right)H_2O \leftrightarrow$$
$$\left(X - A + (2-f)B - E\frac{\gamma_S}{\gamma_B}(k - n + (2-f)p) - \frac{(1-E)\gamma_S}{8}\right)CO_2 + \left(\frac{\gamma_S}{8}(1-E)\right)CH_4 +$$
$$\left(E\frac{\gamma_S}{\gamma_B}\right)C_k H_l O_m N_n P_p + \left(A - nE\frac{\gamma_S}{\gamma_B}\right)NH_4^+ + f\left(B - pE\frac{\gamma_S}{\gamma_B}\right)H_2PO_4^-$$
$$+ (1-f)\left(B - pE\frac{\gamma_S}{\gamma_B}\right)HPO_4^{2-} + \left(A - (2-f)B - E\frac{\gamma_S}{\gamma_B}(n - (2-f)p)\right)HCO_3^-$$

Equation 5.6: AD stoichiometry including P

and for polyphosphate:

$$q[Mg_c K_d Ca_e PO_3] + fqH_2O + (1-f)qHCO_3^- \leftrightarrow (1-f)qCO_2 + fqH_2PO_4^-$$
$$+ (1-f)qHPO_4^{2-} + qcMg^{2+} + qdK^+ + qeCa^{2+}$$

Equation 5.7: PolyP release stoichiometry

Where: i) γ_S and γ_B refer to the electron donating capacity of the substrate and the biomass respectively:

$$\gamma_S = 4X + Y - 2Z - 3A + 5B$$

and

$$\gamma_B = 4k + l - 2m - 3n + 5p$$

ii) E is the fraction of biodegradable COD utilized (where there is no endogenous residue of AD biomass (f_{AD} = 0)) (S_{bpi} - S_{bpe}) that is converted to biomass (Z_{AD}):

$$E = \frac{Z_{AD}}{S_{bpi} - S_{bpe}} = \frac{Y_{AD}(1 + b_{AD}R_S)}{[1 + b_{AD}R_s(1 - Y_{AD})]}$$

iii) Y_{AD} is the yield coefficient (gCOD biomass/gCOD organics hydrolysed)

iv) b_{AD} is the acidogen endogenous respiration rate (/d)

v) R_s is the AD sludge age (d)

vi) The *f* value is the fraction of $H_2PO_4^-$ in the total phosphate species (comprising mainly of $H_2PO_4^-$ and HPO_4^{2-}, which are in equilibrium with each other according to pH.

vii) With the mol/*l* organics hydrolysed and polyP released known, the only unknown in Equation 5.6 and 5.8 is the *f* factor and hence also the AD pH.

Despite the modelling of polyP release, Equation 5.7 does not account for bioprocesses linked to the polyP breakdown. Ikumi and Ekama (2019) generated stoichiometry to model the bioprocesses mediated by PAOs in the AD and their anaerobic digestion. The stoichiometry presented accounts for the potential use of polyP as both an energy source for acetate uptake and PHB production. Different models using glycogen and acetate as the source of reducing agents were also modelled to allow for accepted bioprocess and pCO_2 reconciliation within the AD. These separate pathways will require reconciliation with the inclusion of a new parameter that can be calibrated against pCO_2, pH and alkalinity.

From anaerobic batch tests on the NDEBPR WAS, Harding (2009) noted that it took five (5) to eight (8) days to release practically all the polyP under anaerobic conditions. Whether this is faster than the death rate of the PAOs in the AD has not been confirmed, but it is significantly faster than AS biomass hydrolysis rate in the AD system.

$$Y_{PP}Mg_cK_dCa_ePO_3 + 2CH_3COO^- + (2 - 2Y_{PP})H^+ + 2(H^+ + e^-) \rightarrow C_4H_6O_2 + (2 - Y_{PP})H_2O + Y_{PP}PO_4^{3-} + Y_{PP}cMg^{2+} + Y_{PP}dK^+ + Y_{PP}eCa^{2+}$$

Equation 5.8: Bioprocesses and anaerobic digestion of PAO in an anaerobic digester

The stoichiometry presented can be applied to any biodegradable organics though correct characterization and a careful modelling which separates organics based on their properties. PS, however, contains a significant concentration of short chain fatty acids (SCFA) in the influent, which requires separate consideration.

Sötemann *et al.*' s (2005) AD model models the influent SCFA pool as acetate. In this reaction stoichiometry, the associated and dissociated acetate species are utilized by methanogenic AD biomass with no AD sludge produced in the process. No biomass was modelled to grow from methanogenesis as the biomass yield (Y_{AD}) for acidogenesis was increased to cater for biomass generated from said bioprocess. The detailed stoichiometry is shown in Equations 5.10 and 5.11. As stated by Loewenthal *et al.* (1989), the associated and dissociated acetate species are maintained in equilibrium with each other according to the pH of the AD liquor, whereby higher pH causes a higher fraction of dissociated acetate species.

$$CH_3COOH \rightarrow CH_4 + CO_2$$

Equation 5.9: Methanogenesis of influent undissociated acetate

$$CH_3COO^- + H_2O \rightarrow CH_4 + HCO_3^-$$

Equation 5.10: Methanogenesis of influent dissociated acetate

The final stoichiometry of the AD model for the various municipal sludge types, including WAS from NDEBPR systems, comprises of the combination of Equation 5.6-5.10.

5.3.2 Weak Acid/Base Chemistry Section

The Sötemann *et al.* (2005) AD model uses outputs from the stoichiometric section of the model to predict the weak acid/base chemistry of the AD. The weak acid/base portion of the model relates the partial pressure of CO_2 (pCO_2), aqueous releases, alkalinity and pH. Since the model was developed for the anaerobic digestion of PS and ND AS system WAS, the main components of the model hinged around:

- The proportion of dissolved CO_2 (as H_2CO3) that is converted to bicarbonate (HCO_3^-). This is determined by the quantity of ammonia released during organic degradation that, at neutral pH, uses a proton from the H_2CO_3 to form bicarbonate (HCO_3^-) and saline ammonia NH_4^+, and
- From the rest of the bicarbonate which is produced by the stoichiometric conversion of the influent dissociated acetate species used during the AD process.

Assuming equilibrium is achieved in the AD, the digester pH is calculated using Equation 5.11.

$$\rho_{CO_2} = \frac{\left[HCO_3^-\right] \cdot \left(1 + 10^{pKc1 - pH} + 10^{pH - pKc2}\right)}{10^{-pkHCO2}\left(1 + 10^{pH - pkc1} + 10^{2pH - pkc1 - pkc2}\right)}$$

Equation 5.21: p_{CO2}-pH relationship in an AD

Where: pK'_{HCO2} = -ve log 10 of Henry's law constant for CO_2;

$pK'_{C1} = pK_{C1} + \log_{10}(f_m)$;

$pK'_{C2} = pK_{C2} - \log_{10}(f_m) + +\log_{10}(f_d)$ (Loewenthal *et al.* 1989);

f_m = the monoprotic activity coefficient and

f_d = the diprotic activity coefficient

To allow the modelling of NDEBPR sludge, the weak acid/base chemistry portion of the model must also be extended to account for the impact of polyP breakdown and precipitation in the AD. This was achieved by:

1. Shifting away from a carbon centric pH prediction to a multi-species (carbon, phosphorus, sulphide, ammonia and acetate) system which will consider P releases.
2. Modelling mineral precipitation in the AD: A struvite precipitation model was developed by Loewenthal *et al.* (1995) and introduced into the SS AD model by Harding (2009). This research will extend this struvite precipitation model into a multimineral precipitation model. The mineral precipitates considered to form include amorphous calcium phosphate (ACP), struvite, newberyite, calcite and magnesite.

Loewenthal *et al.* (1995) developed a procedure that will be replicated when modelling multimineral precipitation. Loewenthal *et al.*'s (1995) struvite precipitation modelling assumes that:

1. The ionic strength of the bulk liquid does not vary during precipitation. As precipitation occurs, the number of ions in the bulk liquid decrease which causes a drop in ionic strength and hence the amount of precipitate likely to form. The impact of ionic strength consideration on pH prediction was confirmed by Musvoto *et al.* (2000) to be minimal.
2. Loewenthal *et al.* (1995) also assumed the presence of a limiting reagent in the precipitate formation. This was also confirmed to be adequate by Musvoto *et al.* (2000).

The extension proposed aims at considering five potential precipitates formed. Since several of them have the same limiting reagent, a method was required to decide which precipitate would be modelled to be formed first. The kinetic forward rate was found to be an adequate as it ensured completion of the process and matched observations (Musvoto *et al*., 2000). The precipitates were modelled to precipitate in the order presented in Table 5.1.

Due to the limitations of a steady state model, the multimineral precipitation model created aims at causing each mineral to precipitate sequentially instead of simultaneously as in dynamic models. The amount of precipitate formed was limited by the solubility product (pKsp) and the limiting metal. Similarly, to the Lowenthal *et al*. (1995) procedure, and to allow the model to be run using Visual Basics on Microsoft Excel, the ionic strength of the bulk liquid was not recalculated during the precipitation. The model, however, recalculates the bulk liquid's ionic strength after any one mineral has completely precipitated.

5.4 Model Set-Up

To allow the comparison of the impact of various stoichiometric pathways for PAO bioprocesses in the AD and investigate the potential energy transfer from the AS system to the AD, the models are associated with each possible PAO stoichiometry was divided into several sections: (i) the characterization (as presented by Harding. (2009) for all possible models), kinetics of sludge hydrolysis (using saturation kinetics formulation as presented by Sötemann *et al.* (2005) for all possible models), stoichiometry (varied to replicate proposed equations from Harding *et al.* (2010) and Ikumi and Ekama (2019)) and weak acid/base chemistry (all models adopted the

Table 5.1: Multimineral Precipitation

Chemical name	Chemical composition	Limiting Reagent	Musvoto *et al.* (2000)	
			-Log of Solubility product pKsp	Kinetic constant (K'r)
Struvite	$MgNH_4PO_4$	Magnesium (Mg)	13,16	3000
Amorphous Calcium Phosphate (ACP)	$Ca_3(PO_4)_2$	Calcium (Ca)	25,46	350
Magnesite	$MgCO_3$	Magnesium (Mg)	7	50
Calcite	$CaCO_3$	Calcium (Ca)	6,45	0,5
Newberyite	$MgHPO_4$	Magnesium (Mg)	5,8	0,05
The K'r constants given are as used by Musvoto *et al.* (2000a) in the simulations of aerobic batch tests on effluent from UASB reactor treating wine distillery waste.				

Table 5.2: Models Set-Up

Model:		Model 1	Model 2	Model 3	Model 4
Characterization	Harding (2009) Characterization	✓	✓	✓	✓
Stoichiometry	Sötemann *et al.* (2005)	✓			
	Ikumi and Ekama (2019) polyP disintegration with no external carbon source as reducing agent		✓		
	Ikumi and Ekama (2019) glycogen reducing agent			✓	
	Ikumi and Ekama (2019) acetate reducing agent				✓
Precipitation	No precipitation (infinite solubility)	✓	✓	✓	✓
	Struvite Precipitation	✓	✓	✓	✓
	Multimineral Precipitation	✓	✓	✓	✓

concepts presented by Loewenthal *et al*., 1995). Table 5.2 presents the constituents of each model to ensure a complete analysis of each factor is achieved.

6. Analysis

This section of the report aims at presenting the analysis of the models created and detailed in Chapter 5 to answer the research questions and meet the objectives outlined in Chapter 1. This chapter is divided into two different steady state (SS) analyses:

i) The first analysis is a comparative analysis of the stoichiometry generated by Ikumi and Ekama (2019). The analysis will aim at using a parameter estimation process to highlight which of the stoichiometric pathways presented by Ikumi and Ekama (2019) is most sensitive. It will also allow a deeper understanding towards the behaviour of phosphorus accumulating organisms (PAOs). To ensure the analysis focusses on PAO behaviour only, data from literature and peer reviewed research, specifically the mass ratios from Harding's (2009) nitrifying denitrifying enhanced biological phosphorus removal (NDEBPR) activated sludge (AS) system, will be used to model the influent to the anaerobic digester (AD). This analysis will focus on providing a detailed understanding of each component of the PAO stoichiometric pathway and present the output the way a typical predictive model would.

ii) The second steady state analysis will use data from an augmented biomethane potential (ABMP) test to determine the stoichiometric pathway best approximating the PAO intracellular behaviour. Although ABMPs are typically used to gain information about the dynamics of reactions in the AD, if the duration of the experiment is long enough such that all the biodegradable organics are utilised (the biogas evolutions and nutrient release is halted), the ABMP reactions can be treated as a steady state (SS) AD system. Data from the beginning and end of a forty (40) day ABMP by Maake & Ikumi (2020) will be used to carry out this analysis.

6.1 Steady State Model Pathway Comparison

The first step of the model evaluation will, as previously stated, use influent characterization procedure adopted from Harding (2009) to predict and analyse the AD effluent. The comparative analysis will identify the impact of each parameter in Ikumi and Ekama's (2019) stoichiometry. The analysis will be divided into four main sections:

i) The first will present the influent properties and the characterisation of the influent using the characterization procedure presented by Harding (2009).

ii) The second portion of this section will discuss the hydrolysis of the biomass in the AD using a selected kinetic formulation.

iii) The third section will look at the stoichiometry in the AD. The stoichiometry of the organic breakdown of the biomass and of the impact of PAO anaerobic behaviour will be analysed.

iv) The fourth and final section will investigate the weak acid/base chemistry of the AD. This section will use the outputs of the stoichiometry to predict the effluent pH after mineral precipitation and dissolution as required. The details of the code will be discussed as well as the potential use of minerals as an alkalinity reservoir.

6.1.1 Influent Analysis

6.1.1.1 Influent Data

The influent to the AD was assumed to comprise of an enhanced PAO culture with 65% active PAO biomass and 35% PAO endogenous residue (ER). The percentage split was obtained by modelling the enhanced PAO culture described in Chapter 4 Section 4.1 assuming the system was operated at a sludge retention time (SRT) of ten (10) days. The PAO and endogenous mass fractions assumed are presented in Table 6.1.

The value of f_p=0.38mgP/mgPAOVSS for the PAOs was calculated as the sum of organic (f_p) and inorganic (f_{pp}; due to polyphosphate (polyP)) phosphorus (P) content of the PAO (= 0.03+0.35= 0.38) (Wentzel *et al.*, 1988). From the inorganic P content of the PAO (f_{pp}= 0.35), the ISS/VSS ratio of the PAO was calculated using Wentzel & Ekama's (2004) ISS model. This yielded an ISS/VSS ratio of 1.3mgISS/mgPAOVSS (=3.287*0.35+0.15=1.3mgISS/mgVSS).

Using the mass ratios presented in Table 6.1 and assuming an influent VSS of 3000mgVSS/l (which should have been the aerobic tank concentration in the enhanced PAO culture described in Chapter 4), the influent properties presented in Table 6.2 were generated.

Table 6.1: PAO and endogenous residue assumed mass fractions

Mass fractions	Units	PAO	ER
COD/VSS ratio, f_{cv}	mgCOD/mgVSS	1,481	1,481
N/VSS ratio, f_n	mgN/mgVSS	0,1	0,1
P/VSS ratio, f_p	mgP/mgVSS	0,38	0,03
C/VSS ratio, f_c	mgC/mgVSS	0,512	0,512
ISS/VSS ratio, f_i	mgISS/mgVSS	1,3	0

Table 6.2: WAS used as AD Influent Properties from modelled enhanced PAO culture

Total COD	S_{ti}	4443,0	mgCOD/l
Filtered COD	S_{tsi}	0,0	mgCOD/l
Unbiodegradable soluble COD	S_{usi}	0,0	mgCOD/l
TKN	N_{ti}	300,0	mgN/l
Filtered TKN	N_{tsi}	0,0	mgN/l
Free and Saline Ammonia	N_{ai}	0,0	mgN/l
Influent unbiodegradable N	N_{ousi}	0,0	mgN/l
Total Phosphorus (TP)	P_{ti}	772,0	mgP/l
Filtered TP	P_{tsi}	0,0	mgP/l
Ortho-phosphate	P_{ai}	0,0	mgP/l
Effluent P	P_{ousi}	0,0	mgP/l
Volatile Suspended Solids	VSS	3000,0	mgVSS/l
Inorganic Suspended Solids	ISS	2970,0	mgISS/l
Total Suspended Solids	TSS	5970,0	mgTSS/l
Total Magnesium	Mg^{2+}	124,21	mg/l
Total Potassium	K^{+}	403,69	mg/l
Total Calcium	Ca^{2+}	26,71	mg/l
Soluble Magnesium	Mg^{2+}	0,0	mg/l
Soluble Potassium	K^{+}	0,0	mg/l
Soluble Calcium	Ca^{2+}	0,0	mg/l
Influent alkalinity	Alk_i	300	$mgCaCO_3/l$

The values of bound magnesium, potassium and calcium (i.e. the metal content of the PAOs used to maintain the charge balance of polyphosphate (polyP)) were selected such that the value of q in $C_XH_YO_ZN_aP_b.qMg_cK_dCa_ePO_3$ ranges between 1-1.3 as per Harding's (2009) and Ikumi *et al.*'s (2011) findings.

6.1.1.2 Influent Biodegradable Particulate Characterization

From the influent properties presented in Table 6.2, the sludge characteristics were calculated using the Harding (2009) characterization procedure. The characterization broke-down the biomass into three main components: the biodegradable, unbiodegradable and inorganic portion of the PAO. The biodegradable portion of the PAO refers to that mass of the PAO that can be broken down in the AD, the unbiodegradable portion of the PAO refers to the ER present in the biomass which cannot be broken down in the AD and the inorganic portion of the PAO refers to the polyP stored within the PAO. Table 6.3 presents the results of the characterization.

During the characterization procedure:

i) As per the death regeneration model, 8% of the active PAO biomass was modelled to be unbiodegradable (Dold *et al.*, 1980).

ii) As per Chapter 4 Section 4.1, the influent to the AS system generating this biomass contains only soluble organics. This implies that all the UPO in the AD influent consisted of ER (since there was virtually no UPO in the influent feed to eth AS system to accumulate in the reactor as part of the WAS). The ER was modelled to have the same elemental composition as the active PAO biomass biodegradable portion.

iii) The polyphosphate (polyP) general composition was modelled as $qMg_cK_dCa_ePO_3$ where q is the number of moles of polyP per mol of PAO and ranges between 1-1.3 (Harding, 2009, Ikumi, 2011).

iv) A mass and charge balance must be achieved over the biomass.

Table 6.3: Harding Characterization of PAO Biomass

		BPO	UPO	Inorganic Portion of PAOs			
PAO COD_{in}	S_{PAOi}	2656,9	231,0	Bound Magnesium	Mg^{2+}	124,2	$mgMg^{2+}/l$
PAO N_{in}	N_{PAOi}	179,4	15,6	Bound Potassium	K^{+}	403,7	mgK^{+}/l
PAO P_{in}	P_{PAOi}	53,8	4,7	Bound Calcium	Ca^{2+}	26,7	$mgCa^{2+}/l$
Volatile Suspended Solids	VSS	1794	156	Polyphosphate	PO_3^{-}	682,0	mgP/l
Inorganic Suspended Solids	ISS	269,1	0	ISS content of polyP	ISS	2850,9	mgISS/l
Total Suspended Solids	TSS	2063,1	156				
COD:VSS ratio	fcv	1,481	1,481	1st Iteration			
N:VSS ratio	fn	0,1	0,1			Charge contribution per ion	
P:VSS ratio	fp	0,03	0,03	Charge ratio of magnesium	c	10,2	
C:VSS ratio	fc	0,512	0,512	Charge ratio of potassium	d	10,3	
H:VSS ratio	fh	0,083	0,083	Charge ratio of calcium	e	1,3	
O:VSS ratio	fo	0,291	0,291	Charge of polyP for charge balance	PO_3^{-}	22,0	
ISS/VSS	fi	0,15	0				
				Error			
						Concentration	Percentage (%)
				Error in Magnesium in PAO	Mg^{2+}	0,0	0,0
				Error in Potassium in PAO	K^{+}	0,0	0,0
				Error in Calcium in PAO	Ca^{2+}	0,0	0,0
				Error in Phosphorus in PAO		-4,3	-0,6
Number of moles from COD	n	2,66E-02	2,31E-03	Number of moles of polyP	n	2,20E-02	
Number of moles from VSS	n	2,66E-02	2,31E-03	Number of moles of polyP/mol PAO	q	1,27	
C_X	X	4,43	4,43	Mg^{2+}	c	0,46	
H_Y	Y	7	7	K^{+}	d	0,47	
O_Z	Z	1,89	1,89	Ca^{2+}	e	0,06	
N_a	a	0,74	0,74	PO_3^{-}		1,00	
P_b	b	0,10	0,10				
e^{-}/mol	γ_s	19,22	19,22	P/ISS ratio of polyP		0,24	
COD/mol influent		153,73	153,73	PolyP:VSS ratio	fpp	0,35	mgP/mgVSS
Molar mass	M_r	103,9	103,9	Molar mass	M_r	111,70	g/mol

Table 6.4: Endogenous residue Characterization

Total Unbiodegradable Particulate COD_{in}	S_{upi}	1555,1	mgCOD/l
Total Unbiodegradable Particulate N_{in}	N_{oupi}	105	mgN/l
Total Unbiodegradable Particulate P_{in}	P_{oupi}	31,5	mgP/l
Volatile Suspended Solids	VSS	1050	mgVSS/l
Inorganic Suspended Solids	ISS	0	mgISS/l
Total Suspended Solids	TSS	1050	mgTSS/l
COD:VSS ratio	fcv	1,481	mgCOD/mgVSS
N:VSS ratio	fn	0,1	mgN/mgVSS
P:VSS ratio	fp	0,03	mgP/mgVSS
C:VSS ratio	fc	0,512	mgC/mgVSS
H:VSS ratio	fh	0,08	mgH/mgVSS
O:VSS ratio	fo	0,29	mgO/mgVSS
ISS/VSS	fi	0	mgISS/mgVSS
Number of moles from COD	n	1,01E-02	mol/l
Number of moles from VSS	n	1,01E-02	mol/l
C_X	X	4,43	
H_Y	Y	7	
O_Z	Z	1,89	
N_a	a	0,74	
P_b	b	0,10	
e^-/mol	γ_s	19,22	e^-/mol
COD/mol influent		153,73	gCOD/mol
Molar mass	M_r	103,95	g/mol

During the characterization process, the influent ions (metallic and inorganic) were pre-processed to ensure the influent biomass was both mass and charge balanced. As shown in Table 6.3, however, the sum of the metal ion charges does not fully balance that of the polyphosphate giving rise to a net negative charge. To ensure that charge balance is maintained, the amount of P in polyP is recalculated and the additional P that gave rise to a net negative charge is assumed to be due to experimental errors and added to the orthophosphate reading maintaining a P balance. If the net charge over the polyP were to be positive, this would show as an error in the metal ion measurement. The actual metal content in the polyP would be recalculated keeping the metal ratio (i.e. the value of c, d and e in $Mg_cK_dCa_ePO_3$) constant. A detailed calculation in the characterization of the inorganic portion of the PAO is presented in Chapter 5 Section 5.2.3.

6.1.2 Kinetics of Hydrolysis

For the AD of waste activated sludge (WAS), the kinetics of volumetric sludge hydrolysis is taken as the rate-limiting step since the stoichiometric conversion of the products generated from the hydrolysis process occurs much faster (Sötemann *et al.*, 2005). Hence, in a steady state AD model, once the kinetics of hydrolysis is resolved, the stoichiometry that follows can reach completion towards the AD model prediction of COD removal, biomass generated and methane production. The biodegradable portion of the PAOs are modelled to be hydrolysed according to the saturation kinetics formulation (as described by Sötemann *et al.* (2005)* and explained in Section 2.2.3.2) as they accurately represent the surface breakdown process that is hydrolysis. Assuming the influent PAO characteristics in Table 6.3 and using Sötemann *et al*. (2005) recommended kinetic constants, the hydrolysis of PAOs was modelled. The results are presented in Table 6.5.

Table 6.5: Modelling of the hydrolysis of PAOs (Sötemann *et al.* (2005))

	K_M	5,27	gCODorganics/gCODBiomass.d
	K_S	7,98	gCOD/l
Endogenous residue	Y_{AD}	0,11	/d
Death rate of acidogens	b_{AD}	0,04	/d
Sludge Retention Time	R_s	40,00	d
Influent OHO concentration	S_{bpi}	2,66	gCOD/l
Residual organics concentration	S_{bp}	0,12	gCOD/l
Acidogenic Biomass concentration	Z_{AD}	0,12	gCOD/l
Hydrolysis rate	r_h	0,45	gCOD/l.d
Methane produced	S_m	2,42	gCOD/l

***This first analysis is comparative and is used to determine the most sensitive components of the AD model. As the model focuses mainly on changes to the stoichiometry and weak acid/base chemistry and their impact on the system pH prediction, any kinetics could be used in view of assessing the sensitivity of the model. The Sötemann et al. (2005) kinetics were used as they are well known. Furthermore, the SRT selected ensured maximum COD removal and hence different kinetic constants would have had a low impact. This run did not have any impact on the conclusions drawn but rather assessed as part of a comparative study of the model.*

6.1.3 Stoichiometry

The stoichiometric section of the model inputs the products of sludge hydrolysis into a set of mass and charge balanced bioprocess stoichiometric equations to predict the aqueous phase releases. The stoichiometric analysis presented is divided into three sections:

i. The first models the breakdown of organics resulting in COD (electrons), carbon (C), hydrogen (H), oxygen (O), nitrogen (N) and phosphorus (P) availability towards biogas generation (carbon dioxide and methane), nutrient (N and P) releases and alkalinity.

ii. The second models the breakdown of polyP assuming no energy transfer from the AS system aerobic zone to the AD (Harding *et al.*, 2010). This is achieved through the modelling of polyP breakdown into its constituent OP and metal ions (Mg^{2+}, K^{+} and Ca^{2+}) without uptake of acetate and PHB production in the AD.

iii. The third models the breakdown of polyP and associated OP and metals releases, with acetate uptake and PHB formation. This also models the energy transfer from the AS aerobic zone to the AD as hypothesised in Chapter 1 and presented by Ikumi and Ekama (2019).

6.1.3.1 Stoichiometry of biomass breakdown

The PAO biomass breakdown was modelled according to the extended steady state AD model of Harding *et al.* (2010) that includes organically bound biomass P. The influent elemental composition is critical during this modelling to accurately predict the reactor properties. Using the BPO composition of active PAO biomass that presented in Table 6.3, the releases associated with biomass breakdown were calculated and the results are presented in Table 6.6.

The releases and the reactor pH are dependent on the values of E (ratio of biomass generated to hydrolysed COD) and f (the split between $H_2PO_4^-$ and HPO_4^{2-} ions) and f (the ratio splitting P_T between $H_2PO_4^-$ and HPO_4^{2-} ions). The value of E was calculated from the results of the hydrolysis portion of the model (i.e. 0.18/(2.66-0.45)= 0.08). The value of f is both pH dependent and impacts pH as the concentration of $H_2PO_4^-$ and HPO_4^{2-} ions impact alkalinity. The value of f was only explicitly calculated as the pH assuming infinite solubility of ions was iterated.

Table 6.6: Stoichiometry of PAO biomass breakdown

Ratio of biomass to hydrolysed COD	E	0,05	
split between $H_2PO_4^-$ and HPO_4^{2-}	f	0,33	
Number of moles of water	H_2O	-5,12E-02	mol/l
Number of moles of carbon dioxide	CO_2	2,40E-02	mol/l
Number of moles of methane	CH_4	3,96E-02	mol/l
Number of moles of biomass formed		7,63E-04	mol/l
Number of moles of ammonia released	NH_4^+	1,21E-02	mol/l
Number of moles of P released as	$H_2PO_4^-$	5,68E-04	mol/l
	HPO_4^{2-}	1,16E-03	mol/l
Number of moles of bicarbonate released	HCO_3^-	9,17E-03	mol/l

The value of f was, however, implicitly calculated after the precipitation of each mineral as the $H_2PO_4^-$ and HPO_4^{2-} ion concentration were recalculated to make the system alkalinity equal the calculated alkalinity post precipitation (i.e. final alkalinity = initial alkalinity – 3*amount of struvite precipitated).

6.1.3.2 Stoichiometry of polyP breakdown with no energy transfer

The stoichiometry of polyP breakdown and the resultant pH is dependent upon whether PAOs are assumed to be able to undergo bioprocesses in the AD. The stoichiometry presented by Harding *et al.* (2010) does not model PAO bioprocesses in the AD and hence does not assume energy to be transferred bound within the polyP bond. Harding *et al.*'s (2010) stoichiometry focuses only on the ion releases associated with polyP breakdown. Table 6.7 presents the results.

As shown in Table 6.7, the breakdown of polyP with no energy transfer uses up a significant amount of carbonate alkalinity. The sum of carbonate alkalinity released with biomass breakdown (8.87E-03 mol/l) and carbonate alkalinity used up with polyP breakdown (1.10E-02mol/l) results in a negative carbonate alkalinity highlighting the importance of the influent alkalinity to maintain a stable pH in the AD at SS.

The influent alkalinity is also critical dynamically due to the different rates of carbonate alkalinity release from biomass breakdown and carbonate alkalinity usage from polyP breakdown. Indeed,

Table 6.7: Stoichiometry of polyP breakdown with no energy transfer

split between $H_2PO_4^-$ and HPO_4^{2-}	f	0,33	
Number of moles of water	H_2O	-7,20E-03	mol/l
Number of moles of bicarbonate released	HCO_3^-	-1,48E-02	mol/l
Number of moles of carbon dioxide	CO_2	1,48E-02	mol/l
Number of moles of P released as	$H_2PO_4^-$	7,20E-03	mol/l
	HPO_4^{2-}	1,48E-02	mol/l
Number of moles of magnesium released	Mg^{2+}	5,11E-03	mol/l
Number of moles of potassium released	K^+	1,03E-02	mol/l
Number of moles of calcium released	Ca^{2+}	6,67E-04	mol/l

since polyP breakdown is completed in the first 8-10days in the AD (Harding, 2009) while biomass take 20-40 days to be broken down (Bolzonella *et al.*, 2004), the carbonate alkalinity is used up faster than it is produced in dynamic conditions. If this stoichiometry proves to be the correct one, ADs treating NDEBPR sludge are likely to sour during the start-up (dynamic) phase.

6.1.3.3 Stoichiometry of polyP breakdown with energy transfer

The stoichiometry presented by Ikumi and Ekama (2019) models the impact of energy transfer from the AS system to the AD through the modelling of PAO processes in the AD. Ikumi and Ekama (2019) considered three potential stoichiometric pathways in the formation of poly-B-hydroxybutyrate (PHB):

(i) polyphosphate disintegration without the inclusion of organic compounds as reducing agents,

(ii) glycogen used as reducing agent and

(iii) acetate used as reducing agent. Using the polyP composition presented in Table 6.3 as an input, the results for each biochemical pathway is presented in Table 6.8.

The stoichiometry developed by Ikumi and Ekama (2019) relied on several constants namely Y_{pp} (the ratio of moles of P released to PHB formed), Y_{gl} (the ratio of glycogen broken down to PHB formed) and the percentage of polyP broken down towards bioprocesses. These ratios were obtained from literature on PAO behaviour in the AS system. These values were deemed accurate

since PAOs bioprocesses are modelled to proceed based on their environment. These values also helpful in highlighting the link between the AS system and the AD increasing confidence in the results generated during this analysis. The constant values used were:

i) The ratio of P release to PHB formed was assumed to be 0.33 (Smolders *et al.*, 1995)

ii) The ratio of glycogen to PHB formed was assumed to be 0.37 (Smolders *et al.*, 1995) and

iii) The percentage of polyP used towards bioprocesses was assumed to be 80.5% (Wentzel *et al.*, 1988)

Use of polyphosphate

As shown in Table 6.8, the energy generated from disintegration of polyP (i.e., with the electrons sourced from $NADH_2$ formed aerobically with PHB degradation in the parent NDEBPR AS system) was used for both acetate uptake and PHB formation as per the "Comeau-Wentzel" model (Comeau *et al.*, 1987, Ikumi & Ekama, 2019). In the AD, the PHB is then broken down and the acetate returned to the acetate pool for methane production. Since a portion of the polyP is not used to form PHB (19.5%) (Wentzel *et al.*, 1988), it is broken down as per Harding *et al.*'s (2010) stoichiometry and the energy in the polyP bond is lost as heat in the AD. Despite the decrease in alkalinity associated with polyP breakdown without bioprocesses, this stoichiometry generates alkalinity through P release and is more likely to result in a high pH. However, the high P and metal releases may also cause precipitation in the AD which will impact the system pH.

Use of glycogen as a reducing agent

The results in Table 6.8 present the output of the stoichiometry presented by Ikumi and Ekama (2019) for PAO processes in the AD where polyP is broken down for acetate uptake and glycogen is used as the source of reducing agents to produce PHB.

Table 6.8: Stoichiometry of polyP breakdown with energy transfer

Reducing Agent		PolyP	Glycogen	Acetate	Units
Energy from Inorganic Portion of Biomass to form PHB					
Number of moles of P per mol of PHB formed	Y_{PP}	0,33	0,33	-	
Number of moles of glycogen per mol of PHB formed	Y_{gl}	-	0,37	0,37	
% of polyP released towards bioprocesses		80,5%	80,5%	80,5%	
Number of moles of PolyP		-1,77E-02	-1,77E-02	-1,77E-02	mol/l
Number of moles of glycogen	$C_4H_7O_{3,5}$	-	-1,99E-02	-5,04E-03	mol/l
Number of moles of acetate	CH_3COO^-	-1,07E-01	-5,37E-02	-1,72E-02	mol/l
$(H^+ + e^-)$ generated from polyP breakdown	$(H^+ + e^-)$	-1,07E-01	-	-	mol/l
Number of moles of water	H_2O	8,97E-02	1,39E-02	-8,13E-03	mol/l
Number of moles of PHB formed	$C_4H_6O_2$	5,37E-02	4,15E-02	1,21E-02	mol/l
H^+ ions released	H^+	-7,20E-02	2,33E-02	3,04E-02	mol/l
Number of moles of magnesium released	Mg^{2+}	4,11E-03	4,11E-03	4,11E-03	mol/l
Number of moles of potassium released	K^+	8,31E-03	8,31E-03	8,31E-03	mol/l
Number of moles of calcium released	Ca^{2+}	5,37E-04	5,37E-04	5,37E-04	mol/l
Carbonic Acid	CO_3^{2-}	-	2,08E-02	6,06E-03	mol/l
Phosphoric Acid	PO_4^{3-}	1,77E-02	1,77E-02	1,77E-02	mol/l
PHB breakdown and AD biomass formation					
Number of moles of PHB used	$C_4H_6O_2$	-5,37E-02	-4,15E-02	-1,21E-02	mol/l
Number of moles of water	H_2O	-8,06E-02	-6,23E-02	-1,82E-02	mol/l
Number of moles of carbon dioxide	CO_2	9,40E-02	7,27E-02	2,12E-02	mol/l
Number of moles of methane	CH_4	1,21E-01	9,35E-02	2,73E-02	mol/l
PolyP hydrolysis by extracellular enzymes					
split between $H_2PO_4^-$ and HPO_4^{2-}	f_p	0,52	0,53	0,58	mol/l
split between HCO_3^- and C_T	f_c	0,52	0,53	0,58	mol/l
Number of moles of polyP	n	-4,29E-03	-4,29E-03	-4,29E-03	mol/l
Number of moles of water	H_2O	-4,29E-03	-4,29E-03	4,29E-03	mol/l
Number of moles of bicarbonate released	HCO_3^-	-2,07E-03	-2,02E-03	-1,82E-03	mol/l
Number of moles of carbon dioxide	CO_2	2,07E-03	2,02E-03	1,82E-03	mol/l
Number of moles of P released as	$H_2PO_4^-$	2,22E-03	2,27E-03	2,47E-03	mol/l
	HPO_4^{2-}	2,07E-03	2,02E-03	1,82E-03	mol/l
Number of moles of magnesium released	Mg^{2+}	9,97E-04	9,97E-04	9,97E-04	mol/l
Number of moles of potassium released	K^+	2,01E-03	2,01E-03	2,01E-03	mol/l
Number of moles of calcium released	Ca^{2+}	1,30E-04	1,30E-04	1,30E-04	mol/l

In accordance with literature, this stoichiometry based on the "Mino" model generates more PHB per mol of acetate than the stoichiometry based on the "Comeau-Wentzel" model. Indeed, 77.3% of the acetate is turned into PHB if glycogen is used as a reducing agent versus 50% if polyP disintegration (with aerobically generated $NADH_2$ used for electron transfer) is used as the energy source. However, since more PHB is generated, a higher partial pressure of carbon dioxide (pCO_2) is achieved in the AD due to the breakdown of said PHB. The impact of this increased partial pressure in pH is difficult to predict due to the high releases of carbonate (CO_3^{2}) and phosphate (PO_4^{3-}) ions.

Acetate as a reducing agent

The results presented in Table 6.8 details the stoichiometry generated for PAO processes in the AD when acetate was used as a reducing agent. This stoichiometry was developed to allow for an external carbon source, modelled as acetate, to act as a potential reducing agent. In this stoichiometry, the energy from polyP disintegration is used to take up the acetate in the AD. The acetate is then broken down to produce reducing agents and convert the glycogen and the remaining acetate to PHB.

This stoichiometry produces a significant amount of PHB with a ratio of PHB to acetate equal to 0.705 (70.5%). As shown Table 6.8, the use of acetate as reducing agent:

- Produces a high amount of PHB of the same order of magnitude as the "Mino" model without overwhelming the pCO_2 of the AD,
- It uses less glycogen which generates carbon alkalinity through the release of carbonate ions and
- It uses polyP for acetate uptake which generates phosphate alkalinity through the release of phosphate ions.

A detailed analysis of the stoichiometry generated by Ikumi and Ekama (2019) is presented in Section 2.3

6.1.4 Weak Acid/Base Chemistry

The output from the stoichiometry was used to calculate the initial alkalinity, partial pressure of carbon dioxide (pCO_2) and total species concentration of the AD. Using this information, the impact of precipitation was modelled.

The model first calculated the AD pH and value of f assuming infinite solubility (i.e. no precipitation). The model then ran through the code approximating changes in alkalinity and pH associated with struvite, amorphous calcium phosphate (ACP), magnesite, calcite and newberyite precipitation.

As expected, the stoichiometry presented by Harding *et al.* (2010) which models polyP breakdown with no energy transfer yielded the lowest pH at 6.56 post precipitation predicting digester failure. The stoichiometry by Ikumi and Ekama (2019) yields answers ranging from 6.89-7.00 post precipitation predicting a functional AD.

As shown in Table 6.9, the presence of calcium ions impacts pH post precipitation significantly. Furthermore, all the calcium released in the AD seems to precipitate as is shown by the value of calcium post ACP precipitation which is approximately zero. These results tend to indicate than the anaerobic digestion of calcium high PAOs is more likely to cause AD souring than magnesium high PAOs.

As shown in Table 6.9, the modelling of minerals containing carbon is not appropriate. Indeed, both calcite and magnesite were modelled to dissolve into the AD to increase the system alkalinity, calcium and magnesium concentration. However, the modelling of this dissolution is achieved by increasing the total carbon species concentration. This overwhelms the system by increasing the partial pressure of carbon dioxide to a value larger than one (1) rapidly which cannot take place. This prevents the system from achieving equilibrium but a SS precipitation model allowing for carbonate dissolution would not be achieved.

Table 6.9: pH results

Stoichiometry	Harding (2009)	Ikumi and Ekama (2019)		
Reducing Agent	None	polyP	glycogen	acetate
No precipitation				
pH_no precipitation	6,60	6,91	6,90	7,00
Struvite precipitation				
Amount of struvite formed	2,35E-04	2,31E-03	1,93E-03	2,77E-03
Magnesium post precipitation	4,88E-03	2,80E-03	3,18E-03	2,34E-03
PT post precipitation	2,35E-02	2,14E-02	2,18E-02	2,10E-02
NT post precipitation	1,18E-02	9,75E-03	1,01E-02	9,29E-03
pH_post struvite precipitation	6,59	6,88	6,87	6,97
ACP precipitation				
Amount of ACP formed	2,23E-04	2,23E-04	2,23E-04	2,23E-04
Calcium post precipitation	-1,33E-06	-1,33E-06	-1,33E-06	-1,33E-06
PT post precipitation	2,31E-02	2,10E-02	2,14E-02	2,05E-02
pH_post magnesite precipitation	6,59	6,90	6,89	6,99
Magnesite precipitation				
Amount of Magnesite formed	0,00E+00	0	0	0
Magnesium post precipitation	4,88E-03	2,81E-03	3,18E-03	2,34E-03
pCO2 post precipitation	3,77E-01	4,27E-01	4,25E-01	4,13E-01
pH_post magnesite precipitation	6,59	6,90	6,89	6,99
The value of pCO2 exceeded allowable limits and hence magnesite was disregarded				
Calcite precipitation				
Amount of Calcite formed	0,00E+00	0	0	0
Calcium post precipitation	-1,33E-06	-1,33E-06	-1,33E-06	-1,33E-06
pCO2 post precipitation	3,77E-01	4,27E-01	4,25E-01	4,13E-01
pH_post calcite precipitation	6,59	6,90	6,89	6,99
The value of pCO2 exceeded allowable limits and hence calcite was disregarded				
Newberyite precipitation				
Amount of Newberyite formed	3,51E-03	1,82E-03	2,01E-03	1,41E-03
Mg post precipitation	1,37E-03	9,85E-04	1,18E-03	9,34E-04
PT post precipitation	1,96E-02	1,92E-02	1,94E-02	1,91E-02
pH_post Newberyite precipitation	6,56	6,90	6,89	7,00

6.2 Steady State Model Stoichiometric Pathway Analysis

This section of Chapter 6 aims at evaluating which stoichiometric pathway best represents the behaviour of PAOs in the AD through a comparison between experimental data and model outputs. The results presented will also determine whether an energy transfer takes place between the AS system and the AD a hypothesis presented in Chapter 1.

To achieve this analysis, data generated by Maake & Ikumi (2020) for an ABMP test on WAS containing enhanced PAO cultures will be used. The experimental set-up and requirements for a successful ABMP are presented in Chapter 4 Section 4.3. The ABMP test of Maake and Ikumi (2020) was run to a long solids retention time (>40days) such that all the bioprocesses had completed (as was observed when biogas generation had come to a standstill). Hence, although ABMP data is typically used to assess the kinetics of reactions, the results taken at the beginning and end (40days) of this ABMP data (when all bioprocesses had reached completion) could be analysed in the same fashion as a steady state AD system, operated at a long sludge age.

The analysis performed in this section is divided into five main sections:

i) The first will present the data generated by Maake and Ikumi (2020) for both the ABMP influent and effluent. The influent sludge will then be characterized using the Harding (2009) characterization procedure.

ii) The second will utilize the hydrolysis kinetic constants generated by Maake and Ikumi's (2020) dynamic analysis of the same data to model the hydrolysis process taking place in the AD.

iii) Using the output from the hydrolysis portion of the model, the third section will assess the stoichiometric pathways that represent behaviour of PAOs in the AD system as presented by Ikumi and Ekama (2019)as an extension of the AD stoichiometric model of Sötemann et al (2005).

iv) The fourth section will present the output of the multimineral precipitation model which will help determine the impact of precipitation on the AD's pH.

v) And finally, the fifth section will present a global comparison between the proposed SS AD model output and the experimental data.

6.2.1 Sludge influent properties and characterization

6.2.1.1 Maake and Ikumi (2020) ABMP data

Maake & Ikumi (2020) performed an ABMP test on an enhanced PAO culture. The ABMP lasted 40 days with tests being done daily for the first ten (10) days and the last five (5) days of the experiment. The seed used by Maake & Ikumi (2020) to anaerobically digest PAOs was sourced from a WAS fed AD which had reached steady state. One litre (1l) of seed and feed sludge was used to during the ABMP test to ensure the data generated was representative of the AD characteristics and enhanced PAO culture respectively.

Table 6.10: Maake and Ikumi (2020) data

Maake and Ikumi (2020)		Influent Data	Effluent Data	Units
Total COD	S_t	5440,00	2520,00	mgCOD/l
Filtered COD	S_{ts}	0,00	-	mgCOD/l
Unbiodegradable soluble COD	S_{us}	0,00	-	mgCOD/l
TKN	N_t	366,28	-	mgN/l
Filtered TKN	N_{ts}	0,00	-	mgN/l
Free and Saline Ammonia	N_a	2,90	-	mgN/l
Influent unbiodegradable N	N_{ous}	0,00	-	mgN/l
Total Phosphorus (TP)	P_t	446,50	563,40	mgP/l
Filtered TP	P_{ts}	0,00	-	mgP/l
Ortho-phosphate	P_a	184,20	308,70	mgP/l
Effluent P	P_{ous}	0,00	-	mgP/l
Volatile Suspended Solids	VSS	3633,8	1660,00	mgVSS/l
Inorganic Suspended Solids	ISS	1137,00	1060,00	mgISS/l
Total Suspended Solids	TSS	4770,80	2720,80	mgTSS/l
Total Magnesium	TMg^{2+}	49,40	49,40	mgMg/l
Total Potassium	TK^{+}	245,00	245,00	mgK/l
Total Calcium	TCa^{2+}	42,50	42,50	mgCa/l
Soluble Magnesium	SMg^{2+}	0,00	49,40	mgMg/l
Soluble Potassium	SK^{+}	0,00	245,00	mgK/l
Soluble Calcium	SCa^{2+}	0,00	42,50	mgCa/l
Influent alkalinity	Alk	211,50	Dependent on reducing agent.	$mgCaCO_3/l$
Gas produced		-	739,5	ml
pH		7,01	6,69	

- The N content of the sludge was calculated using an assumed TKN/VSS ratio, f_n=0.1mgN/mgVSS (Sötemann *et al.*, 2007). The influent TKN was calculated by multiplying by the influent VSS by the given f_n and adding the influent FSA reading (influent TKN = (0.1*3633.8) + 2.9 = 363.4 + 2.9 = 366.3mgN/l).
- The influent alkalinity was calculated using a glass box model (Gaszynski *et al.*, 2019, Ikumi, 2011, Maake & Ikumi, 2020) knowing the influent and effluent pH. The procedure towards using a glass box model is presented in Chapter 2 Section 2.2.4.1.

6.2.1.2 Influent Biodegradable Particulate Characterization

The influent properties presented in Table 6.10 were characterized and are presented in Table 6.11. The characteristics presented in Table 6.11 were obtained from the measured data generated by Maake and Ikumi (2020).

- 32% of the influent VSS was UPO generated as ER in the AS system (obtained from Maake & Ikumi's (2020) analysis),
- As per the death regeneration model, 8% of the PAO biomass was modelled to be unbiodegradable (Dold *et al.*, 1980). This unbiodegradable portion of the PAO was also modelled not to contribute ISS as per Wentzel & Ekama's (2004) ISS model.
- The polyphosphate (polyP) general composition was $qMg_cK_dCa_ePO_3$ where q is the number of moles of polyP per mol of PAO (Harding, 2009).

From the sludge characterization, the PAOs were calculated to have a P-PP to VSS ratio f_{pp}=0.14mgP-PP/mgVSS. This value is significantly higher than the organic P content of the biomass (f_p=0.025mgP/mgVSS) confirming the enhanced state of the culture. This value, however, is much lower than the maximum 0.35mgP-PP/mgPAOVSS reported by Wentzel *et al.* (1988). The low polyP content could be attributed a low concentration of magnesium ions (Mg^{2+}) and a high concentration of potassium ions (K^+) in the polyP composition. However, because the impact of the metal ion ratio is still unknown, this cannot be conclusively stated. Furthermore, the low f_{pp} value explains the value of q_Φ = 0.5 when Harding (2009) reported a value of q_Φ ranging between 1-1.3. The P/ISS ratio is within expectations due to the amount of inorganic P content in the sludge.

Table 6.11: Influent Characterization

		BPO	UPO		Inorganic Portion of PAOs		
PAO COD_{in}	S_{PAOi}	3403,3	295,9	Bound Magnesium	Mg^{2+}	49,40	$mgMg^{2+}/l$
PAO N_{in}	N_{PAOi}	229,1	19,9	Bound Potassium	K^{+}	245,00	mgK^{+}/l
PAO P_{in}	P_{PAOi}	68,2	5,9	Bound Calcium	Ca^{2+}	42,50	$mgCa^{2+}/l$
Volatile Suspended Solids	VSS	2273,3	197,7	Polyphosphate	PO_3^{-}	337,49	mgPP/l
Inorganic Suspended Solids	ISS	341,0	0,0	ISS of polyP		796,00	
Total Suspended Solids	TSS	2614,3	197,7	1^{st} Iteration			
COD:VSS ratio	fcv	1,497	1,497			Charge per ion	
N:VSS ratio	fn	0,101	0,100798	Charge ratio of magnesium	c	4,07	
P:VSS ratio	fp	0,03	0,03	Charge ratio of potassium	d	6,27	
C:VSS ratio	fc	0,51	0,51	Charge ratio of calcium	e	2,12	
H:VSS ratio	fh	0,08	0,08	Charge of polyP for charge balance	PO_3^{-}	10,90	
O:VSS ratio	fo	0,29	0,29	Error			
ISS/VSS	fi	0,15	0			Concentration	Percentage (%)
				Error in Magnesium in PAO	Mg^{2+}	0,0	0,0
				Error in Potassium in PAO	K^{+}	0,0	0,0
				Error in Calcium in PAO	Ca^{2+}	0,0	0,0
				Error in Phosphorus in PAO	PO_3^{-}	48,2	14,3
Number of moles from COD	n	2,25E-02	1,96E-03	Number of moles of polyP		1,09E-02	
Number of moles from VSS	n	2,25E-02	1,95E-03	Number of moles of polyP/mol PAO	q	0,5	
C_X	X	4,31	4,31	Mg^{2+}	c	0,37	
H_Y	Y	7	7	K^{+}	d	0,58	
O_Z	Z	1,82	1,82	Ca^{2+}	e	0,19	
N_a	a	0,73	0,73	PO_3^{-}		1,00	
P_b	b	0,10	0,10				
e^{-}/mol	γ_s	18,91	18,91	P/ISS ratio of polyP		0,48	
COD/mol influent		151,25	151,25	PolyP:VSS ratio	fpp	0,14	mgP/mgVSS
Molar mass	M_r	101,1753	101,1753	Molar mass	M_r	118,33	g/mol

Table 6.12: Unbiodegradable Particulate Characterization

Total Unbiodegradable Particulate COD_{in}	S_{upi}	1740,8	mgCOD/l
Total Unbiodegradable Particulate N_{in}	N_{oupi}	117,2	mgN/l
Total Unbiodegradable Particulate P_{in}	P_{oupi}	34,9	mgP/l
Volatile Suspended Solids	VSS	1162,8	mgVSS/l
Inorganic Suspended Solids	ISS	0,0	mgISS/l
Total Suspended Solids	TSS	1162,8	mgTSS/l
COD:VSS ratio	fcv	1,497	mgCOD/mgVSS
N:VSS ratio	fn	0,101	mgN/mgVSS
P:VSS ratio	fp	0,03	mgP/mgVSS
C:VSS ratio	fc	0,512	mgC/mgVSS
H:VSS ratio	fh	0,08	mgH/mgVSS
O:VSS ratio	fo	0,29	mgO/mgVSS
ISS/VSS	fi	0	mgISS/mgVSS
Number of moles from COD	n	1,15E-02	mol/l
Number of moles from VSS	n	1,15E-02	mol/l
C_X	X	4,31	
H_Y	Y	7	
O_Z	Z	1,82	
N_a	a	0,73	
P_b	b	0,10	
e^-/mol	γ_s	18,91	e^-/mol
COD/mol influent		151,25	gCOD/mol
Molar mass	M_r	101,1753	g/mol

Table 6.13: Kinetics of hydrolysis

Hydrolysis Kinetics Constant Maake& Ikumi (2020)	K_M	2,64	gCODorganics/gCODBiomass.d
	K_S	9,00	gCOD/l
Endogenous residue	Y_{AD}	0,11	/d
Death rate of acidogens	b_{AD}	0,04	/d
Sludge Retention Time	R_s	40,00	d
Influent OHO concentration	S_{bpi}	3,40	gCOD/l
Residual organics concentration	S_{bp}	0,36	gCOD/l
Acidogenic Biomass concentration	Z_{AD}	0,14	gCOD/l
Hydrolysis rate	r_h	0,26	gCOD/l,d
Methane produced	S_m	9,28	gCOD/l

6.2.2 Kinetics of hydrolysis

To achieve accurate methane and effluent COD predictions, the kinetics of hydrolysis need to be adapted to the PAO substrate. Maake & Ikumi (2020) analysed dynamic ABMP data and generated hydrolysis kinetic constants for PAOs. The analysis of saturation kinetics constants yielded a value of K_M=2.64gCODorganics/gCODorganics.d and K_S=9.11gCOD/l. The output to the kinetics portion of the model is presented in Table 6.13.

6.2.3 Stoichiometry

The stoichiometric portion of the model used the sludge characteristics presented in Table 6.11 and the output from the kinetics of hydrolysis in Table 6.13 to model COD removal and associated N, P and alkalinity releases. The organic and inorganic stoichiometry were modelled separately.

6.2.3.1 Stoichiometry of biomass breakdown

The PAO biomass breakdown was modelled according to Sötemann *et al.*'s (2005) stoichiometry with the P extension proposed by Harding *et al.* (2010). Table 6.14 presents the stoichiometric results of organic PAO breakdown. These releases were then used to model the AD's weak acid/base chemistry and estimate the AD's pH.

6.2.3.2 Stoichiometry of polyP breakdown with no energy transfer

If polyP is transferred to the AD with no energy, PAOs are unable to undergo bioprocesses in the AD. The stoichiometry presented by Harding *et al.* (2010) does not model PAO bioprocesses in the AD and is hence used to model this alternative. Table 6.15 presents the results of polyP breakdown with no energy transfer.

As previously discussed, the breakdown of polyP with no associated bioprocesses results in a decrease in the AD alkalinity due to HCO_3^- ions being used up despite associated P releases.

Table 6.14: Biomass stoichiometric breakdown

Ratio of biomass to hydrolysed COD	E	0,05	
split between H2PO4- and HPO42-	f	0,23	
Number of moles of water	H_2O	-6,38E-02	mol/l
Number of moles of carbon dioxide	CO_2	3,00E-02	mol/l
Number of moles of methane	CH_4	5,07E-02	mol/l
Number of moles of biomass formed		9,77E-04	mol/l
Number of moles of ammonia released	NH_4^+	1,53E-02	mol/l
Number of moles of P released as	$H_2PO_4^-$	5,07E-04	mol/l
	HPO_4^{2-}	1,68E-03	mol/l
Number of moles of bicarbonate released	HCO_3^-	1,14E-02	mol/l

Table 6.15: PolyP breakdown stoichiometry with no energy transfer

Select value of q.	q=	0,48	
split between H2PO4- and HPO42-	f	0,23	
Number of moles of water	H_2O	-2,52E-03	mol/l
Number of moles of bicoarbonate released	HCO_3^-	-8,38E-03	mol/l
Number of moles of carbon dioxide	CO_2	8,38E-03	mol/l
Number of moles of P released as	$H_2PO_4^-$	2,52E-03	mol/l
	HPO_4^{2-}	8,38E-03	mol/l
Number of moles of magnesium released	Mg^{2+}	1,18E-03	mol/l
Number of moles of potassium released	K^+	7,30E-03	mol/l
Number of moles of calcium released	Ca^{2+}	6,17E-04	mol/l

Table 6.16: Stoichiometry of polyP breakdown with energy transfer

Reducing Agent		PolyP	Glycogen	Acetate	Units
Energy from Inorganic Portion of Biomass to form PHB					
Number of moles of P per mol of PHB formed	Y_{PP}	0,33	0,33	-	
Number of moles of glycogen per mol of PHB formed	Y_{gl}	-	0,37	0,37	
% of polyP released towards bioprocesses		80,5%	80,5%	80,5%	
Number of moles of PolyP		-8,77E-03	-8,77E-03	-8,77E-03	mol/l
Number of moles of glycogen	$C_4H_7O_{3,5}$	-	-9,83E-03	-2,50E-03	mol/l
Number of moles of acetate	CH_3COO^-	-5,32E-02	-2,66E-02	-8,50E-03	mol/l
$(H^+ + e^-)$ generated from polyP breakdown	$(H^+ + e^-)$	-5,32E-02	-	-	mol/l
Number of moles of water	H_2O	4,44E-02	6,87E-03	-4,02E-03	mol/l
Number of moles of PHB formed	$C_4H_6O_2$	2,66E-02	2,06E-02	5,99E-03	mol/l
H^+ ions released	H^+	-3,56E-02	1,15E-02	1,50E-02	mol/l
Number of moles of magnesium released	Mg^{2+}	1,64E-03	1,64E-03	1,64E-03	mol/l
Number of moles of potassium released	K^+	5,04E-03	5,04E-03	5,04E-03	mol/l
Number of moles of calcium released	Ca^{2+}	8,54E-04	8,54E-04	8,54E-04	mol/l
Carbonic Acid	CO_3^{2-}	-	1,03E-02	3,00E-03	mol/l
Phosphoric Acid	PO_4^{3-}	8,77E-03	8,77E-03	8,77E-03	mol/l
PHB breakdown and AD biomass formation					
Number of moles of PHB used	$C_4H_6O_2$	-2,66E-02	-2,06E-02	-5,99E-03	mol/l
Number of moles of water	H_2O	-3,99E-02	-3,08E-02	-8,99E-03	mol/l
Number of moles of carbon dioxide	CO_2	4,65E-02	3,60E-02	1,05E-02	mol/l
Number of moles of methane	CH_4	5,98E-02	4,62E-02	1,35E-02	mol/l
PolyP hydrolysis by extracellular enzymes					
split between $H_2PO_4^-$ and HPO_4^{2-}	f_p	0,37	0,37	0,39	mol/l
split between HCO_3^- and C_T	f_c	0,37	0,37	0,39	mol/l
Number of moles of polyP	n	-2,12E-03	-2,12E-03	-2,12E-03	mol/l
Number of moles of water	H_2O	-2,12E-03	-2,12E-03	2,12E-03	mol/l
Number of moles of bicarbonate released	HCO_3^-	-1,33E-03	-1,33E-03	-1,31E-03	mol/l
Number of moles of carbon dioxide	CO_2	1,33E-03	1,33E-03	1,31E-03	mol/l
Number of moles of P released as	$H_2PO_4^-$	7,91E-04	7,96E-04	8,19E-04	mol/l
	HPO_4^{2-}	1,33E-03	1,33E-03	1,31E-03	mol/l
Number of moles of magnesium released	Mg^{2+}	3,96E-04	3,96E-04	3,96E-04	mol/l
Number of moles of potassium released	K^+	1,22E-03	1,22E-03	1,22E-03	mol/l
Number of moles of calcium released	Ca^{2+}	2,07E-04	2,07E-04	2,07E-04	mol/l

6.2.3.3 Stoichiometry of polyP breakdown with energy transfer

The stoichiometry presented by Ikumi and Ekama (2019) models the impact of energy transfer from the AS system to the AD through the modelling of PAO processes in the AD. To allow for a complete model and ensure no potential biochemical pathways are ignored, Ikumi and Ekama (2019) considered three potential reducing agents namely polyphosphate, glycogen and acetate. Using the polyP characterization presented in Table 6.11 as an input, the results for each biochemical pathway is presented in Table 6.16.

The stoichiometry developed by Ikumi and Ekama (2019) relied on several PAO anaerobic constants obtained from the AS system. These constants highlighted both the link between the AS system and the AD and the fact that PAOs act according to the environment. The constants were:

i) The ratio of P release to PHB formed which assumed to be 0.33 (Smolders et al., 1995)

ii) The ratio of glycogen to PHB formed which was assumed to be 0.37 (Smolders et al., 1995) and

iii) And the percentage of polyP used towards bioprocesses which was assumed to be 80.5% (Wentzel et al., 1988).

Use of polyphosphate

The disintegration of polyP directly, without an external carbon source used as a reducing agent (electron transfer represented by $NADH_2$),was divided into three sections into the model:

- 80.5% of the polyP was used to manufacture PHB as per the "Comeau-Wentzel" model and Wentzel *et al.*'s (1988) observations. This increased the system's alkalinity through P releases
- 19.5% of the polyP was not released through bioprocesses and anaerobically digested. This release caused a decrease in the system alkalinity through bicarbonate utilization.
- The PHB formed was then anaerobically digested increasing the partial pressure of CO_2 (pCO_2)

The P release was accompanied by metal releases to maintain the charge balance on the biomass. Table 6.16 presents the stoichiometric output with this polyP disintegration.

Use of glycogen as a reducing agent

The results in Table 6.16 present the output of the stoichiometry presented by Ikumi and Ekama (2019) for PAO processes in the AD where polyP is broken down for acetate uptake and glycogen is used as the source of reducing agents to produce PHB.

Acetate as a reducing agent

The results presented in Table 6.16 detail the stoichiometry generated for PAO processes in the AD when acetate was used as a reducing agent. This stoichiometry allowed for an external carbon source to act as a potential reducing agent.

6.2.4 Weak Acid/Base Chemistry

Using the initial alkalinity, the output from the stoichiometry and a multimineral precipitation model, the AD system's pH was calculated. For this analysis, the multimineral precipitation model was simplified to remediate to issues associated with magnesite and calcite precipitation shown in Table 6.9. The multimineral precipitation model now only calculates the AD's pH at infinite solubility and after struvite, ACP and Newberyite precipitation. In the model, the value f, the fraction of HPO_4^{2-} to total phosphorus ions was only explicitly calculated at infinite solubility. Iterating f during precipitation was not achievable due to the changing total species concentration and limitations of Microsoft Excel.

The results presented in Table 6.17 will be used to identify the impact of Ikumi and Ekama's (2019) stoichiometry and the multimineral precipitation model on the AD. The pH predicted by the model will be compared to the empirical pH measured by Maake & Ikumi (2020) at 6.69. Figure 6.1 presents a graphical representation of this comparison.

Table 6.17: pH results

Stoichiometry	Harding (2009)	Ikumi and Ekama (2019)		
Reducing Agent	None	polyP	glycogen	Acetate
No precipitation				
pH_no precipitation	6,41	6,68	6,68	6,70
Struvite Precipitation				
Amount of struvite formed	3,45E-03	1,55E-03	1,53E-03	1,51E-03
Magnesium post precipitation	4,63E-03	3,59E-03	3,56E-03	3,54E-03
PT post precipitation	1,65E-02	1,46E-02	1,46E-02	1,46E-02
NT post precipitation	1,87E-02	1,68E-02	1,68E-02	1,68E-02
pH_post struvite precipitation	6,55	6,71	6,72	6,73
ACP precipitation				
Amount of ACP formed	2,06E-04	3,54E-04	3,54E-04	3,54E-04
Calcium post precipitation	-1,23E-06	-2,12E-06	-2,12E-06	-2,12E-06
PT post precipitation	1,61E-02	1,39E-02	1,39E-02	1,39E-02
pH_post ACP precipitation	6,47	6,69	6,69	6,70
Newberyite precipitation				
Amount of Newberyite formed	2,05E-03	1,61E-03	1,59E-03	1,56E-03
Mg post precipitation	2,58E-03	1,98E-03	1,96E-03	1,98E-03
PT post precipitation	1,41E-02	1,23E-02	1,23E-02	1,23E-02
pH_post Newberyite precipitation	6,40	6,67	6,67	6,68

Figure 6.1: Comparison between empirical and model predicted pH

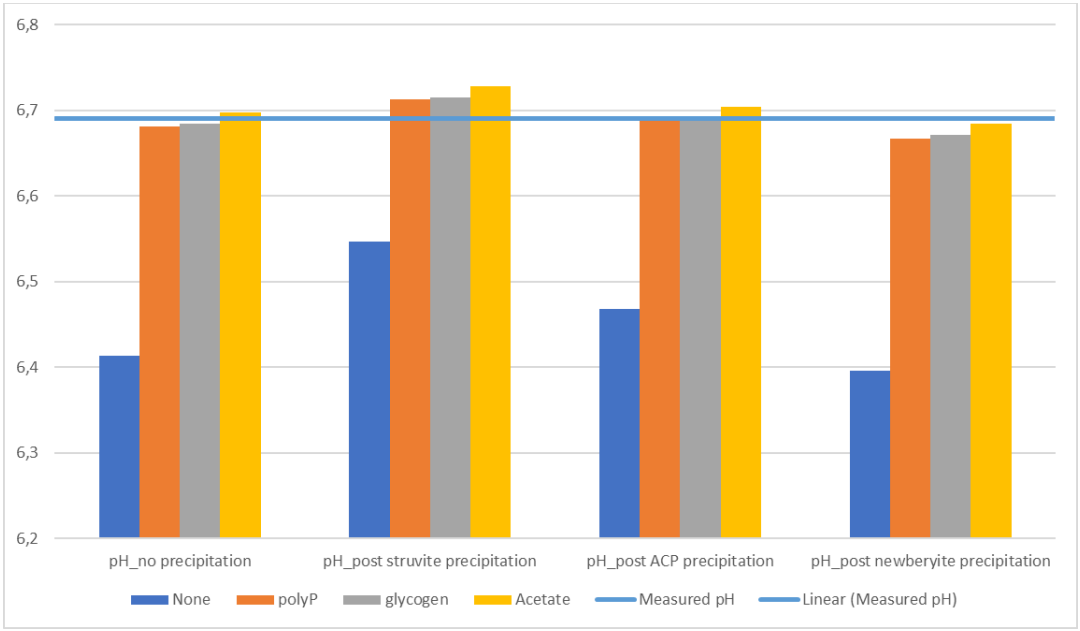

Maake & Ikumi (2020) reported a pH of 6.69 after the 40 days ABMP was carried out. As shown in Figure 6.1, this pH was approximated by:

i) The model using glycogen as a reducing agent post ACP precipitation with a pH=6.69,

ii) The model using polyP disintegration without an external carbon source used as a reducing agent post ACP precipitation with a pH=6.69 and

iii) The model using acetate as reducing agent post multimineral precipitation with a pH=6.68

These results show that PAO processes do take place in the AD as the model assuming no bioprocesses in the AD yielded the worse results. The results also indicated, however, that the model and the data generated could not be used to identify which reducing agent is used during PAO intracellular processes. The analysis also indicates that the data generated by Maake and Ikumi (2020) shows evidence that an energy transfer does take place between the AS system and the AD. However, since the experimental pH was approximated several times, it cannot be conclusively stated that polyP should be used as the source of energy for PAO bioprocesses.

6.2.5 Model Analysis

The data presented in Figure 6.1 and Table 6.17 show accurate AD pH predictions. To increase confidence in these results, a comparison between the ABMP effluent data and the AD model predicted data must also take place. Table 6.18 presents this comparison.

Table 6.18 shows that the predicted effluent COD, VSS, ISS and TSS are within range of the experimental data reported by Maake and Ikumi's (2020). Indeed, they respectively achieved a 97.5%, 95.8%, 103.0% and 98.5% match. Since Maake and Ikumi (2020) did not have N data, an analysis of the N prediction could not be achieved. The accurate pH estimation, however, do validate the N releases as they impact the AD pH significantly (Sötemann *et al.*, 2005). Severe discrepancies can be seen between the predicted and measured P and metals readings. This disparity in data was attributed to experimental error as, as shown in Table 6.10, P and metal balances were not achieved over the experimental data.

To increase confidence in the models generated, mass balances were carried out. Table 6.19 presents the results of the mass balances performed over each AD model created.

Table 6.18: Comparison between Maake and Ikumi (2020) effluent data and model output

SS AD model results		Maake & Ikumi (2020)	Model Output
Total COD	S_{te}	2520,00	2585,3
Filtered COD	S_{tse}	-	0
Unbiodegradable soluble COD	S_{use}	-	0
TKN	N_{te}	-	366,3
Filtered TKN	N_{tse}	-	230,2
Free and Saline Ammonia	N_{ae}	-	230,2
Influent unbiodegradable N	N_{ouse}	-	0
Total Phosphorus (TP)	P_{te}	563,40	446,50
Filtered TP	P_{tse}	-	405,69
Ortho-phosphate	P_{ae}	308,70	405,69
Effluent P	P_{ouse}	-	0
Particulate Volatile Suspended Solids	VSSe	1660,00	1732,3
Inorganic Suspended Solids	ISSe	1060,00	1028,6
Total Suspended Solids	TSSe	2720,80	2760,9
Total Magnesium	TMg^{2+}_e	-	49,40
Total Potassium	TK^{+}_e	493,50	245,00
Total Calcium	TCa^{2+}_e	24,30	42,50
Soluble Magnesium	SMg^{2+}_e	-	49,40
Soluble Potassium	SK^{+}_e	-	245,00
Soluble Calcium	SCa^{2+}_e	-	42,50
Gas		739,5	-
pH of effluent		6,69	-

Table 6.19: Model Balances

Balances	Harding (2009) (%)	Ikumi and Ekama (2019) (%)		
		PolyP	Glycogen	Acetate
COD	100	100	100	100
Nitrogen	100	100	100	100
Phosphorus	100	100	100	100
Magnesium	100	100	100	100
Potassium	100	100	100	100
Calcium	100	100	100	100

7. Conclusion

This research aimed, through the generation of experimental data and the creation of an anaerobic digestion model, to generate knowledge that will help obtain a better understanding of the intracellular bioprocesses of phosphorus accumulating organisms (PAOs) when fed to AD systems. This chapter aims at concluding and presenting the results of this research. This chapter will also highlight whether the objectives presented in Chapter 1 were met.

7.1 Anaerobic Digestion Model for treatment of NDEBPR Sludge

Anaerobic digestion (AD) is a sludge treatment protocol where organics are broken down in the absence of oxygen and nitrates to achieve increased sludge stabilization. This process also ensures resource recovery in the form of methane which can be used to generate electricity. Sötemann *et al.* (2005) developed a steady state (SS) AD model that predicted the reactor and effluent properties of the digester when treating primary sludge (PS) and waste activated sludge (WAS) from a Modified Ludzach Ettinger (MLE) system (N rich sludge). Harding *et al.* (2010) extended Sötemann *et al.*'s (2005) model allowing for the modelling of the P fraction of the influent sludge and P releases associated with said sludge's breakdown.

7.1.1 Model Development

This research further extends the model to allow the prediction of the reactor and effluent properties of an AD treating sludge from nitrifying-denitrifying enhanced biological phosphorus removal (NDEBPR) activated sludge (AS) systems (N and P rich sludge). This was achieved by:

- Modelling the behaviour of PAOs in the NDEBPR sludge in the AD. The behaviour of PAOs were modelled through the inclusion of stoichiometry generated by Ikumi and Ekama (2019) to approximate PAO intracellular processes. The stoichiometry modelled the uptake of acetate, the breakdown of glycogen and polyphosphate (poly) and the manufacture of poly-β-hydroxybutyrate (PHB) in the AD. Due to the lack of an accepted theory of PAO intracellular processes, Ikumi and Ekama (2019) allowed for multiple pathways for PAO bioprocesses developing equations using polyP (in accordance to the

"Comeau-Wentzel" model), glycogen (in accordance to the "Mino" model) and acetate (an external carbon source) as potential reducing agents.

- Modelling the impact of precipitation in the AD. This was done by extending the SS struvite precipitation model proposed by Loewenthal *et al.* (1995) to a multimineral precipitation model.

The AD model generated was built in five main sections:

i) The first section characterized the sludge according to the method presented by Harding *et al.* (2010). The characterization procedure separated the sludge into three components: the biodegradable, unbiodegradable and the inorganic portions. The PAO biomass was modelled to have a biodegradable, unbiodegradable and inorganic fraction. 8% of the active biomass was modelled to be unbiodegradable in the AD system in accordance with the death regeneration model (Dold *et al.*, 1980). The inorganic portion of the biomass (i.e., the polyP stored in the PAO) was assumed to have a general composition of $Mg_cK_dCa_e.PO_3$ (Harding, 2009).

ii) The second used saturation kinetics of hydrolysis to predict the effluent COD. Saturation kinetics were used to model the hydrolysis of the sludge because it modelled the nature of the hydrolysis process, a surface process, best. From the hydrolysis portion of the model the predicted effluent COD, COD removal and the amount of biogas generated were predicted.

iii) The third section of the model used the output from the saturation kinetics of hydrolysis and stoichiometry to assess releases in the AD. The stoichiometry used aimed at assessing whether PAOs did or did not undergo bioprocesses (polyp release and associated PHB formation) in the AD (i.e., Harding *et al.* (2010) vs Ikumi and Ekama (2019)) and the best stoichiometric pathway that would represent these potential bioprocesses).

iv) The fourth section used metallic and ionic releases from the third stage of the model to estimate the pH of the AD. The pH was calculated assuming both no precipitation took place in the AD (i.e., infinite ionic solubility) and multimineral precipitation took place in the AD. The multimineral precipitation allowed for the precipitation of struvite, amorphous

calcium phosphate (ACP), magnesite, calcite and newberyite precipitation in that order based on kinetic rates.

v) The fifth and final section ensured mass balances were maintained over each stage of the steady state AD model

7.1.2 Model Analysis

7.1.2.1 Steady State Pathway Analysis

A comparative analysis of the PAO pathways in the model showed that the weak acid/base chemistry portion of the AD model was the most sensitive portion of the model. The multimineral precipitation model was built to allow both the precipitation and dissolution model of minerals to ensure equilibrium was achieved. However, the modelling of magnesite and calcite proved problematic. The dissolution of magnesite and calcite was seen to overwhelm the model resulting in a partial pressure of carbon-dioxide (pCO_2) large than one (1) which cannot be achieved. A bypass was placed in the model to prevent this from happening.

To reduce operating time, prevent errors in the model and because this portion of the model was bypassed for a range of influent properties during the comparative analysis, the portion of the model was removed. The final multimineral precipitation model only considered the precipitation of struvite, ACP and newberyite.

7.1.2.2 Metabolic Pathway Analysis

To assess the validity of each model and determine which stoichiometric pathway best approximated PAO behaviour, data from an enhanced PAO culture 40-day augmented biomethane potential (ABMP) test was used. The influent, saturation kinetic rates and effluent data sourced from, Maake and Ikumi (2020) were fed to the model to compare the results.

The details of the influent characterization, hydrolysis process, stoichiometry and weak acid/base chemistry sections of the model are presented in Chapter 6 Section 6.2.1, 6.2.2, 6.2.3 and 6.2.4 respectively. Table 7.1 presents a comparison between the model and empirical effluent properties. Figure 7.1 presents a SS pH comparison between each stoichiometry and the empirical pH

Table 7.1: Weak Acid/Base Chemistry model output

SS AD model results		Empirical Data	Model Output			
		Maake and Ikumi (2020)	Harding et al. (2009)	Ikumi and Ekama (2019)		
				PolyP	Glycogen	Acetate
Total COD	S_{te}	2520,00	2585,3			
Filtered COD	S_{tse}	-	0			
Unbiodegradable soluble COD	S_{use}	-	0			
TKN	N_{te}	-	366,3			
Filtered TKN	N_{tse}	-	230,2			
Free and Saline Ammonia	N_{ae}	-	230,2			
Influent unbiodegradable N	N_{ouse}	-	0			
Total Phosphorus (TP)	P_{te}	563,40	446,50			
Filtered TP	P_{tse}	-	405,69			
Ortho-phosphate	P_{ae}	308,70	405,69			
Effluent P	P_{ouse}	-	0			
Particulate Volatile Suspended Solids	VSSe	1660,00	1732,3			
Inorganic Suspended Solids	ISSe	1060,00	1028,6			
Total Suspended Solids	TTSSe	2720,80	2760,9			
Total Magnesium	TMg^{2+}_e	-	49,40			
Total Potassium	TK^{+}_e	493,50	245,00			
Total Calcium	TCa^{2+}_e	24,30	42,50			
Soluble Magnesium	SMg^{2+}_e	-	49,40			
Soluble Potassium	SK^{+}_e	-	245,00			
Soluble Calcium	SCa^{2+}_e	-	42,50			
Gas	ml	739,5	771			
pH of effluent assuming infinite ionic solubility		6,69	6,41	6,68	6,68	6,70
pH post struvite precipitation			6,55	6,71	6,72	6,73
pH post ACP precipitation			6,47	6,69	6,69	6,70
pH post newberyte precipitation			6,40	6,67	6,67	6,68

Figure 7.1: pH comparison between empirical and modelled pH

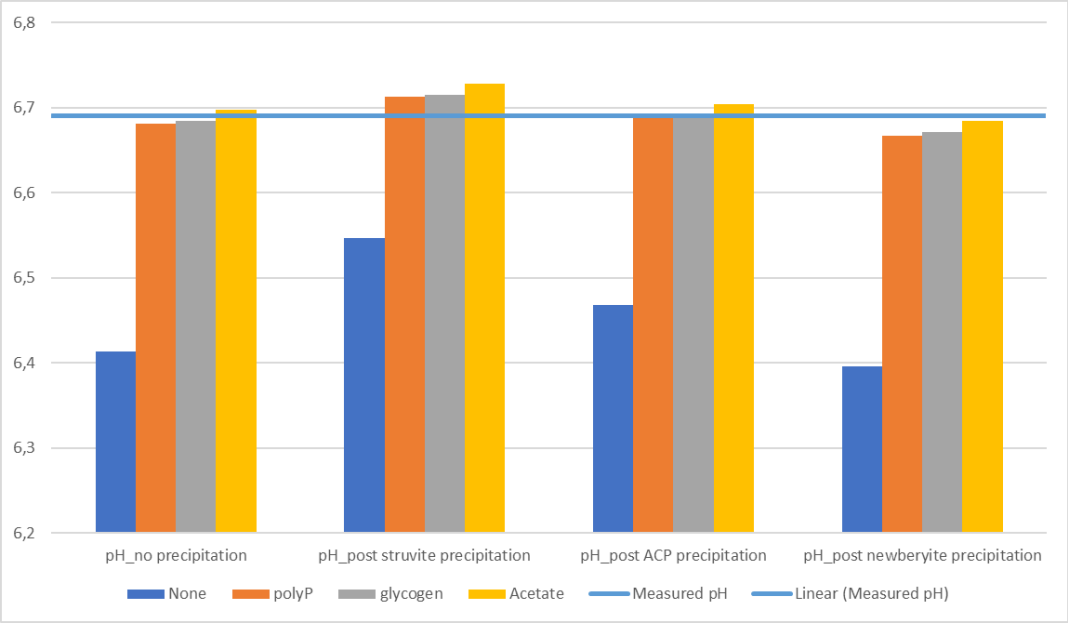

As shown in Table 7.1, the model generated achieved a high degree of correlation with the effluent data measured by Maake and Ikumi (2020):

- A COD, VSS, ISS and TSS balance was achieved with respectively a 97.5%, 95.8%, 103.0% and 98.5% match.
- The metal and P balance were not achieved. However, since Maake and Ikumi (2020) could not achieve a metal and P balance over the ABMP reactor, it was unlikely that a balance could be achieved.
- The SS AD model predicted reasonable outputs approximating the reactor's pH.

7.1.2.3 Steady State AD model Closure

Due to the high degree of correlation between the model and the experimental data, it can be concluded that a SS AD model accurately predicting reactor and effluent properties when treating NDEBPR sludge was developed.

From the model, it can also be concluded that:

i) PAOs do undergo bioprocesses of polyP breakdown and associated PHB uptake in the AD.

ii) The SS AD model generated, by itself, does not allow this research to determine where energy required for PAOs for intracellular processes originates and hence if an energy transfer does take place between the AS system and the AD. If an energy transfer does take place, it means that the magnitude of this energy transfer is small and does not impact the AD at SS (or how it impacts the AD is yet unknown). The sum of this research and the dynamic analysis presented by Ikumi and Ekama (2019) seems to warrant that polyP be used as a reducing agent for PAO processes.

iii) The findings of this thesis seem to show that a multimineral precipitation model in required even at steady state. The multimineral precipitation model generated during this research was, however, reduced due to issues linked to the modelling of precipitation and dissolution of carbon-based minerals.

7.2 Further Research

This research and the AD model developed to meet the objectives outlined in Chapter 1 give rise to new questions to ensure completion of the AD model developed.

7.2.1 Further Testing of the model

Due to the inability of this research to run and generate data from a SS AD, it is recommended that ADs be operated, and their contents modelled to confirm the findings of this research. ABMPs from these ADs should also be carried out to provide new data towards the hydrolysis rate of PAOs in the AD. The data generated which will help derive general PAO hydrolysis constants similar to the ones presented by Sötemann *et al.* (2005).

Further research in this precipitation model is also required to ensure that its replicates the system well or presents an easier interface as a decision-making tool. Indeed, the failure to model the precipitation of carbon-based minerals limits the accuracy of the model and its extension is to be encouraged. This dissolution model generated as part of this research used precipitates as alkalinity reservoirs that were not measured by 5pt titration. Data is required to calibrate this portion of the multimineral precipitation model.

7.2.2 PolyP hydrolysis Kinetics

In this research, data from a forty (40) day ABMP was used to test the accuracy of the model developed. The long SRT ensured all the polyP stored in the PAO would be released into the AD. Since Harding (2009) reported polyP release to last for eight (8) to ten (10) days and the alkalinity in the influent and from the biomass was shown to be critical, it is recommended that a kinetic equation regarding polyP breakdown by PAOs for bioprocesses be added to the AD model. This equation will allow the accurate modelling of aqueous phase releases in the AD at short retention times as well as AD reactor alkalinity and pH.

8. References

Angelidaki, I., Alves, M., Bolzonella, D., Borzaconni, L., Campos, J.L., Guwy, A.J., Kalyuzhnyi, S.V., Jenicek, P. et al. 2009. Defining the biomethane potential (BMP) of solid organic wastes and energy crops: a proposed protocol for batch assays. *Water Science and Technology*.8.

APHA. 1975. *Standard Methods For the Examination of Water and Wastewater.* Fourteenth.

Batstone, Keller, J., Angelidaki, I., Kalyuzhnyi, S.V., Pavlostathis, S.G., Rozzi, A., Sanders, W.T.M., Siegrist, H. et al. 2002. The IWA Anaerobic Digestion Model No 1 (ADM1).

Bolzonella, D., Pavan, P., Battistoni, P. & Cecchi, F. 2004. Mesophilic anaerobic digestion of waste activated sludge: influent of the solid retention time in the wastewater treatment process. *Process Biochemistry.* 40:7. DOI:10.1016/j.procbio.2004.06.036.

Botha, R.F. & Ekama, G.A. 2015. Characterization of organics for anaerobic digestion by modelling augmented biochemical potential test results.

Brdjanovic, D., van Loosdrecht, M.C.M., Hooijmans, C.M., Mino, T., Alaerts, G.J. & Heijnen, J.J. 1998. Effect of phosphate limitation on the anaerobic metabolism of phosphorus accumulating microorganisms. *Applied Microbiology and biotechnology.* 50(2):3.

Comeau, Y., Oldham, W.K., Hall, K.J. & Hancock, R.E.W. 1987. Biochemical Model for Enhanced Biological Phosphorus Removal. *Water Research.* 20(12):11.

Dold, P.L., Ekama, G.A. & Marais, G.v.R. 1980. A general model for the activated sludge process. *Prog. Wat. Technol.*:30.

Ekama, G.A., Sotemann, S.W. & Wentzel, M.C. 2007. Biodegradability of activated sludge organics under anaerobic conditions. *Water Research.* 41(1):8.

Gaszynski, C.E., Ekama, G.A. & Ikumi, D.S. 2019. Utilisation of augmented batch tests to determine sludge characteristics. *Watermatex 2019.* 2019.

Harding, T.H. 2009. A Steady State Stoichiometric Model Describing The Anaerobic Digestion Of Biological Excess Phosphorus Removal Waste Activated Sludge. University of Cape Town.

Henze, M., van Loosdrecht, M.C.M., Ekama, G.A. & Brdjanovic, D. 2008. *Biological Wastewater Treatment: Principles, Modelling and Design.* IWA Publishing.

Hu, Z., Wentzel, M.C. & Ekama, G.A. 2002. Anoxic Growth of phosphate accumulating organisms (PAOs) in biological nutrient removal activated sludge systems. *Water Research.* 36:11.

Ikumi, D.S. 2011. Plantwide Integrated Biological, Chemical and Physical Bioprocesses Modelling of Wastewater Treatment Plants in Three Phases (Aqueous-Gas-Solid). University of Cape Town.

Ikumi, D.S. & Ekama, G.A. 2019. Plantwide Modellig - Anaerobic Digestion of Waste Sludge from Parent Nutrient (N&P) Removal Systems.

Ikumi, D.S., Harding, T.H. & Ekama, G.A. 2014. Biodegradability of wastewater and activated sludge organics in anaerobic digestion. *Water Research.* 56:13. DOI:10.1016/j.watres.2014.02.008.

Ikumi, D.S., Harding, T.H., Vogts, M., Lakay, M.T., Mafungwa, H., Brouckaert, C. & Ekama, G.A. 2015. *Mass Balances Modelling Over Wastewater Treatment Plants III*. (No. 1822/1/14). Cape Town.

Kruk, D.J., Elektorowicz, M. & Oleszkiewicz, J.A. 2014. Struvite precipitation and phosphorus removal using magnesium sacrificial anode. *Chemosphere.* 10.1016/j.chemosphere.2013.12.036. DOI:10.1016/j.chemosphere.2013.12.036.

Kuba, T., Smolders, G.J.F., van Loosdrecht, M.C.M. & Heijnen, J.J. 1993. Biological phosphorus removal from wastewater by anaerobic-anoxic sequencing batch reactor. *Water Science and Technology.* 27(6):12.
Lahav, O. & Loewenthal, R.E. 1993. Measurement of VFA in anaerobic digestion: The five point titration revised. *Water SA.* 26(3):5.
Lee, H. & Yun, Z. 2014. Comparison of biochemical characteristics between PAO and DPAO sludges. *Journal of Environmental Sciences.* 26:8. DOI:10.1016/S1001-0742(13)60609-9.
Loewenthal, R.E., Kornmuller, U.R.C. & van Heerden, E.P. 1995. Modelling Struvite Precipitation in Anaerobic Treatment Systems. *Water Science and Technology.* 30(12):10.
Maake, A. & Ikumi, D.S. 2020. *The utilisation of augmented batch tests to comprehensively characterize waste sluge containing enhanced cultures of polyphosphate accumulating organisms.* Cape Town: University of Cape Town.
Marti, N., Bouzas, A., Seco, A. & Ferrer, J. 2008. Struvite precipitation assessment in anaerobic digestion processes. *Chemical Engineering Journal.* 141:8. DOI:10.1016/j.cej.2007.10.023.
McCarty, P.L. 1974. Anaerobic processes. *International*
Association of Water Pollution Research (IAWPR) now IWA. 1974.
Mino, T., van Loosdrecht, M.C.M. & Heijnen, J.J. 1988. Microbiology and biochemistry of the enhanced biological phosphate removal process. *Water Research.* 32(11):15.
Murnleitner, E., Kuba, T., van Loosdrecht, M.C.M. & Heijnen, J.J. 1997. An integrated metabolic model for the aerobic and denitrifying biological phosphorus removal. *Biotechnology and Bioengineering.* 54(5):17.
Musvoto, E.V., Wentzel, M.C., Loewenthal, R.E. & Ekama, G.A. 2000. Integrated Chemical-Physical Processes MOodelling - I. Development of a Kinetic-Based MODEL FOR MIXED WEAK ACID/BASE SYSTEMS. *Water Research.* 34(6):11.
Nielsen, J. & Villadsen, J. 1994. *Bioreaction Engineering Principles.* United States of America: Plemum Publishing Corporation.
Oehmen, A., Lemos, P.C., Carvalho, G., Yuan, Z., Keller, J., Blackall, L.L. & Reis, M.A.M. 2007. Advances in enhanced biological phosphorus removal. *Elsevier.* 02(30):30. DOI:10.1016/j.watres.2007.02.030.
Owen, F.W., Stuckey, D.C., Healy, J.B., Young, L.Y. & McCarty, P.L. 1978. Bioassay for Monitring Biochemical Methane potential and Anaerobic Toxicity. *Water Research.* 13:8.
Parkin, F.G. & Owen, F.W. 1986. Fundamentals of Anaerobic Digestion of Wastewater Sludges. *Journal of Environmental Management.* 112(5).
Pereira, H., Lemos, P.C., Reis, M.A.M., Crespo, J.P.S.G., Carrondo, J.T. & Santos, H. 1996. Model for Carbon Metabolism in Biological Phosphorus Removal Processes based on In Vivo C-NMR Labelling Experiments. *Water Research.* 30(9):11. DOI:0043-1354/96.
Pijuan, M., Oehmen, A., Baeza, J.A. & Yuan, Z. 2008. Characterizing the biochemical activity of full-scale enhanced biological phosphorus removal systems: A comparison. *Biotechnology and Bioengineering.* 10.1002/bit.21502. DOI:10.1002/bit.21502.
Raposo, F., De la Rubia, M.A., Fernandez-Cegri, V. & Borja, R. 2011. Anearobic digestion of solid organic substrates in batch mode : An overview relating to methane yields and experimental procedures. *Renewable and Sustainable Energy Reviews.* 16:17. DOI:10.1016/j.rser.2011.09.008.
Rittmann, B.E. & McCarty, P.L. 2001. Environmental Biotechnology: Principles and Applications.
Sathasivan, A. 2011. Biological Phosphorus Removal Processes for Wastewater Treatment. *Water and Wastewater Treatment Technologies.*16.

Seviour, R.J., Mino, T. & Onuki, M. 2003. The microbiology of phosphorus removal in activated sludge systems. *FEMS Microbiology Reviews.* 10.1016/S0168-6445(03)00021-4:29. DOI:10.1016/S0168-6445(03)00021-4.
Smolders, G.J.F., van der Meij, J., van Loosdrecht, M.C.M. & Heijnen, J.J. 1993. Model of the Anaerobic Metabolism of the biological phosphorus removal process-Stoichiometry and pH influence. *Biotechnology and Bioengineering.*
Smolders, G.J.F., van der Meij, J., van Loosdrecht, M.C.M. & Heijnen, J.J. 1994. Stoichiometry model of the aerobic metabolism of the biological phosphorus removal process. *Biotechnology and Bioengineering.* 43(6):10. DOI:10.1002/bit.260430605.
Smolders, G.J.F., van der Meij, J., van Loosdrecht, M.C.M. & Heijnen, J.J. 1995. A structured metabolic model for anaerobic and aerobic stoichiometry and kinetics of the biological phosphorus removal process. *Biotechnology and Bioengineering.* 47:11.
Sötemann, S.W., Ristow, N.E., Wentzel, M.C. & Ekama, G.A. 2005. A steady state model for anaerobic digestion of sewage sludges. *Water SA.* 31(4):6.
Sötemann, S.W., Ristow, N.C., Wentzel, M.C. & Ekama, G.A. 2007. A Steady State Model for Anaerobic Digestion of Sewage Sludge. *Water SA.* 31(4). DOI:10.4314/wsa.v31i4.5143.
van Loosdrecht, M.C.M., Smolders, G.J.F., Kuba, T. & Heijnen, J.J. 1997. Metabolism of micro-organisms responsble for enhanced biological phosphorus removal from wastewater. *Kluwer Academic Publishers.*8.
Varga, E., Hauduc, H., Barnard, J., Dunlap, P., Jimenez, J., Menniti, A., Schauer, P. & Lopez Vasquez, C.M. Eds. 2018. Recent Advances in Bio-P Modelling- a new approach verified by full-scale observations. Quebec, Canada.
Vlekke, G.J.F.M., Comeau, Y. & Oldham, W.K. 1988. Biological phosphate removal from wastewater with oxygen or nitrate in sequencing batch reactors. *Environmental Technology Letters.* 9(8):791-796. DOI:10.1080/09593338809384634.
Wentzel, M.C. & Ekama, G.A. 2004. A predictive model for the reactor inorganic suspended solids concentration in activated sludge system. *Water Research.* 38:14. DOI:10.1016/j.watres.2004.08.005.
Wentzel, M.C., Ekama, G.A. & Marais, G.v.R. 1990. Kinetics of Nitrification Denitrification Biological Excess Phosphorus Removal Systems - A Review. *Water Science and Technology.*
Wentzel, M.C., Loewenthal, R.E., Ekama, G.A. & Marais, G.v.R. 1988. Enhanced polyphosphate organism culture in activated sludge systems part 1. *Water SA.* 14(2).
Wentzel, M.C., Lotter, L.H., Ekama, G.A., Loewenthal, R.E. & Marais, G.v.R. 1991. Evaluation Of Biochemical Models For Biological Excess Phosphorus Removal. *Water Science and Technology.* 23:5.
Yagci, N., Artan, N., Cokgor, E.U., Randall, C.W. & Orhon, D. 2003. Metabolic Model for Acetate Uptake by a Mixed Culture of Phosphate- and Glycogen-Accumulaiting Organisms Under Anaerobic Conditions. *Wiley InterScience.* 10.1002/bit.10765. DOI:10.1002/bit.10765.
Zhou, Y., Pijuan, M., Zeng, R.J. & Yuan, Z. 2008. Involvment of the TCA cycle in anaerobic metabolism of polyphosphate accumulating organisms (PAOs). *Water Research.* 43:11. DOI:10.1016/j.watres.2008.12.008.